2021-06

TESTING AND INTEGRATION OF CUBESAT X-BAND SOFTWARE DEFINED RADIO WITH MOBILE CUBESAT COMMAND AND CONTROL (MC3) GROUND STATION

Claybaugh, Allyson A.

Monterey, CA; Naval Postgraduate School

NAVAL POSTGRADUATE SCHOOL

MONTEREY, CALIFORNIA

THESIS

TESTING AND INTEGRATION OF CUBESAT X-BAND SOFTWARE DEFINED RADIO WITH MOBILE CUBESAT COMMAND AND CONTROL (MC3) GROUND STATION

by

Allyson A. Claybaugh

June 2021

Thesis Advisor: Wenschel D. Lan
Co-Advisor: Giovanni Minelli

THIS PAGE INTENTIONALLY LEFT BLANK

REPORT DOCUMENTATION PAGE			Form Approved OMB No. 0704-0188

1. AGENCY USE ONLY *(Leave blank)*	2. REPORT DATE June 2021	3. REPORT TYPE AND DATES COVERED Master's thesis

4. TITLE AND SUBTITLE TESTING AND INTEGRATION OF CUBESAT X-BAND SOFTWARE DEFINED RADIO WITH MOBILE CUBESAT COMMAND AND CONTROL (MC3) GROUND STATION	5. FUNDING NUMBERS RGNNU
6. AUTHOR(S) Allyson A. Claybaugh	
7. PERFORMING ORGANIZATION NAME(S) AND ADDRESS(ES) Naval Postgraduate School Monterey, CA 93943-5000	8. PERFORMING ORGANIZATION REPORT NUMBER
9. SPONSORING / MONITORING AGENCY NAME(S) AND ADDRESS(ES) DoD Space	10. SPONSORING / MONITORING AGENCY REPORT NUMBER

11. SUPPLEMENTARY NOTES The views expressed in this thesis are those of the author and do not reflect the official policy or position of the Department of Defense or the U.S. Government.

12a. DISTRIBUTION / AVAILABILITY STATEMENT Approved for public release. Distribution is unlimited.	12b. DISTRIBUTION CODE A

13. ABSTRACT (maximum 200 words)

A proven CubeSat form factor is leading to increasingly ambitious payloads and mission requirements, resulting in more data products and the need for higher space-to-ground transmission rates. This thesis contributes to the Naval Postgraduate School (NPS) CubeSat project and Mobile CubeSat Command and Control (MC3) initiative to increase network capacity through X-band downlinks. The Space Systems Academic Group at NPS is developing and fielding a 6U CubeSat with an X-band software-defined radio (SDR) payload, constructed using commercial-off-the-shelf hardware and operated via the MC3 ground station network. The objective of this thesis research was verification of end-to-end compatibility between the X-band SDR payload and MC3 ground station receivers. Research, testing, and analysis determined radio frequency signal parameters and communications standards that enable transmission of data from the X-band SDR payload to the AMERGINT satTRAC SDR and Kratos quantumRadio SDR receivers. Simulation (through MathWorks Simulink models) and interoperability testing were conducted. Research culminated in demonstration of a successful baseband link from payload SDR hardware to both ground station receivers, with a QPSK-modulated, PN11 data transmission. Further functional and environmental testing will ensure the X-band SDR payload can effectively communicate on-orbit with the MC3 network.

14. SUBJECT TERMS software-defined radio, SDR, X-Band, CubeSat, Mobile CubeSat Command and Control, MC3, ground station, receiver, MathWorks, MATLAB, Simulink, on-orbit, end-to-end, testing, compatibility, Naval Postgraduate School, NPS	15. NUMBER OF PAGES 123
	16. PRICE CODE

17. SECURITY CLASSIFICATION OF REPORT	18. SECURITY CLASSIFICATION OF THIS PAGE	19. SECURITY CLASSIFICATION OF ABSTRACT	20. LIMITATION OF ABSTRACT
Unclassified	Unclassified	Unclassified	UU

NSN 7540-01-280-5500

Standard Form 298 (Rev. 2-89)
Prescribed by ANSI Std. 239-18

THIS PAGE INTENTIONALLY LEFT BLANK

Approved for public release. Distribution is unlimited.

TESTING AND INTEGRATION OF CUBESAT X-BAND SOFTWARE DEFINED RADIO WITH MOBILE CUBESAT COMMAND AND CONTROL (MC3) GROUND STATION

Allyson A. Claybaugh
Lieutenant, United States Navy
BS, Creighton University, 2013

Submitted in partial fulfillment of the
requirements for the degree of

MASTER OF SCIENCE IN SPACE SYSTEMS OPERATIONS

from the

NAVAL POSTGRADUATE SCHOOL
June 2021

Approved by: Wenschel D. Lan
Advisor

Giovanni Minelli
Co-Advisor

James H. Newman
Chair, Space Systems Academic Group

THIS PAGE INTENTIONALLY LEFT BLANK

ABSTRACT

A proven CubeSat form factor is leading to increasingly ambitious payloads and mission requirements, resulting in more data products and the need for higher space-to-ground transmission rates. This thesis contributes to the Naval Postgraduate School (NPS) CubeSat project and Mobile CubeSat Command and Control (MC3) initiative to increase network capacity through X-band downlinks. The Space Systems Academic Group at NPS is developing and fielding a 6U CubeSat with an X-band software-defined radio (SDR) payload, constructed using commercial-off-the-shelf hardware and operated via the MC3 ground station network. The objective of this thesis research was verification of end-to-end compatibility between the X-band SDR payload and MC3 ground station receivers. Research, testing, and analysis determined radio frequency signal parameters and communications standards that enable transmission of data from the X-band SDR payload to the AMERGINT satTRAC SDR and Kratos quantumRadio SDR receivers. Simulation (through MathWorks Simulink models) and interoperability testing were conducted. Research culminated in demonstration of a successful baseband link from payload SDR hardware to both ground station receivers, with a QPSK-modulated, PN11 data transmission. Further functional and environmental testing will ensure the X-band SDR payload can effectively communicate on-orbit with the MC3 network.

THIS PAGE INTENTIONALLY LEFT BLANK

TABLE OF CONTENTS

LIST OF FIGURES

LIST OF TABLES

THIS PAGE INTENTIONALLY LEFT BLANK

LIST OF ACRONYMS AND ABBREVIATIONS

A/D	analog-to-digital
AD	Analog Devices
ADC	analog-to-digital converter
ASIC	application specific integrated circuit
ASK	amplitude shift keying
BER	bit error rate
BERT	bit error rate test
BPSK	binary phase shift keying
C2	command and control
CDS	CubeSat Design Specification
COTS	commercial off-the-shelf
CSLI	CubeSat Launch Initiative
D/A	digital-to-analog
dB	decibels
DOD	Department of Defense
DSP	digital signal processor
EHF	extremely high frequency
EM	electromagnetic
f	frequency
FCC	Federal Communications Commission
FEC	forward error correction
FPGA	field-programmable gate array
FSK	frequency shift keying
FVEY	Five Eye
GHz	gigahertz
GUI	graphical user interface
IEEE	Institute of Electrical and Electronics Engineers
IF	intermediate frequency
ISC2N	International SmallSat Command and Control Network
ISS	International Space Station

ITU-R	International Telecommunications Union - Radio
Kbps	kilobits per second
km	kilometers
LFSR	linear-feedback shift register
LNA	low noise amplifier
LOS	line-of-sight
LPF	low pass filter
LV	launch vehicle
Mbps	megabits per second
MC3	Mobile CubeSat Command and Control
MHz	megahertz
NASA	National Aeronautics and Space Administration
NIWC	Naval Information Warfare Center
NOC	network operations center
NPS	Naval Postgraduate School
NTIA	National Telecommunications and Information Administration
NTM	national technical means
OQPSK	offset quadrature phase shift keying
PDR	preliminary design review
PN	pseudo-random noise
PSK	phase shift keying
QPSK	quadrature phase shift keying
R&D	research and development
RF	radio frequency
RFBE	RF back end
RFFE	RF front end
RGT	remote ground terminal
RxBERT	Received Bit Error Rate
SATRN	Satellite Agile Transmit and Receive Network
SDR	software-defined radio
SHF	super high frequency
SNR	signal-to-noise ratio

SoC	system on a chip
SoM	system on a module
SSAG	Space Systems Academic Group
SWaP	size, weight, and power
SwD	Software Devices
THz	terahertz
TIC	Terahertz Imaging Camera
TT&C	telemetry, tracking, and control
UHF	ultra high frequency
VPN	virtual private network

THIS PAGE INTENTIONALLY LEFT BLANK

ACKNOWLEDGMENTS

I would like to thank my thesis advisors, Dr. Wenschel Lan and Dr. Giovanni Minelli, for their support, guidance and enthusiasm every step of the way during my research and education. A special thanks also goes to Mr. David Rigmaiden for his invaluable expertise and assistance.

I feel honored and blessed for the opportunity the U.S. Navy gave me to pursue a master's degree in Space Systems at NPS. I am incredibly grateful for the SSAG professors, faculty and peers who impacted my time as a graduate student and fostered my discovery of a new passion for the space field.

Lastly, an important thank you to my family for your love and encouragement, for your unwavering belief in me, and for always being "over my shoulder."

THIS PAGE INTENTIONALLY LEFT BLANK

I. INTRODUCTION

This thesis research builds upon preceding work on the Naval Postgraduate School (NPS) 6U CubeSat project and Mobile CubeSat Command and Control (MC3) X-band initiative. The Space Systems Academic Group (SSAG) at NPS is developing and fielding the "Mola" 6U CubeSat. Operated via the MC3 network (the collaborative, NPS-led system of small satellite ground stations), Mola will be implemented for X-band downlink demonstration in support of mission goals. The objective of this thesis is verification of end-to-end compatibility between a MC3 ground station and the Mola CubeSat's X-band Software-Defined Radio (SDR), a payload designed and constructed through previous thesis research [1], [2], [3] with commercial off-the-shelf (COTS) hardware. The testing pursued in this study aims to find the required parameters, and associated software configurations, to achieve mission-ready interoperability between the payload SDR and commercial SDR receivers at the NPS MC3 ground station. Ultimately, verified parameters will be implemented for operational demonstration of the X-band SDR payload.

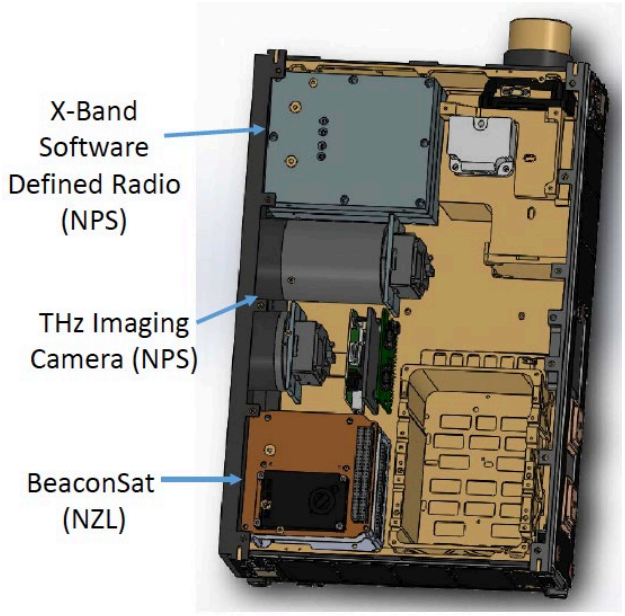

Figure 1. Mola preliminary payload configuration with SDR. Source: [4].

Though CubeSats have successfully utilized SDR technology on-orbit, X-band SDRs are a more recent and emerging endeavor for CubeSat communications. CubeSat developers have to balance communications systems with more stringent size, weight, and power (SWaP) requirements. Expanding the capacity of CubeSat communications technology to include X-band SDRs is advantageous for the Department of Defense (DOD) and space-faring entities of the United States. X-band SDRs offer enticing features such as greater bandwidth, higher data rates, advanced modulation schemes and increased resiliency against environmental interference such as attenuation. Additionally, this research contributes to the mission of continued International SmallSat Command and Control Network (ISC2N) ground station development and standardization for Five Eye (FVEY) partners [4]. The flight iteration of the Mola CubeSat, encompassing the X-band SDR payload, will help create future coalition advantages and substantially enhance CubeSat communications posture in an increasingly contested space environment.

A. CUBESATS

The term "small satellite" (SmallSat) signifies a satellite that weighs less than 300 kg. Cube satellites (CubeSats) are a distinct category of small satellites that follow specific standards for size, form factor and mass. CubeSat sizes are based on the standard unit "U." Approximately a 10 cm cube (10 cm x 10 cm x 10 cm) constitutes 1U with an associated mass of 1 to 1.33 kg [5]. CubeSats fall within the "nanosatellite" classification of small spacecraft, which have a mass between 1 to 10 kg, or 1U to 12U in CubeSat vernacular. Modern-day CubeSats typically conform to common sizes of 1U, 1.5U, 2U, 3U, 6U or 12U [6], as depicted in Figure 2 .

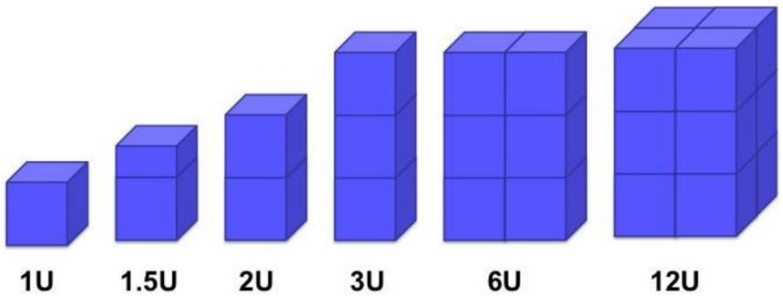

Figure 2. CubeSat standard sizes. Source: [6].

The CubeSat concept was initially forged in 1999 as a joint effort between professors at Cal Poly SLO and Stanford University's Space Systems Development Laboratory [7]. Originally intended for educational purposes by providing universities easier, quicker and cheaper access to scientific space exploration, today CubeSats serve a variety of functions and are capable of advanced missions. The standardized, streamlined components of CubeSats facilitate mass production and overall cost reduction for CubeSat developers. Accessibility, utility and cost-effectiveness fuels a CubeSat industry that attracts academic institutions, government organizations, private contractors and commercial companies alike. However, taking advantage of innovative CubeSat technologies does not occur without design trade-offs. CubeSats have shorter mission life, reduced maturity of onboard electronics, and less fuel storage for station-keeping requirements than the larger, exquisite, more expensive spacecraft. Conversely, short life expectancies give engineers the trade space to choose cheaper, less redundant COTS components. Condensed CubeSat development cycles provide the opportunity to evaluate designs more frequently and implement the latest technologies.

The CubeSat Design Specification (CDS) is an online resource maintained by California Polytechnic State University, San Luis Obispo (Cal Poly SLO) that outlines baseline CubeSat design and testing requirements. The purpose of the CDS is to safeguard CubeSat program missions and establish preliminary design criterion that optimizes spacecraft compatibility with available dispensers and launch opportunities [7]. Specifications contained within the current revision of the CDS include mechanical details such as acceptable center of gravity locations, and recommended placement for separation mechanisms and deployment switches. Ultimately, mission requirements related to the particular launch vehicle that gives a CubeSat its ride to space overrule the CDS.

A CubeSat typically receives its ride to space as a secondary payload on a launch vehicle (LV). For example, the Naval Postgraduate School's PropCube 3 ride-shared aboard an Atlas V LV in October 2015, with successful deployment into the desired orbit [8]. The CubeSat is mated to the LV with a sealed dispenser that provides protection and timely release when the vehicle achieves orbit [5]. Various dispensers exist on the market. The National Aeronautics and Space Administration (NASA) announced its CubeSat

Launch Initiative (CSLI) in 2010, offering CubeSat developers a low-cost deployment method via auxiliary payload launch opportunities [9]. In return NASA benefits from the scientific research, planetary exploration and/or technology demonstrations of its hosted CubeSats. Figure 3 shows the LVs utilized by CSLI for CubeSat launches. Through CSLI, NASA is able to leverage mutually-beneficial partnerships to foster collaborative technology advancement on par with the organization's strategic objectives. NASA celebrated its 100th CSLI mission on February 19, 2020, with the deployment of the Hyper-Angular Rainbow Polarimeter CubeSat from Northrup Grumman's 12th Commercial Resupply to the International Space Station (ISS).

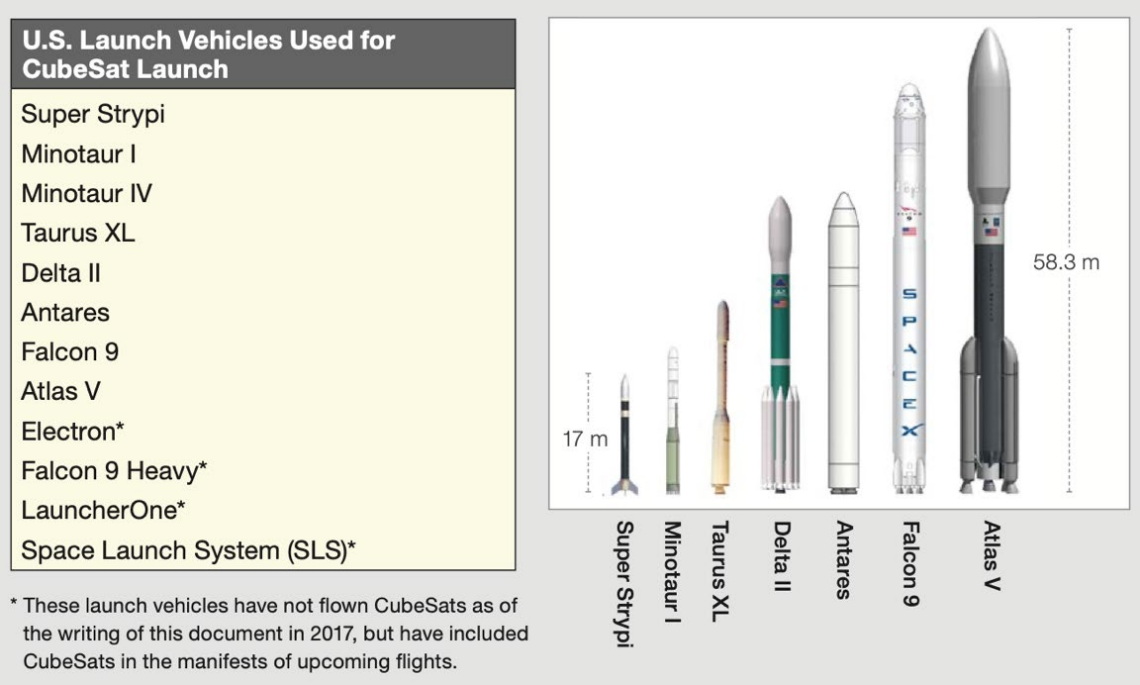

Figure 3. U.S. launch vehicles used for CubeSat launches. Source: [5].

B. MOBILE CUBESAT COMMAND AND CONTROL (MC3) X-BAND INITIATIVE

NPS collaborates with DOD and U.S. government missions, commercial enterprises, public universities and foreign partners to conduct CubeSat/SmallSat operations and research through the Mobile CubeSat Command and Control (MC3) ground

station network. The MC3 network is composed of multiple low-cost Remote Ground Terminals (RGTs) that are geographically dispersed across the United States [10]. NPS serves as the primary Network Operations Center (NOC), administering the network through its ground station node on campus in Monterey, California. At this time, MC3 ground stations utilize Ultra High Frequency (UHF) and S-band radio frequencies for command and control (C2) of small satellites in low-earth orbit (LEO).

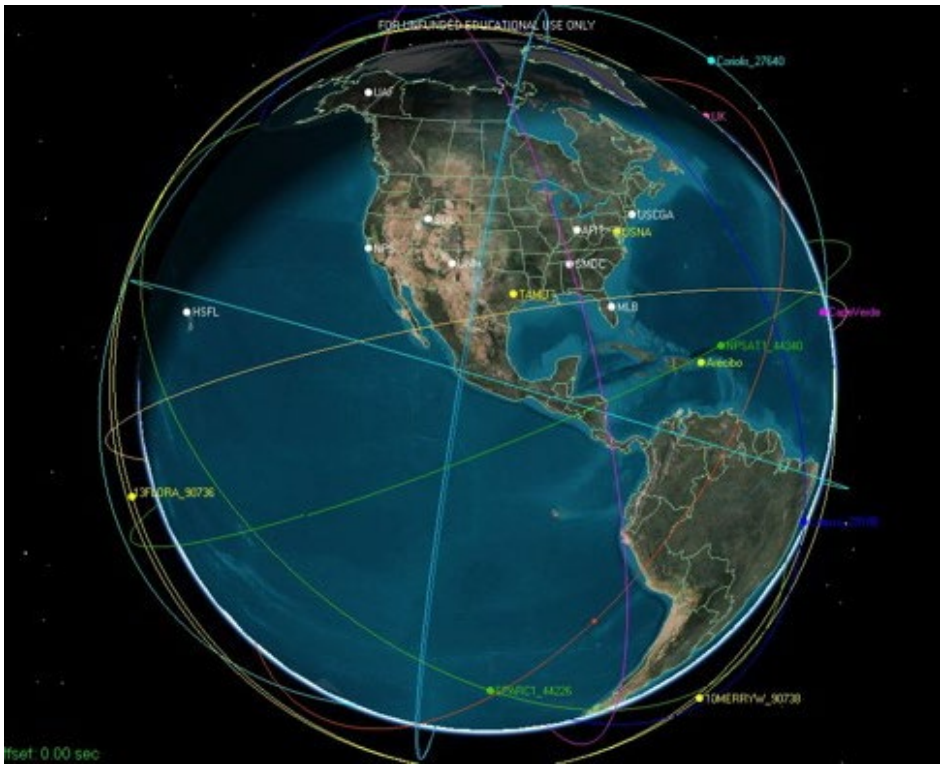

Figure 4. NPS MC3 network terminal snapshot. Source: [1].

The anticipation of increased data requirements for future spacecraft pointed MC3 research toward the support of higher bandwidth, X-band downlinks. The MC3 X-band initiative aims to increase capacity by adding X-band communications capability to the network. Specifically, the SSAG at NPS is attacking the objective of demonstrating low-cost X-band SDR technology for small satellites. As discussed in [11], research objectives of the X-band SDR include:

- 1U SDR payload made of COTS hardware and readily-available software.
- S-band uplink and X-band downlink.
- Line-of-sight (LOS) data transmissions.
- Compatibility with MC3 ground stations.
- Digital phase or frequency shift keying modulation.
- Data rate of 5 to 10 megabits per second (Mbps).
- Forward error correction coding.
- Bit error rate (BER) of less than 10E-5.

The AMERGINT satTRAC system was acquired for the MC3 ground station at NPS, a cutting edge SDR capable of receiving waveforms transmitted by X-band systems. This thesis work ensures the SSAG's X-band SDR can effectively communicate with the AMERGINT SDR, and/or with the currently-operational Kratos quantumRadio SDR, advancing the MC3 X-band initiative toward full fruition.

C. SOFTWARE-DEFINED RADIO (SDR)

Due to the flexibility that software technology offers over traditional hardware radio components, and considerably smaller supporting components for the field-programmable gate array (FPGA), the use of SDRs for CubeSat communications is becoming increasingly popular. Hardware radios enact pre-defined parameters, and are unable to adopt new schemes on-orbit. SDRs are attractive for space applications because of their ability to alter communication configurations on-orbit without the need to physically change hardware components on the satellite. A software-defined-radio is more agile in that it enables different modes, frequencies and modulations via software changes at the ground station. Replacing hardware equipment with software is also more favorable for meeting size requirements in small spacecraft design.

D. METHODOLOGY

The research, testing and analysis pursued in this thesis determined the radio frequency (RF) signal parameters and communications standards that enable successful transmission of data from the X-band SDR payload to the AMERGINT satTRAC SDR and Kratos quantumRadio SDR receivers. Simulation (through MathWorks Simulink models) and end-to-end testing was conducted, altering parameters to achieve a successful link from payload to ground station receiver. Varying communications configurations were attempted, with a focus on Quadrature Phase Shift Keying (QPSK) modulation, and the goal of establishing viable parameters for the flight iteration of X-band payload and subsequent functional 6U CubeSat. This thesis contributes toward final flight build and integration for the Mola CubeSat, currently slated for launch in late 2022.

THIS PAGE INTENTIONALLY LEFT BLANK

II. BACKGROUND

The following chapter provides relevant background material to properly frame the objectives, methods, testing and analysis pursued in this thesis. A brief expansion on MC3 components precedes a deeper dive into the science and technology behind digital communications. Next, a discussion on the principal devices behind this research (SDRs), and how link budget analysis drives procedures and system performance estimates, prepares the reader for later chapters on testing and results. Requisite information is provided to ensure clarity on the determination of parameters and software configurations for successful data transmissions between CubeSat payload SDR, and ground terminal SDR. This chapter concludes with an overview of the AMERGINT satTRAC system and Kratos quantumRadio SDR used in this research, in the pursuit of interoperability between the MC3 network and Mola's X-band SDR.

A. MC3 ARCHITECTURE AND MISSIONS

The Mobile CubeSat Command and Control (MC3) ground station network seeks to construct a common-use framework for the operations and communications of a variety of SmallSat missions. Established in 2012 to connect a handful of institutions designing SmallSats on behalf of the U.S. government, the MC3 network facilitated material and technology-sharing in a tight-budget research and development (R&D) setting [12]. The network now has nine active ground stations and three international partners (outlined in Table 1).

Table 1. MC3 ground stations. Adapted from [12].

Site	Location	Capability
Naval Information Warfare Center (PCH)	Pearl City, HI	UHF/S-band/X-band
Naval Postgraduate School (NPS)	Monterey, CA	UHF/S-band/X-band
Space Dynamics Laboratory (SDL)	Logan, UT	UHF/S-band
University of New Mexico/ Cosmiac (UNM)	Albuquerque, NM	UHF/S-band
Air Force Institute of Technology (AFIT)	Dayton, OH	UHF/S-band
US Coast Guard Academy (USCGA)	New London, CT	S-band
Malabar Transmitter Annex (MLB)	Palm Bay, FL	UHF/S-band
University of Alaska, Fairbanks (UAF)	Fairbanks, AK	S-band
Army Space and Missile Defense Command (SMDC)	Huntsville, AL	S-band/X-band

The MC3 network endeavors to give participants seamless access to, and effective operation of, their spacecraft [10]. Inherent in MC3 architecture is an emphasis on utilizing "COTS devices where possible to achieve a low-cost, yet reliable ground segment for small satellite missions" [12]. MC3 ground stations utilize SDRs and convenient, open-source, commercially available software (i.e., GNU Radio and MathWorks MATLAB) to bolster flexibility in communications waveforms and protocols. The AMERGINT satTRAC system employed with this thesis research joins the Kratos quantumRadio and National Instruments USRP-2922 as commercial SDRs presently in use at MC3 RGTs. The frequency ranges currently licensed to MC3 are shown in Table 2.

Table 2. MC3 frequency allocations. Adapted from [12].

Band	Frequency	Designator
UHF uplink	449.75-450.25 MHz	12K5F1D 43K0F1D
UHF downlink	902-928 MHz	115KG1D
S-band uplink	2025-2110 MHz	2M00G2D 2M45G1D
S-band downlink	2200-2290 MHz	1M60G1D 2M00G2D 2M45G1D
X-band uplink	7190-7250 MHz	(in progress)
X-band downlink	8025-8400 MHz	(in progress)

Additional critical capabilities of the network include the Satellite Agile Transmit and Receive Network (SATRN) software, fast-track radio licensing, and assimilation into cloud-based infrastructure [12]. SATRN is MC3's main software specified to handle CubeSat/SmallSat operations, and ensures interconnectivity between the autonomous, geographically separated network nodes. Operators dispersed throughout the network are able to control their satellites remotely through the virtual private network (VPN).

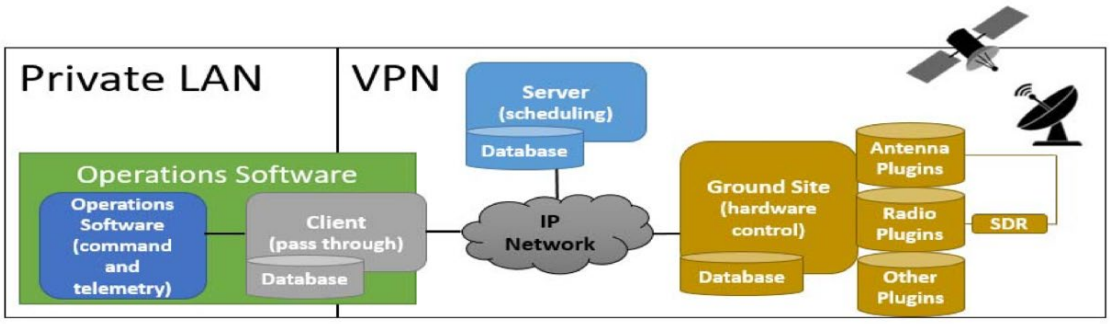

Figure 5. SATRN architecture. Source: [12].

B. MOLA SPACECRAFT

The MC3 network participates in a DOD-driven effort that charged NPS with producing two 6U CubeSats as orbiting test platforms for risk-reduction efforts. The Otter CubeSat will follow 6–9 months behind Mola, in order to effectively incorporate lessons

learned. With anticipated launches in 2022 and 2023, the Mola and Otter 6U CubeSats will support ISC2N ground station development, international payload-to-bus interface standardization, and demonstration of a FVEY federated space system by 2025 [4]. Through the research, design, and employment of these small spacecraft, the SSAG develops space-based capabilities in close coordination with international partners such as New Zealand.

Mola constitutes a multi-payload mission, including three additional payloads to the X-band transmitter of this thesis research. The X-band SDR payload will transmit imagery and functional data from the Terahertz Imaging Camera (TIC), a first of its kind payload demonstrating potential imaging capability in the terahertz (THz) range in the space environment. The third payload is the Korimako Beacon, a New Zealand R&D effort that measures the download capacity per ground station node [4]. Mola's fourth payload is a Passive Retroreflector, built by the Naval Information Warfare Center (NIWC). With an associated threshold objective of ground station coverage to the NPS and New Zealand sites, a mission requirement of the Mola project is to perform telemetry, tracking, and control (TT&C) and data distribution through MC3 and ISC2N ground stations. Mola's spacecraft design will utilize the Astro Digital Corvus-6 bus, which features several data interfaces and a 3U space to house the payloads, as shown in Figure 6. The proposed payload layout is depicted in Figure 7.

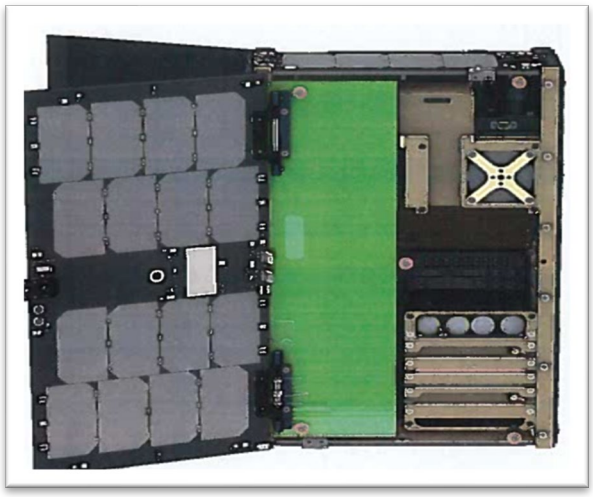

Figure 6. Astro Digital Corvus-6 bus with 3U payload space (green). Source: [1].

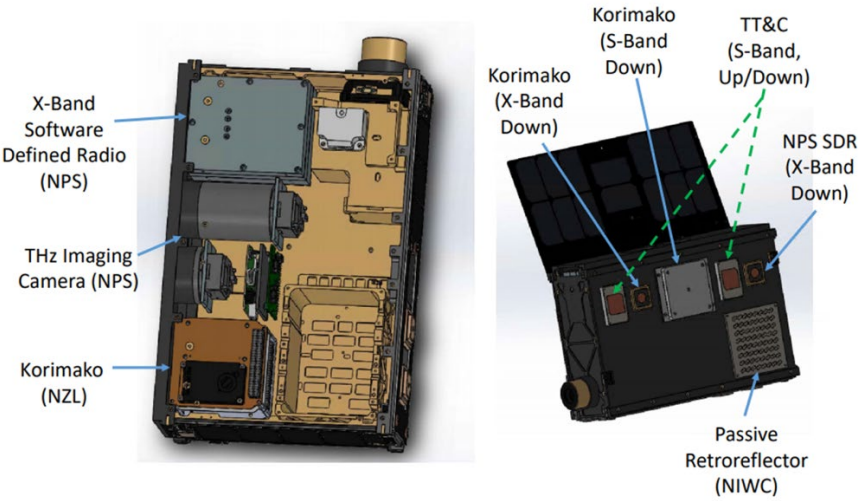

Figure 7. Mola payloads layout. Source: [4].

C. RADIO FREQUENCY

Maxwell's work in the field of electromagnetism, and the ensuing discovery of radio waves by Heinrich Hertz in 1886, profoundly impacted the evolution of modern-day communications [13]. Figures 8 and 9 illustrate where radio waves fall within the electromagnetic (EM) spectrum, accentuating the most readily recognized applications of radio frequency (RF) channels.

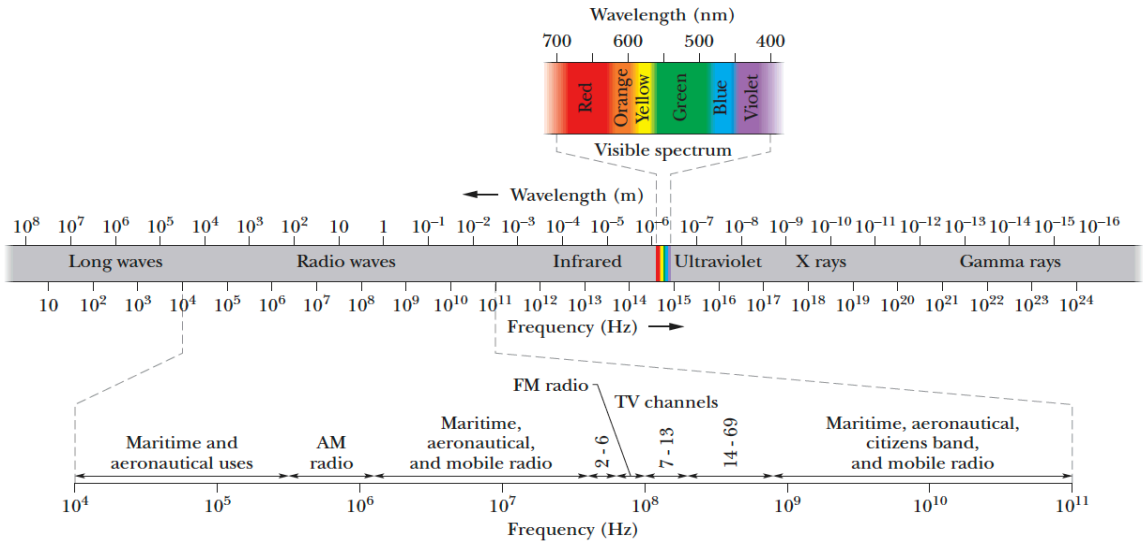

Figure 8. Electromagnetic spectrum. Source: [13].

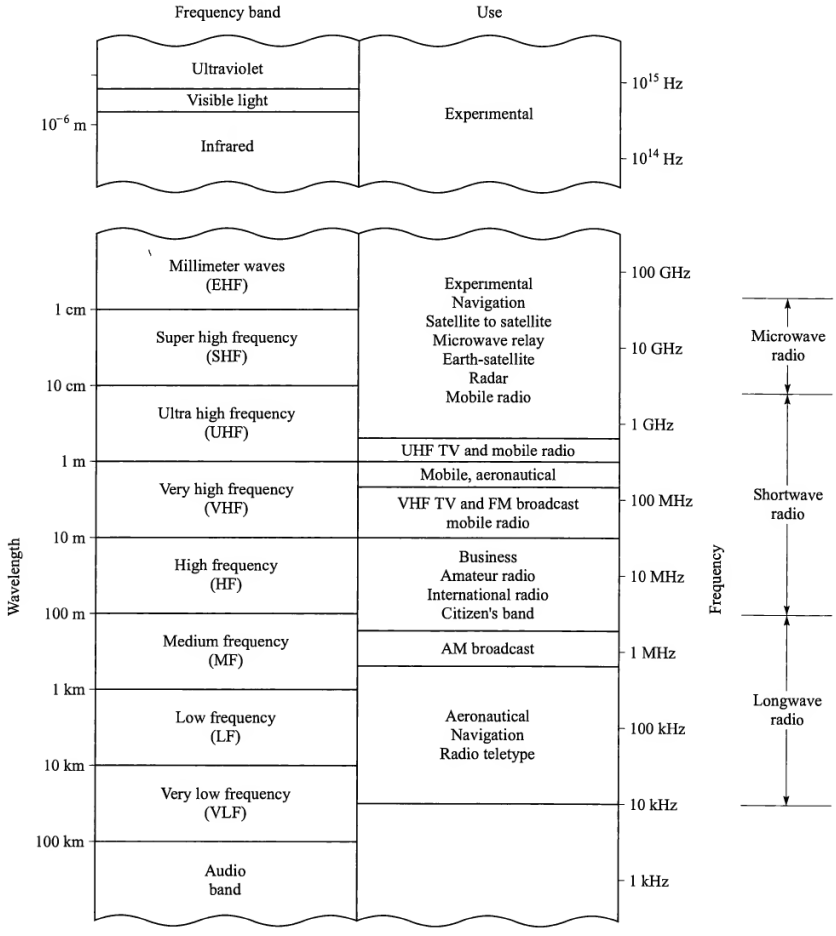

Figure 9. Radio frequency spectrum. Source: [14].

Radio waves propagate through free space by means of ground-wave propagation, sky-wave propagation, or line-of-sight (LOS) propagation [14]. This thesis research deals with LOS propagation, executing testing procedures that simulate the transmission of communication signals in a straight path from one antenna to another through the ionosphere, as a satellite passes over its ground station. An RF communication link utilizes a carrier signal, oscillating at a fixed frequency in a well-recognized sine wave pattern. The manner in which information is added to the carrier wave (i.e., modulation) will be discussed at length later on. The principal frequency bands of satellite communications (SATCOM) are ultra high frequency (UHF), super high frequency (SHF) and extremely high frequency (EHF), diagramed in Figure 9. The RF spectrum is further divided into narrower letter-designated bands, appropriated by the International Telecommunication Union - Radio communication sector (ITU-R) and the Institute of Electrical and Electronic Engineers (IEEE) [3]. Satellite system operations are conducted in bands L to Ka (see Figure 10). The X-band of the spectrum resides in the SHF region, at 8–12 GHz.

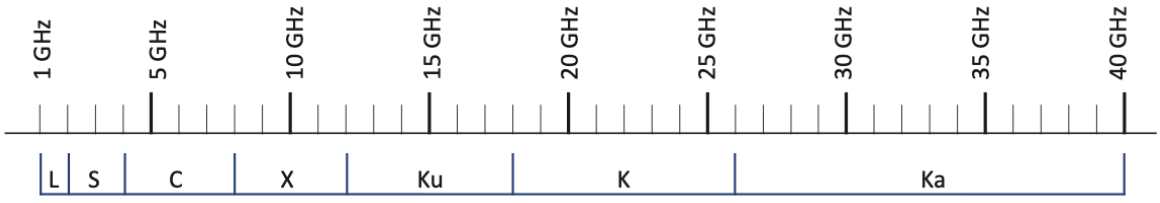

Figure 10. Radio frequency bands used for satellite communications links. Source: [15].

As frequency increases, wavelength of the radio wave shortens, creating more available bandwidth and information capacity on the carrier signal. A substantiated CubeSat form factor is leading to increasingly ambitious payloads and mission requirements, resulting in more data products and the subsequent need for higher space-to-ground data transmission rates. Through the MC3 X-band initiative and Mola CubeSat project, the SSAG is developing infrastructure that responds to this emerging need of the small satellite community. To achieve necessary throughput, the MC3 network seeks to establish an X-band communication capability, leveraged for downlink with Mola's X-

band SDR payload. The 8025–8400 MHz (8.025-8.400 GHz) frequency range was applied in design, assembly and testing of the X-band payload, in preceding thesis work [1]. This frequency range exists safely under 10 GHz, which is key for avoiding the frequent signal propagation losses caused by rain in the atmosphere for upper SHF frequencies [14].

In the United States, the task of radio spectrum regulation and frequency allocation is shared by two organizations: the National Telecommunications and Information Administration (NTIA), and the Federal Communications Commission (FCC). The NTIA administers spectrum for federal use, while the FCC handles non-federal applications [16].

D. DIGITAL COMMUNICATIONS

Communication signals are described as the physical embodiment of information transferred along a "channel" (physical medium or electromagnetic path between a transmitter and receiver). Communications channels may be comprised of "wires, coaxial cables, fiber optic cables, and in the case of RF, links, waveguides, the atmosphere, or empty space" [17]. Analog signals vary with time in a continuous manner (i.e., RF waves). Digital signals are discrete, predefined sequences of symbols (i.e., binary 1's and 0's) [18]. Electrical hardware and RF wave transmission channels are subject to noise, interference and distortion, so it is imperative that communications systems account for these signal disturbances. A digital communications receiver is capable of receiving a noise-perturbed signal and resolving which waveform was transmitted, correcting errors upon receipt [17]. An analog communications receiver, on the contrary, regenerates the transmitted waveform as is.

Digital radio systems receive analog RF signals and transform them into discrete digital signals through sampling, quantization and decoding. This process is reversed for radio transmissions. During digital radio transmission, information provided by the source undergoes a source encoding process, which creates a bit stream of binary digits representative of the original message [14]. This bit stream goes through a channel encoder, which introduces redundancy into the sequence that "can be used at the receiver to overcome the effects of noise and interference encountered in the transmission of the signal through the channel" [14]. In order to transmit from the antenna, the digital binary content

must be added to an analog RF carrier wave. The digital modulator performs this task. The particular modulation scheme employed by the modulator determines the power required for the transmission to successfully reach the receiver [19].

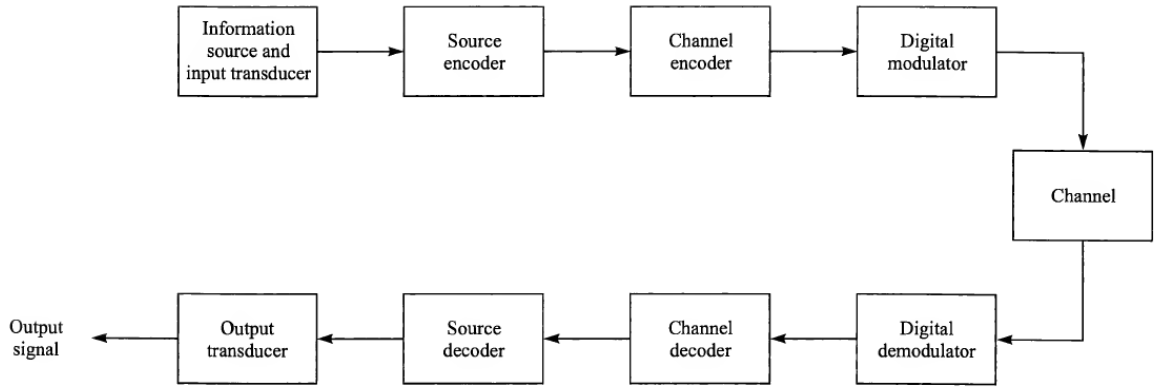

Figure 11. Basic elements of a digital communication system. Source: [14].

Signals propagated by a source transmitter are received by the destination receiver's antenna and converted to electrical signals. These weak signals are sent to the radio's RF front end (RFFE), which houses equipment that modifies the signal via amplification, down-conversion and filtering, prior to further processing by the RF back end (RFBE) [20]. The main components of a digital radio receiver system, listed in order of signal processing occurrence and depicted in subsequent figures, are:

1. *Low-noise amplifier (LNA).* Inside the RFFE, administers high voltage gain to amplify the signal with minimal noise contribution [21].
2. *Local oscillator.* Generates a complex sinusoidal waveform for mixing with the amplified signal.
3. *Sinusoidal mixer.* Mixes the signals to generate a lower carrier frequency, while maintaining original signal information content. Signal down-conversion is either to baseband (~ 0 Hz) or intermediate frequency (IF) (70-1200 MHz), depending on the radio technology [2].

4. *Low pass filter (LPF).* Filters the new signal to remove any inadvertently produced harmonic images [2].

5. *Analog-to-digital converter (ADC).* Digitizes the signal through sampling and quantization [21].

6. *Digital signal processor (DSP).* Extracts information content from the digitized signal for further translation to intended format (i.e., data, text, video, etc.) [20].

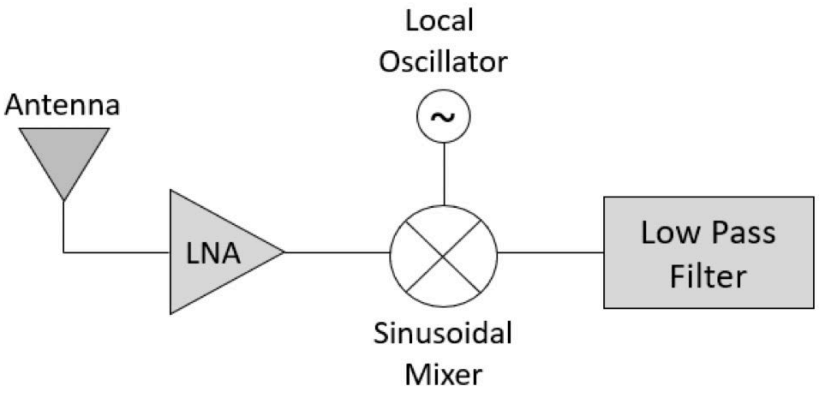

Figure 12. Digital radio RFFE components. Source: [2].

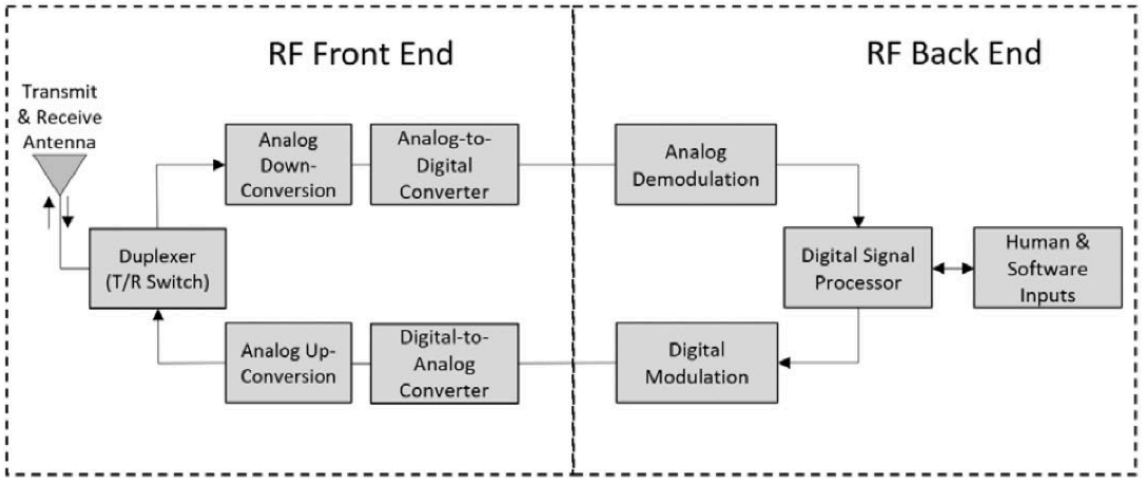

Figure 13. Example radio architecture with RFFE and RFBE functional areas. Source: [2].

A feature that distinguishes one digital radio receiver architecture from another is its method of received signal down-conversion. Direct conversion ("homodyne") receivers utilize a one-step process to down-convert a received analog RF signal into digital baseband. Super-heterodyne receivers perform two or more down-conversions [22]. This architecture first down-converts the received signal to an IF, then applies signal filtering again before conversion to baseband frequency. Advantages to super-heterodyne receivers include additional filtering opportunities to remove unwanted harmonic images, effective RF selectivity, and less internal noise interference and amplification [22]. The SDR receiver implemented in this thesis work, the AMERGINT satTRAC system, has a super-heterodyne architecture.

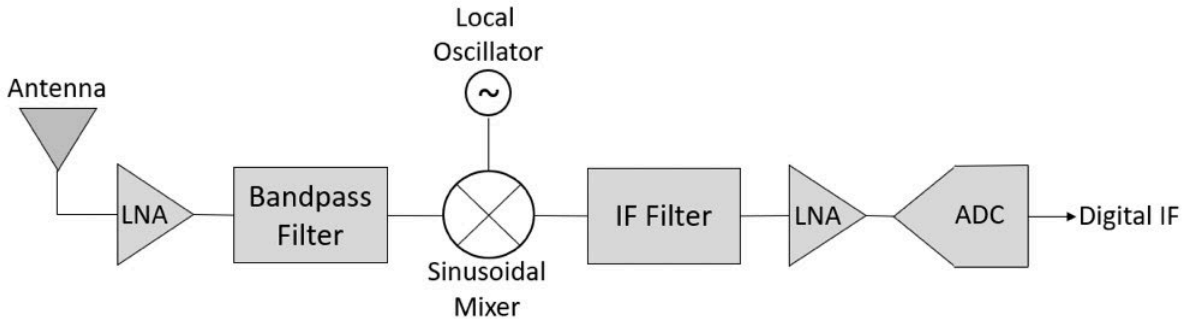

Figure 14. Super-heterodyne receiver diagram. Source: [2].

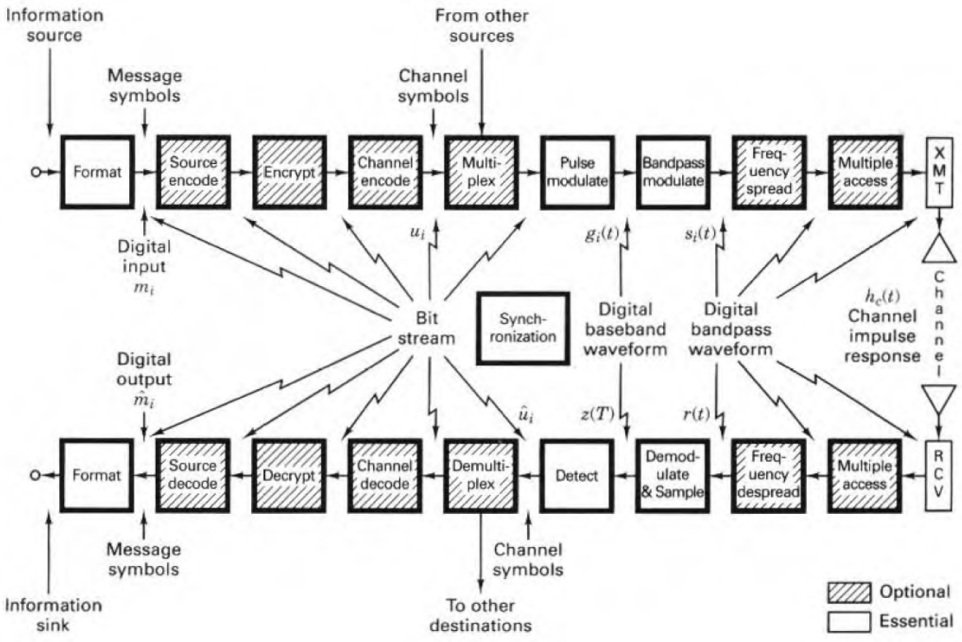

Figure 15. Block diagram of a typical digital communication system. Source: [17].

1. Modulation and Demodulation

Digital modulation is the process of altering the carrier analog signal to portray the data to be transmitted. Demodulation describes the reverse process, or the reconstruction of an analog waveform from the digitized signal. A modem (short for modulator/demodulator) can vary different features of the RF sine wave to capture the information content, for interpretation by a modem at the intended destination. Modulation techniques include amplitude shift keying (ASK), frequency shift keying (FSK), and phase shift keying (PSK). These techniques add data to a signal through variation of the waveform attributes designated in their perspective titles. The modulated parameter is keyed from one discrete value to another [18]. PSK is preferred for SATCOM due to its added protection against noise effects [23]. Binary phase shift keying (BPSK) is one of the least complicated modulation schemes, encoding bits through 180° phase shifts, portrayed for visualization in Figure 16 [15].

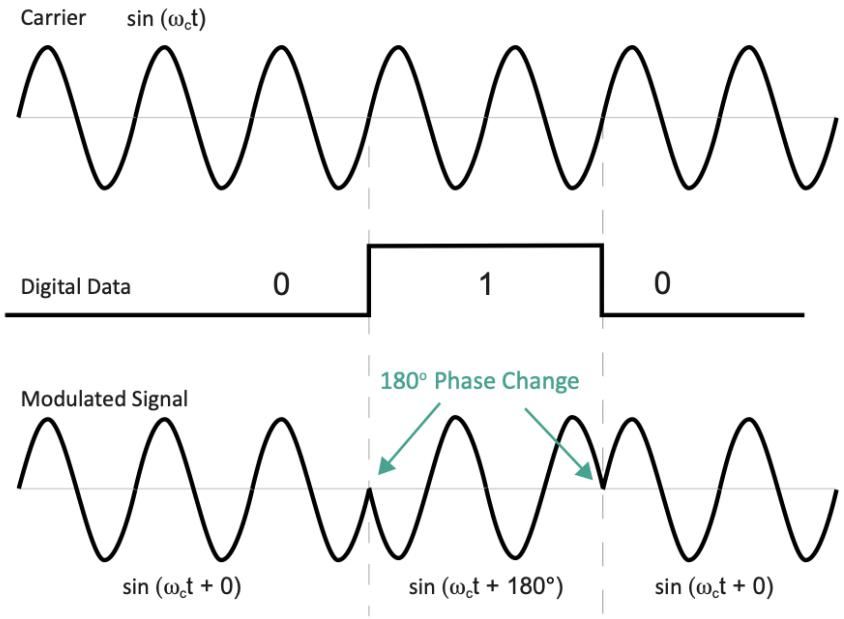

Figure 16. BPSK modulation. Source: [15].

This thesis research aimed to test and establish links between Mola's X-band SDR and MC3's AMERGINT SDR that employed quadrature phase shift keying (QPSK) modulation methods. In QPSK modulation, the phase of the carrier signal shifts to one of four possible positions (45°, 135°, -45°, or -135°). Each position, or symbol, represents two bits [24]. Figure 17 illustrates these quadrature bit positions in a constellation diagram, and Figure 18 shows what the modulation looks like on the waveform. QPSK modulation has the potential to double the possible data rate, a valuable option for X-band communications.

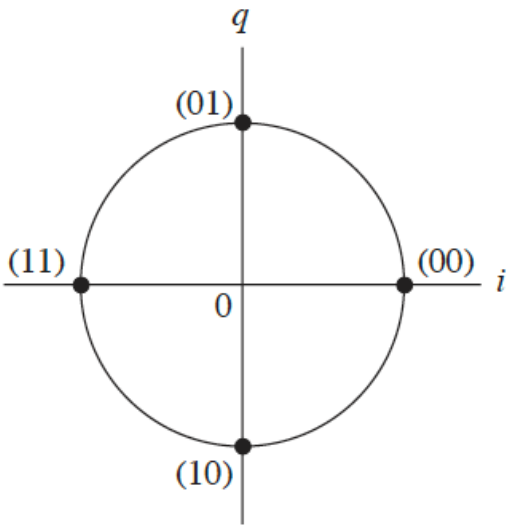

Figure 17. QPSK signal constellation. Source: [18].

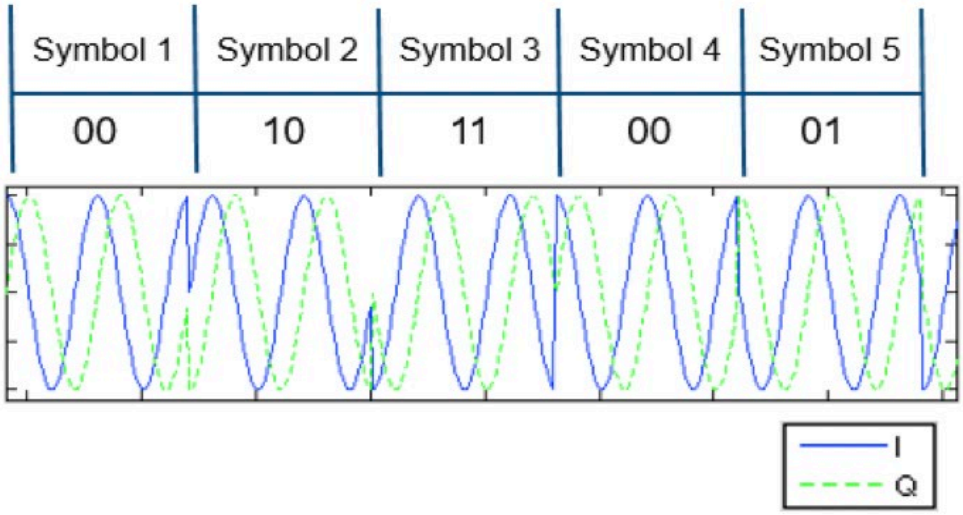

Figure 18. QPSK modulation. Source: [24].

IQ constellation diagrams are graphical representations of demodulated signals. Each point denotes one demodulated symbol, where the x-axis is the amplitude of the I (in-phase) channel and the y-axis is the Q (quadrature) channel output [25], [26]. A QPSK modulator partitions the incoming bit stream into I and Q channels [25]. The IQ diagram should match the constellation diagram of the particular modulation being applied to the signal. Figure 19 provides a screenshot of an IQ plot from AMERGINT satTRAC's user

interface during a QPSK loopback test, and may be compared to Figure 17 for emphasis. The distance between points signifies the error probability of the signal, and adding more power increases the distance between points (see Figure 20) [24]. IQ diagrams are highly useful for system troubleshooting because they allow the radio user to visualize properties such as "modulation type, signal-to-noise ratio, carrier lock, symbol lock, carrier phase offset, and symbol jitter" [26].

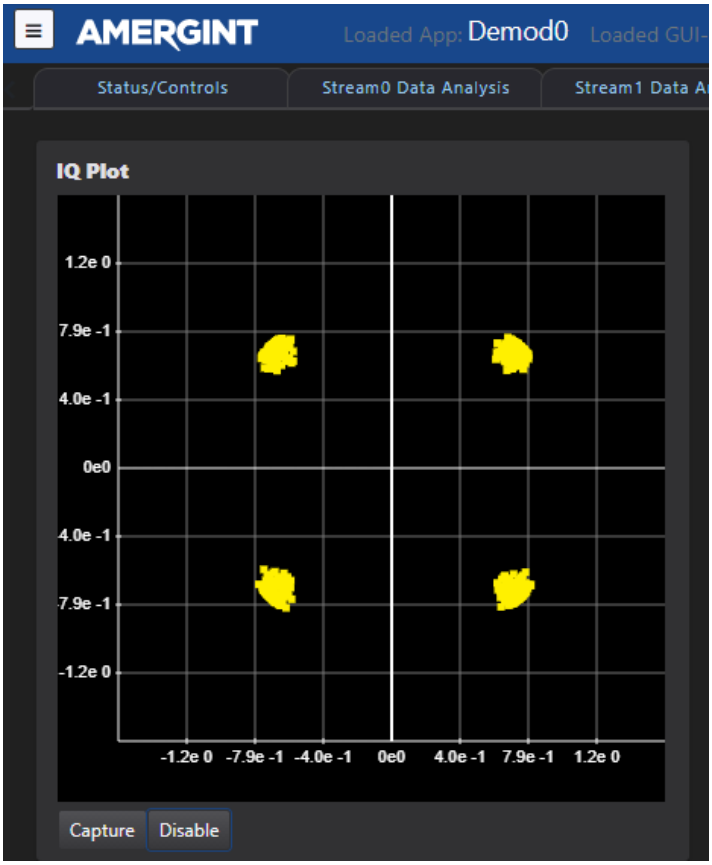

Figure 19. IQ plot screenshot. Source: AMERGINT satTRAC user interface.

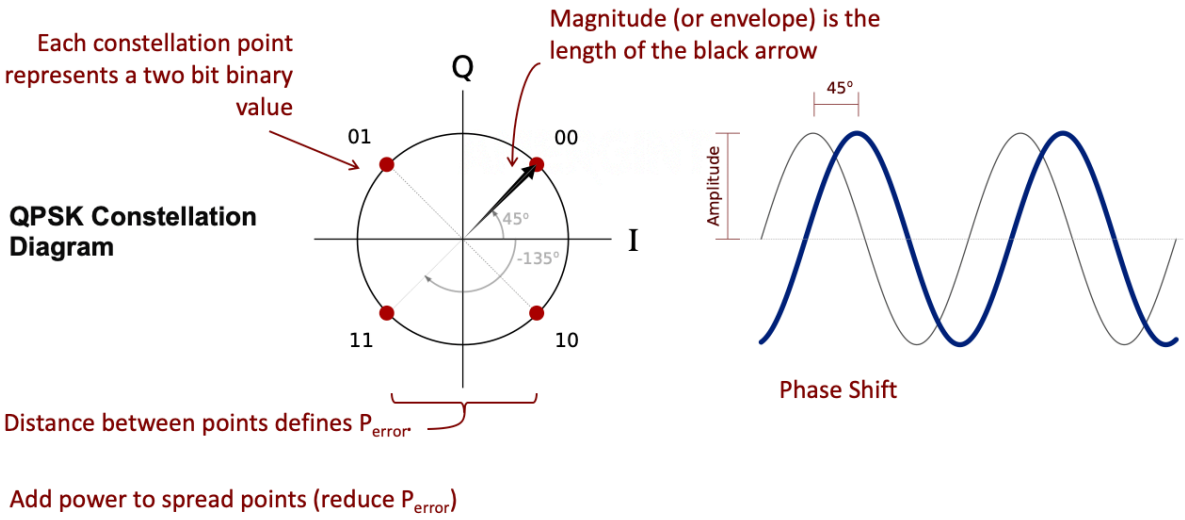

Figure 20. QPSK constellation diagram, detailed. Source: [24].

2. Sampling and Quantization

In [27], sampling is defined as the "conversion of a continuous-time signal into a discrete-time signal obtained by taking the samples of the continuous-time signal at discrete-time instants." The minimum sampling rate (or frequency) is called the Nyquist rate, equal to twice the bandwidth of the signal. Sampling above the Nyquist rate is ideal because it allows for errorless reconstruction of the signal from the spectrum samples taken [27]. Sampling above the Nyquist rate creates favorable guard bands that provide space for low pass filter implementation [18]. Equation (1) portrays this proper sampling frequency (f_s) according to the Nyquist sampling theorem, based on signal bandwidth (W) [18].

$$f_s \geq 2W \tag{1}$$

Conversely, an under sampled signal at a frequency below the Nyquist rate leads to samples with spectral overlapping, referred to as aliasing [27]. In this case, content from the original signal is cut-off and incomplete, thus preventing full signal reconstruction. Figure 21 depicts the spectra resultant of the described sampling scenarios. In a digital radio system, the sampling rate also drives system bandwidth (i.e., the highest input frequency that the system can handle and process) [2].

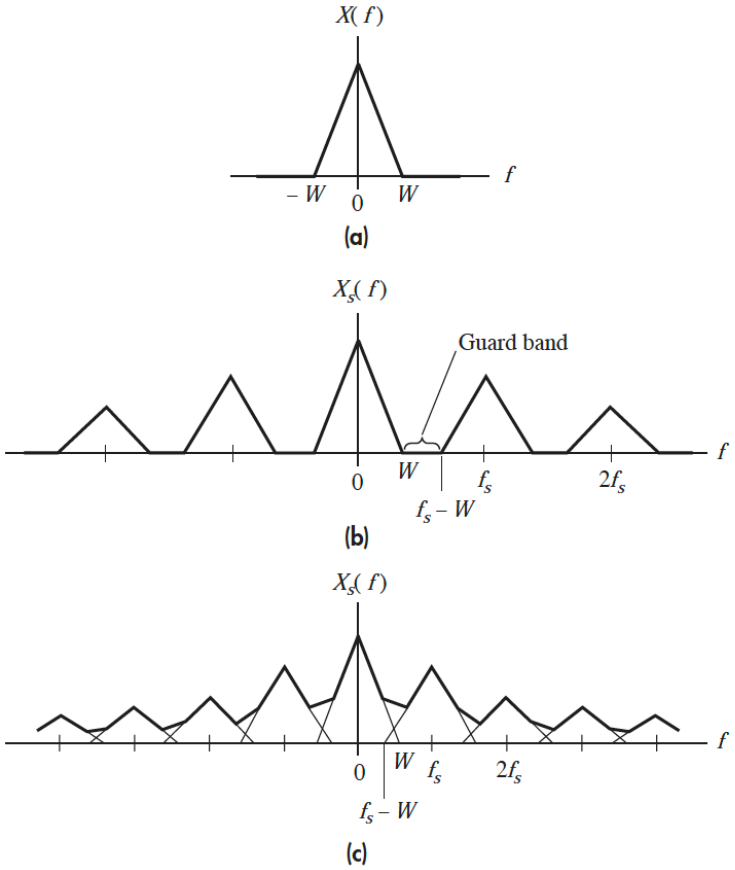

Figure 21. Sampling spectra: (a) signal, (b) proper sampling, (c) under-sampled aliasing. Source: [18].

After samples are collected from the signal, the digitization process continues through quantization, whereby captured spectra values are converted into discrete digital values via the ADC [27]. The bit resolution of the ADC determines the number of bits used to digitize an analog signal.

E. SOFTWARE-DEFINED RADIOS

The Wireless Innovation SDR Forum, in conjunction with the IEEE, defines the software-defined radio as a "radio in which some or all of the physical layer functions are software defined" [28]. Grayver [20] describes SDRs as "a class of reconfigurable/reprogrammable radios whose physical layer characteristics can be significantly modified via software changes." Prior to the 1980s, most wireless

communication systems were designed via fixed, hard-wired models, utilizing technologies like application-specific integrated circuits (ASICs) [29]. Technological advancements in digital processing, and digital-to-analog (D/A) and analog-to-digital (A/D) conversion, enabled radio functions that were typically fulfilled by hardware components to instead be performed by software. The implementation of software adds versatility, size reduction, and robustness to wireless communications systems. Additionally, in lieu of changing the physical hardware to enact different waveforms, this may be accomplished by reprogramming the software/firmware of the SDR. In the context of space applications, software changes are done by operators at the ground station, eliminating the need to physically alter equipment on the spacecraft itself in order to achieve the same effect. Wyglinski outlines several key characteristics of the SDR platform in the following list:

- *Multifunctionality*: Possessing the ability to support multiple types of radio functions using the same digital communication system platform.
- *Global mobility*: Transparent operation with different communication networks located in different parts of the world (i.e., not confined to just one standard).
- *Compactness and power efficiency*: Many communication standards can be supported with just one SDR platform.
- *Ease of manufacturing*: Baseband functions are a software problem, not a hardware problem.
- *Ease of upgrading*: Firmware updates can be performed on the SDR platform to enable functionality with the latest communication standards. [29]

In [20], Grayver expands on two additional advantages of the SDR: lowered costs and "reduced obsolescence (future-proofing)." Lower overall material and manufacturing costs further expands the utility and applicability of SDRs to multiple markets. Future-proofing refers to the SDR's ability to keep pace with the "cutting-edge," so to speak. Inherent in the ingenuity of SDR technology is an ability to adapt to the latest communication practices and requirements. The reconfigurable/reprogrammable characteristic protects an SDR from becoming antiquated, a valuable feature that is "especially important to radios with long life cycles such as those in military and aerospace applications" [20].

SDRs are characterized as radios that perform received signal digitization at a phase downstream from the antenna (and vice versa for transmitted signals). Digitization customarily follows wideband filtering, low noise amplification of the received signal, and down-conversion to a lower frequency [22]. Down-conversion to baseband is accomplished through analog mixers and/or a digital signal processor (DSP). An SDR uses software to establish baseband radio features such as error correction coding and modulation. Digital signal processing occurs via flexible and reconfigurable functional blocks [22]. Pertinent radio modules/design options may be stored in memory and activated when a particular functional block is required to provide communications [20]. Through automation or human operator, communication parameters can be altered in real-time. RFFE operations (i.e., transmission carrier frequency) are also administered via software.

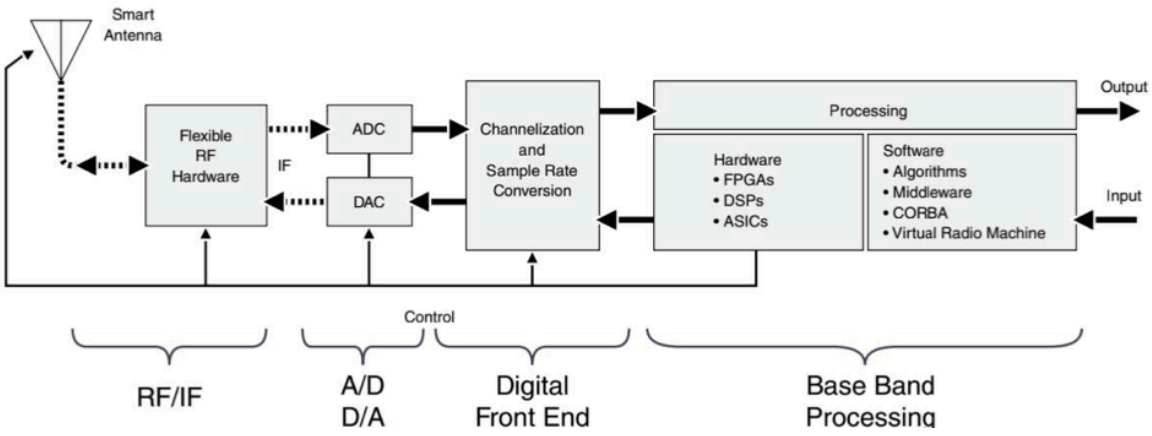

Figure 22. Block diagram of SDR transceiver. Source [30].

F. LINK BUDGET ANALYSIS

The "link" describes the complete communications path from information source to destination, inclusive of all the encoding, modulation, and signal processing steps, from transmitter through the channel to the receiver [17]. Link analysis encompasses calculations of the gains and losses affecting an RF signal, comparing signal power to noise power. The product of such analysis is the link budget, an invaluable estimation technique for determining communication system performance. The link budget is used to discern

system trade-offs, understand interdependencies, and mathematically account for various noise sources and system processes [17].

1. Equations

The basic link budget equation for received signal power is given as [19]

$$P_{Rx} = P_{Tx} + G_{Tx} + G_{Rx} + L_{Tx+Rx} \tag{2}$$

The variables, typically expressed in decibels (dB), are defined as follows: received signal power (P_{Rx}), transmitted signal power (P_{Tx}), transmit antenna gain (G_{Tx}), receive antenna gain (G_{Rx}), and total losses (L_{Tx+Rx}). The total losses figure includes all losses associated with the radio equipment (i.e., line losses and antenna pointing losses), free space dispersion, and signal propagation through the atmosphere [19]. Losses hinder the power of the signal, and are therefore subtracted. Gains, which conversely enhance the power of the signal, are added. Free space loss (L_S) is the largest contributing loss factor, calculated using separation distance between antennas in km (S), and signal frequency in GHz (f). Free space loss is calculated as shown in Equation (3) [19]

$$L_s = 92.45 + 20\log(S) + 20\log(f) \tag{3}$$

Gain describes the way antennas amplify signals. Antenna gain is the result of concentrating the isotropic RF. For parabolic reflector antennas, gain can be expressed as a function of antenna efficiency (η), diameter (D), and signal frequency (λ), as follows [19]

$$G = \eta\left(\frac{\pi D}{\lambda}\right)^2 = \eta\left(\pi D\frac{f}{c}\right)^2 \tag{4}$$

Or translated to dB format, where frequency (f) is in GHz:

$$G = 20.4 + 20\log(f) + 20\log(D) + 20\log(\eta) \tag{5}$$

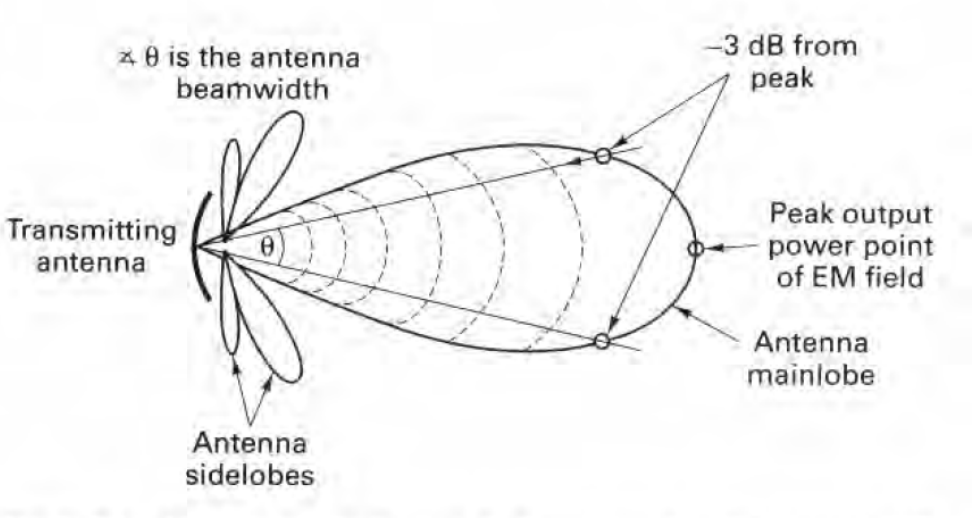

Figure 23. Antenna gain generation. Source: [17].

The broad definition of noise is any in-band EM energy generated from sources outside of those designed to positively support the communications link [19]. Though various sources of noise have the potential to impair a communications signal, early link analysis for SATCOM antennas focuses on estimates of antenna noise temperatures and/or RF losses within antenna feed equipment. Sklar explains in [17] that overall noise can be calculated from Boltzmann's constant (κ), system temperature ($T°$), and signal bandwidth (W). In the context of link equations, overall noise (N) is given in [17] as

$$N = \kappa \times T^{\circ} \times W \quad (Watts) \tag{6}$$

The signal-to-noise ratio (SNR) describes the ratio of signal strength to signal noise. In digital communications, the ratio of energy per bit to noise density (E_b/N_0) is more often used, especially when considering bit error rate (BER) prediction. E_b/N_0 is defined as the "value of bit energy per noise power spectral density required to yield a specified error probability" [17]. Both the SNR (S/N) and E_b/N_0 are unitless figures of merit calculated via the following equations

$$\frac{S}{N} = \frac{P_t \times G_t \times G_r}{L_s \times \kappa \times T^{\circ} \times W} \quad (unitless\ ratio) \tag{7}$$

$$\frac{E_b}{N_0} = \frac{P_t \times G_t \times G_r}{L_s \times \kappa \times T^{\circ} \times R_b} \quad \left(unitless\ ratio\right) \tag{8}$$

$$E_b \Big/ N_0 = P_t + G_t + G_r - L_s - \kappa - T^{\circ} - R_b \quad \left(db\right) \tag{9}$$

Link margin calculations, using Equation (10), reveal the amount of safety margin above what is required for a successful link. The link margin equation determines the difference between the required E_b/N_0 and the achieved E_b/N_0. A positive link margin indicates a closed link (i.e., the signal is detected by the receiver). A negative link margin indicates an unsuccessful link.

$$M = \left(\frac{E_b}{N_0}\right)_{achieved} - \left(\frac{E_b}{N_0}\right)_{required} \tag{10}$$

2. Bit Error Rate (BER)

When it comes to system performance, the ability to successfully detect signals in the presence of noise, with tolerable error probability (message quality), is of paramount interest to the radio user [17]. The Bit Error Rate (BER) is the dominant performance metric for communications links. BER of a digital RF receiver system, with digital modulation, is defined as the probability that a bit traversing the receiver system is received in error (i.e., the odds that a logical "1" bit is received incorrectly as a logical "0" bit) [31]. During BER testing (BERT) of a receiver system, the BER is described as "the percentage of erroneous bits received divided by the total number of bits received" [31]. BER is inversely proportional to SNR. As a signal is disrupted by noise or interference, the SNR decreases, thereby increasing the BER. Digital communication systems have distinct required BER values, which facilitate the achievement of intelligible signals.

Probability of bit quantization errors increases as bit energy (E_b) decreases and approaches the associated noise level of a communications link [19]. Quantization error is directly proportional to the number of bits per symbol, for a fixed E_b. Given a specific modulation scheme and coding rate, BER may be anticipated as a function of the E_b/N_0

[19]. Estimated BER vs E_b/N_0 graphs are a useful tool for link analysis. The curves depicted in Figure 24 enable prediction of the specific E_b/N_0 required to support a desired BER, for a particular modulation.

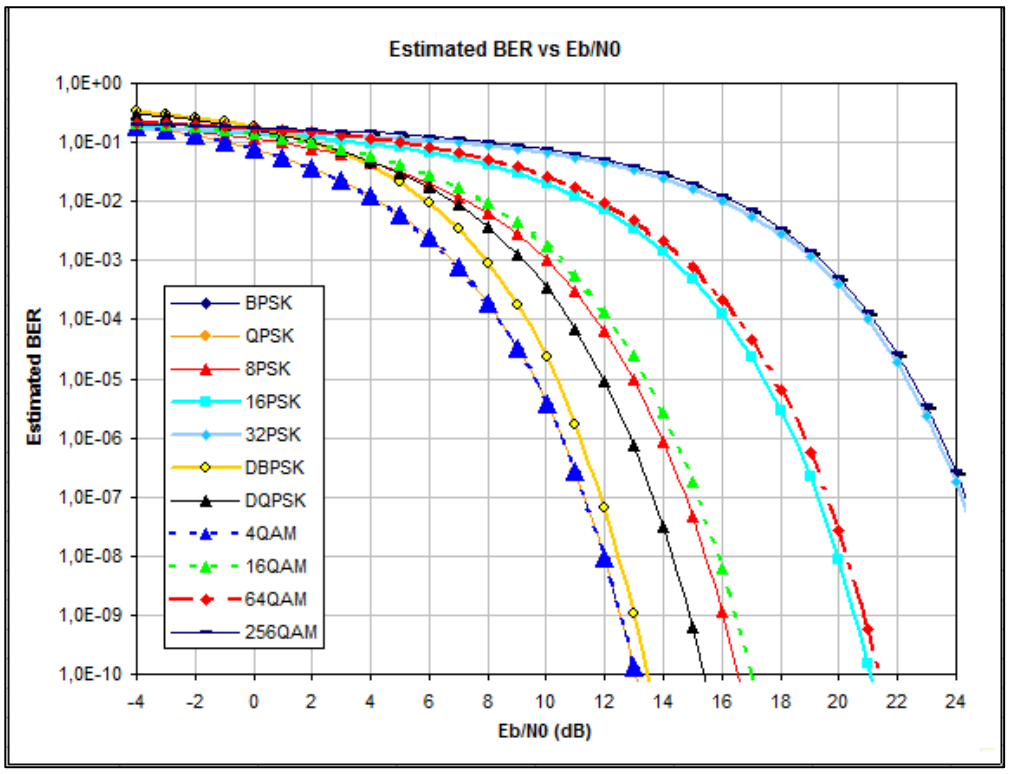

Figure 24. Predicted BER curves as a function of E_b/N_0. Source: [32].

G. GROUND STATION RECEIVERS OVERVIEW

The following section describes the two radio receiver test-subjects of this research, the AMERGINT satTRAC and Kratos quantumRadio SDRs. The AMERGINT system is a new addition to MC3 network efforts, acquired in support of the SSAG's objective of demonstrating low-cost X-band SDR technology for CubeSats. The Kratos SDR, on the other hand, is already operational at MC3 ground stations, effectively enabling C2 for various small satellite missions (though not yet through X-band downlinks). Thesis research objectives sought to establish the successful transmission of data from Mola's X-band SDR payload to both (or at least one) of the designated receivers, while comparing performance and utility.

1. AMERGINT satTRAC System

AMERGINT Technologies advertises the satTRAC Modem/Baseband unit as a high-performance software modem with configurable user interfaces, built-in testing, published open interfaces, and reliable customer support [33]. The AMERGINT satTRAC system is capable of supporting all commonly used frequencies/waveforms for payload downlinks and TT&C of small satellites. The modem features configurable RF bands, softFEP applications for implementation of all modulation/demodulation and baseband processing functions, and narrowband and wideband data rates [34]. The satTRAC SDR consists of a Signal Converter RFFE, a software-defined modem RFBE on a Dell R740 server, and AMERGINT's SOFTLINK Product Architecture (i.e., softFEP software applications); interfaced via a standard 1GB ethernet connection. A block diagram of the entire transceiver chain is provided in Figure 25.

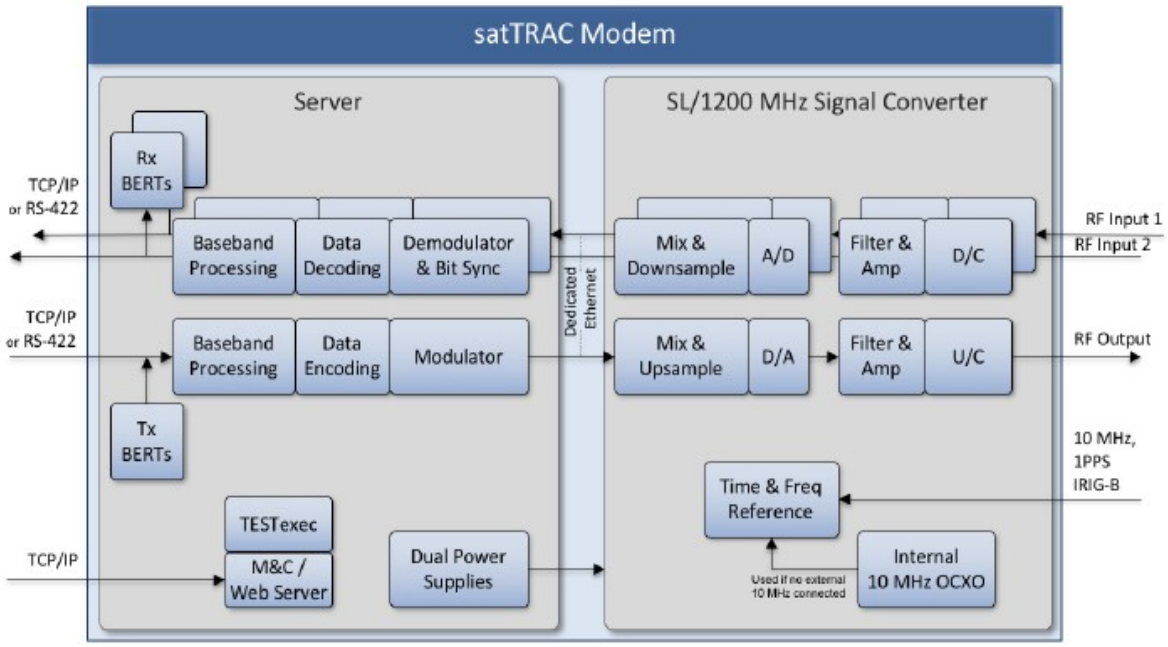

Figure 25. AMERGINT satTRAC system functional block diagram. Source: [26].

The satTRAC Signal Converter (Figure 26) performs the SDR's analog transmit and receive roles, and is managed through the softFEP applications. Signal conversion

technology “conditions, filters, down converts, samples, and decimates to a digitized IF over Ethernet” [34]. As a heterodyne receiver architecture, the satTRAC SDR down-converts received analog signals into a 70 MHz IF prior to digital sampling. Next, samples are digitally translated down to baseband frequency. The applied process resists analog image generations that could negatively impact the received SNR [2]. Baseband data is routed to the selected modulator (QPSK or BPSK, for example) and subsequently converted to RF data before transmission.

Figure 26. Depiction of satTRAC signal converter front plate. Source: [26].

The satTRAC system’s general functions are summarized in the following list:

- BPSK, QPSK command and telemetry modulation.
- Command and telemetry demodulation data is sent via TCP/IP, and/or to an Rx BERT.
- Bi-Phase L, NRZ-L, NRZ-M, and NRZ-S PCM encoding and decoding.
- Bit Error Rate (BERT) transmit and receive, with selectable PN patterns.
- Rate 1/2 convolutional encoding and decoding.
- External frequency reference, 10MHz.
- **Web-Based User Interface:** The system has a user-configurable UI for standalone operations. The UI runs in a web browser window, enabling the system to be controlled remotely. Users can change labels, add/delete fields and widgets, and change the conditional logic under status fields and indicators.
- **Software Application Programming Interface:** A software API allows customers to support the system from their monitor and control application. The system uses the Ground Equipment Monitor Standard (GEMS) for this interface. [26]

The manufacturer boasts the following key performance metrics of the satTRAC modem:

- **Spectral Purity:** High compression points and multi-rate digital filtering insure NTIA compliance. That means < -65 dBc.
- **Noise Figure (Receiver):** The noise figure targets high performance test and measurement applications, exceeding most ground station needs.
- **Implementation Loss (BER):** The measured implementation loss for satTRAC is well below 0.7 dB across a typical Eb/N0 range, often within 0.25 dB of theory.
- **Output Power Range:** satTRAC's outputs have an accuracy of better than 0.5 dB over the output power range and over the specified temperature range.
- **Dynamic Range:** An instantaneous dynamic range of 80 dB enables multi-carrier reception on a single RF/IF input. [33]

AMERGINT's softFEP applications are accessed through the graphical user interface (GUI). The system's "Modem Overview" window allows the user to control and/or discern how data is flowing through the SDR. Visually represented in flow diagram fashion, the component blocks, arrows and status indicators show data movement through the system. Figure 27 pictures an example "Modem Overview" interface. The user may click on displayed components to "select the desired uplink and downlink modes, configure the modem parameters affecting these modes, and generate/acquire the command and telemetry data" [26]. Green indicators signify that data is flowing, while gray indicates that no data is flowing. The flow of data can be started, stopped and routed through the drop-down boxes. The satTRAC transceiver features an internal spectrum analyzer to effectively measure noise density and band power, identify a signal's peak, and make marker-delta measurements. Another valuable tool built into the system is an IQ constellation diagram (i.e., a graphical representation of the demodulated received signal). Both of these tools may be accessed by clicking on the appropriate components of the "Modem Overview" window.

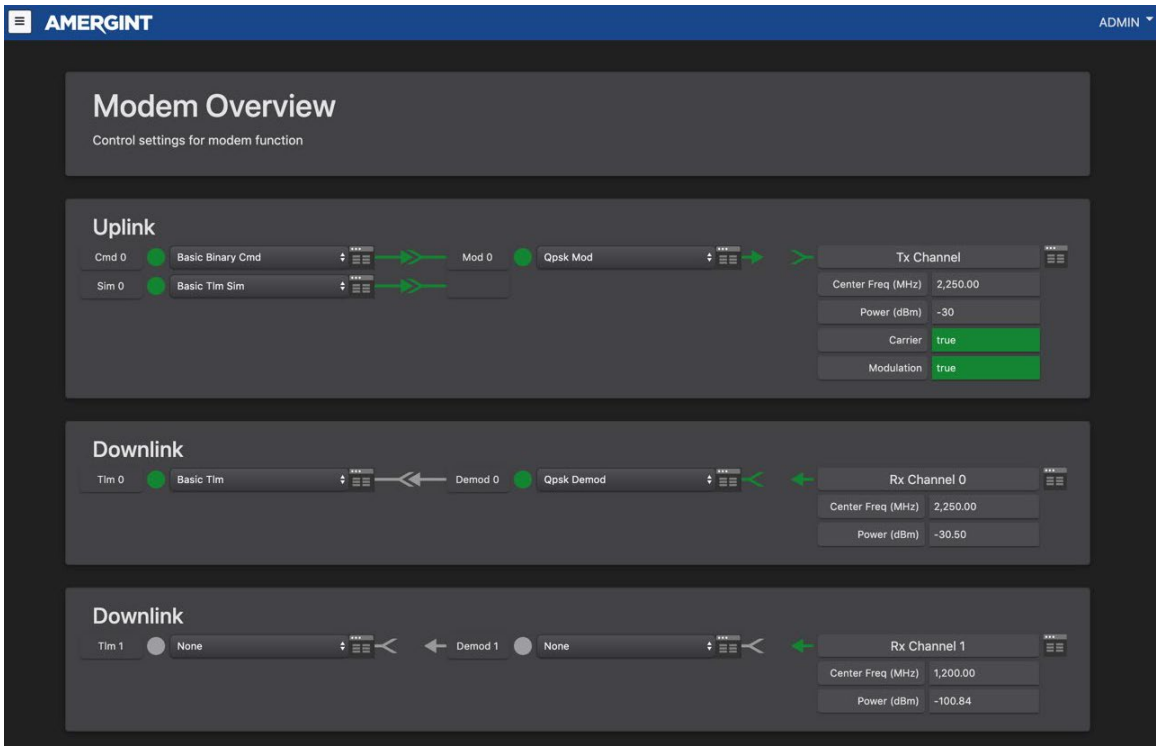

Component/App	Description
Cmd	Control and status the command data to be transmitted.
Sim	Control and status the simulated data to be transmitted.
Mod	Control and status the modulators.
Tx Channel	Control and status the outgoing signal.
Rx Channel	Control and status the incoming signal.
Demod	Control and status the demodulators.
Tlm	Control and status the telemetry processors.

Figure 27. Modem overview with component descriptions. Source: [26].

Figure 28 presents an overall block diagram showing the integration of softFEP applications to form the satTRAC SDR. The bottom half receiver components are of most interest to this thesis research, for the satTRAC equipment was acquired by NPS to function as a ground station receiver for future CubeSats of the MC3 network. “Rx In” interfaces

with the Signal Converter receive ports, “Demod” receives the digital samples and defines modulation type and anticipated data rate, and “TLM” receives the demodulated bits and provides further processing [2].

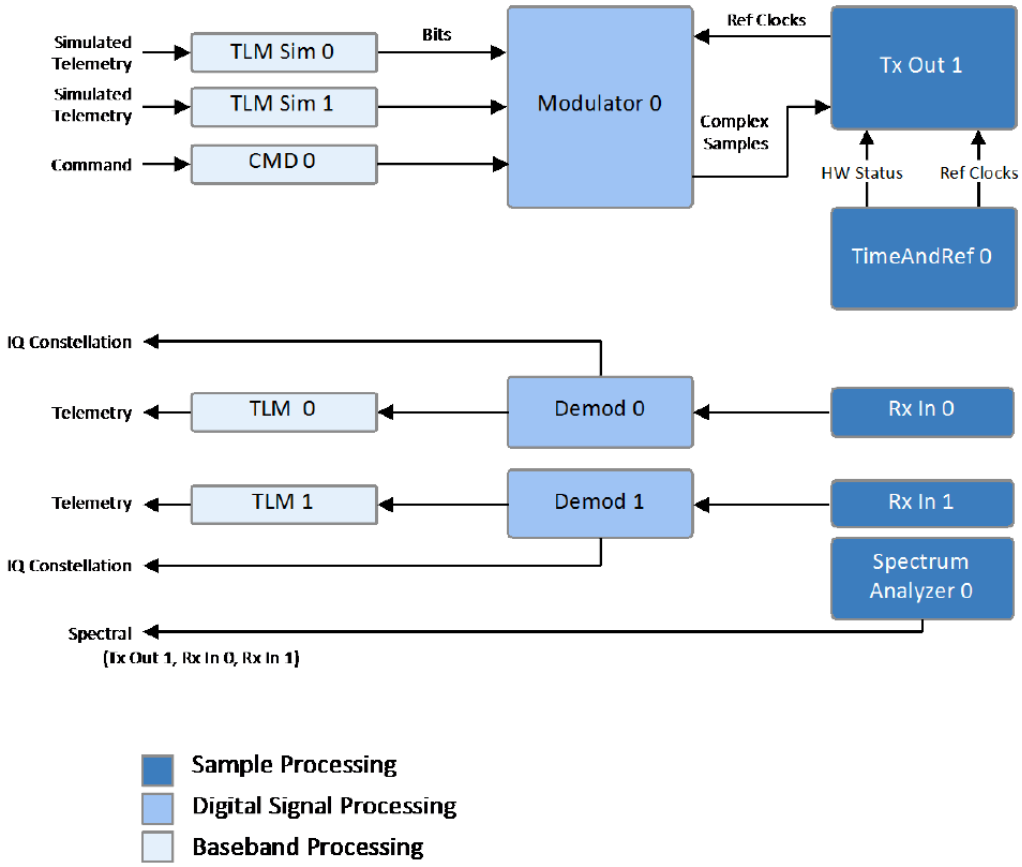

Figure 28. Modem operations block diagram. Source: [26].

Additional SDR parameters can be altered through the “Software Devices (SwD) Overview” module. The user is able to search for available softFEP applications by name and open up parameter characteristics for viewing and editing. Figure 29 captures a snapshot of the SwD Overview screen, in this case depicting the characteristics of the Received Bit Error Rate (RxBERT) module. The “App Manager” screen offers an additional way for a user to easily monitor application statuses. The various applications are listed, color coded, and accessible through simply clicking on an application name to open the user interface for a specific app (see Figure 30).

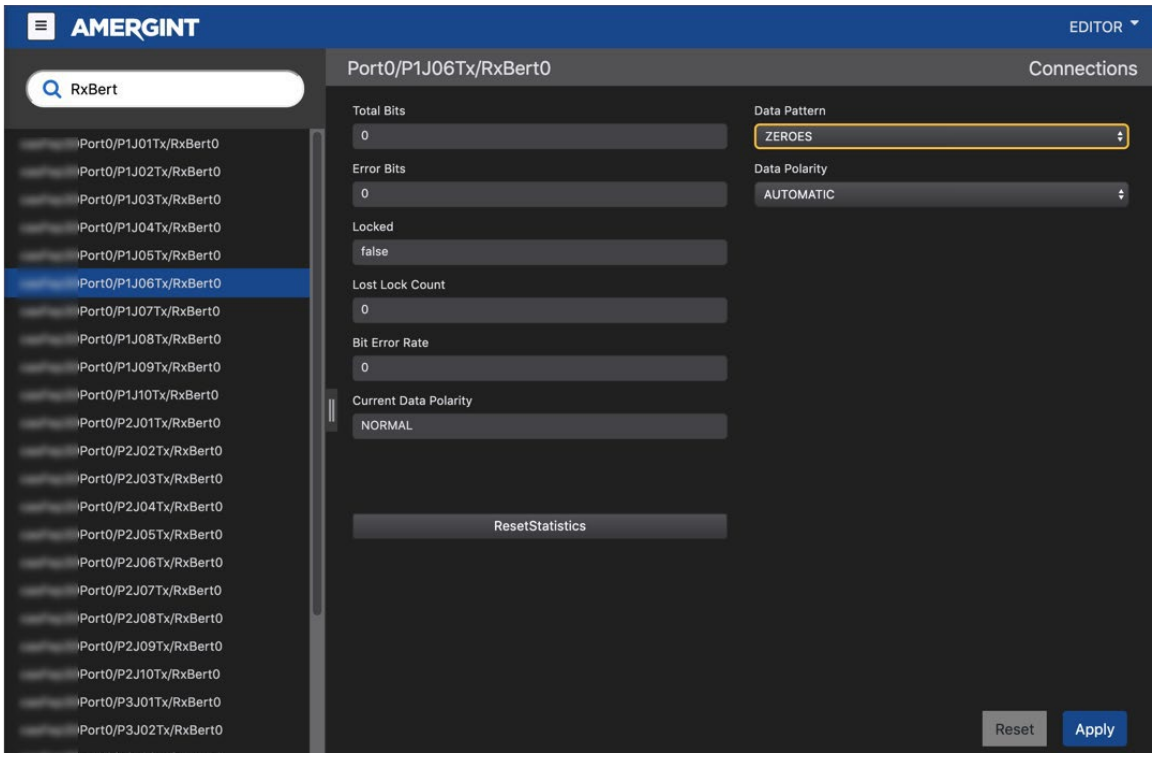

Figure 29. SwD overview window. Source: [26].

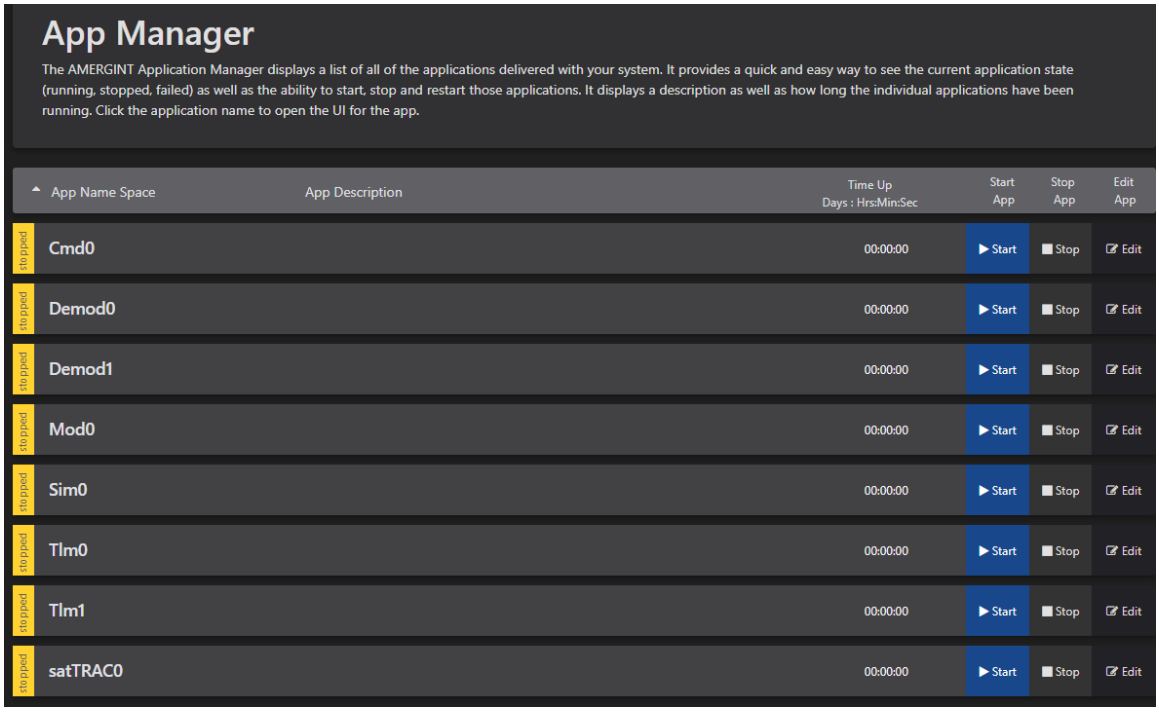

Figure 30. Application Manager window. Source: satTRAC GUI.

Several U.S. government organizations have employed satTRAC's technology, including NASA, the Air Force, and commercial industry partners such as Northrop Grumman, Raytheon and Lockheed Martin [35].

2. Kratos SpectralNet Lite Digitizer and quantumRadio SDR

Though implementing the newly-acquired AMERGINT satTRAC heterodyne receiver into MC3 ground stations was a focus of this thesis research, the currently in-use, established Kratos SDR receiver was also utilized for testing and integration purposes. Kratos Defense & Security Solutions, Inc. develops and fields cost-effective technology related to U.S. national security, with satellite communications systems as a main specialty [36]. The Kratos quantumRadio (qRadio) product is advertised as a robust, ground station software modem for RF signal processing, specifically designed to meet the evolving requirements of satellite operations. Highlighted benefits include common cloud compatible infrastructure, industry standard interfaces, proven field performance, improved scalability, added flexibility, and increased automation [37]. Key features of this SDR, as promoted by the manufacturer, are listed below:

- quantumRadio can be used on-premise, in a private cloud or with a cloud provider.
- Suitable for all types of programs from single satellites to large constellations.
- Compatible with widely used space radios.
- Performs telemetry, commanding and ranging functions.
- Built in test functions that reduce costs and minimize Integration and Test (I&T) efforts.
- Configurable as mission requirements change or as new missions come online.
- Standard TCP/IP, GEMS, REST, and VITA-49 interfaces make integration simple and protects long term investments.
- Minimize hardware footprint and costs with pure software implementation.
- Access and control from anywhere via the web. No client software to install or maintain. [37]

The Kratos receiver employed at MC3 ground stations consists of the SpectralNet Lite Digitizer and qRadio SDR. The SpectralNet Lite Digitizer serves as the system's RFFE, while qRadio constitutes the RFBE with signal processing software running on a

Dell R440 server. A homodyne receiver, the Kratos digitizer utilizes Analog Digital's RFSoC AD9364 chip to perform direct down-conversion of received analog signals into digital IF [2]. The front plate of the SpectralNet Lite Digitizer is annotated in Figure 31. The qRadio system, depicted in Figure 32, executes RFBE functions such as modulation, demodulation, and bit synchronization. Specific Kratos performance features and capabilities are summarized in Appendix A.

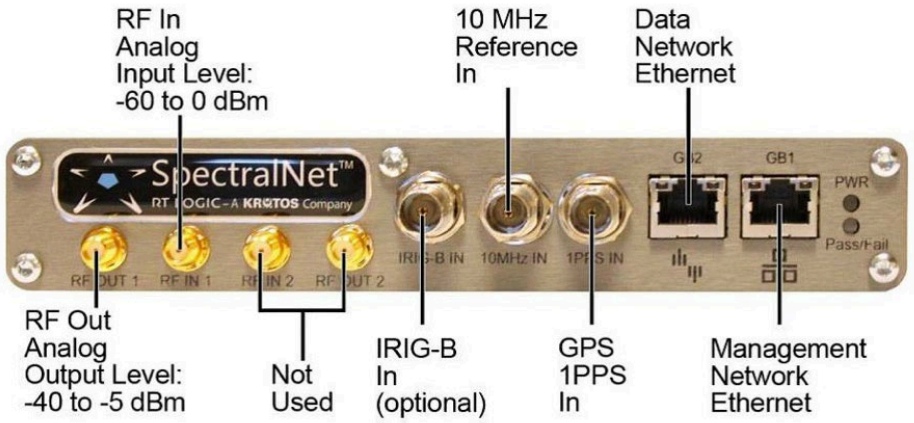

Figure 31. SpectralNet lite digitizer. Source: [38].

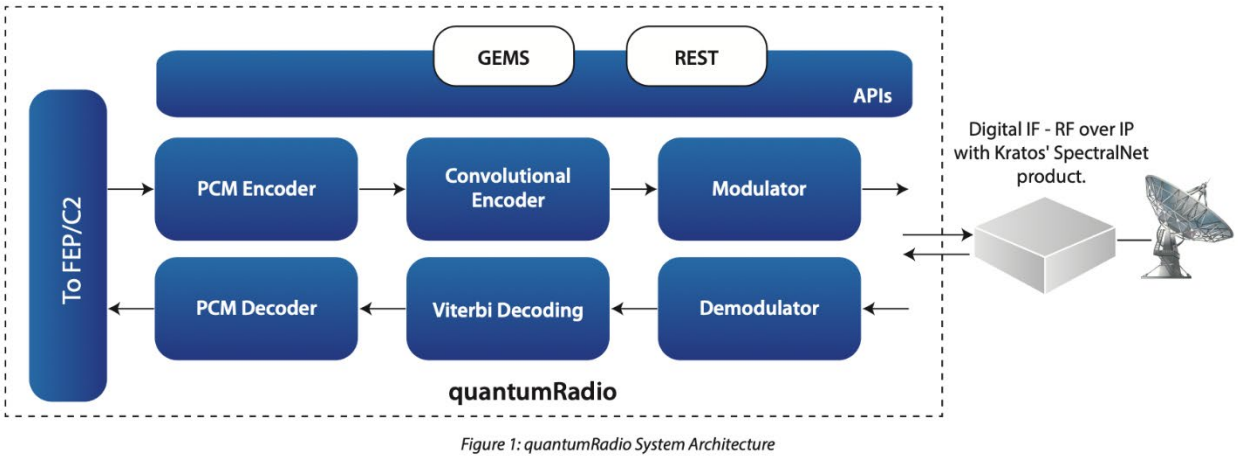

Figure 32. Kratos quantumRadio system architecture. Source [37].

As opposed to AMERGINT satTRAC's single, all-encompassing GUI, the Kratos system employs two separate GUIs via proprietary software to access and operate the digitizer and SDR. The SpectralNet GUI allows the user to set analog input/output RF and power parameters for digitizer hardware. The qRadio GUI provides user access to RFFE parameter inputs through VMware software. As depicted in Figure 33, the two Kratos components are interconnected by way of digital IF waveforms that are formatted as packetized data streams via the open-standard VITA-49 protocol, and transferred through a 1GbE cable [38]. Screenshots of each GUI are provided for example in Figures 34 and 35.

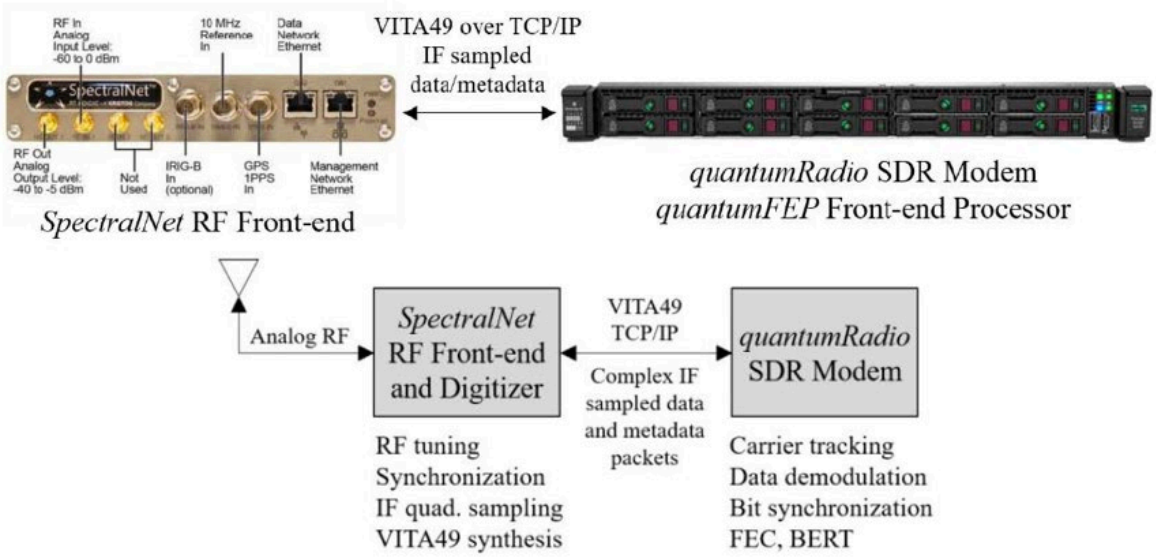

Figure 33. Kratos SpectralNet Lite Digitizer and qRadio SDR system components. Source: [39].

Figure 34. SpectralNet GUI screenshot. Source: SpectralNet GUI.

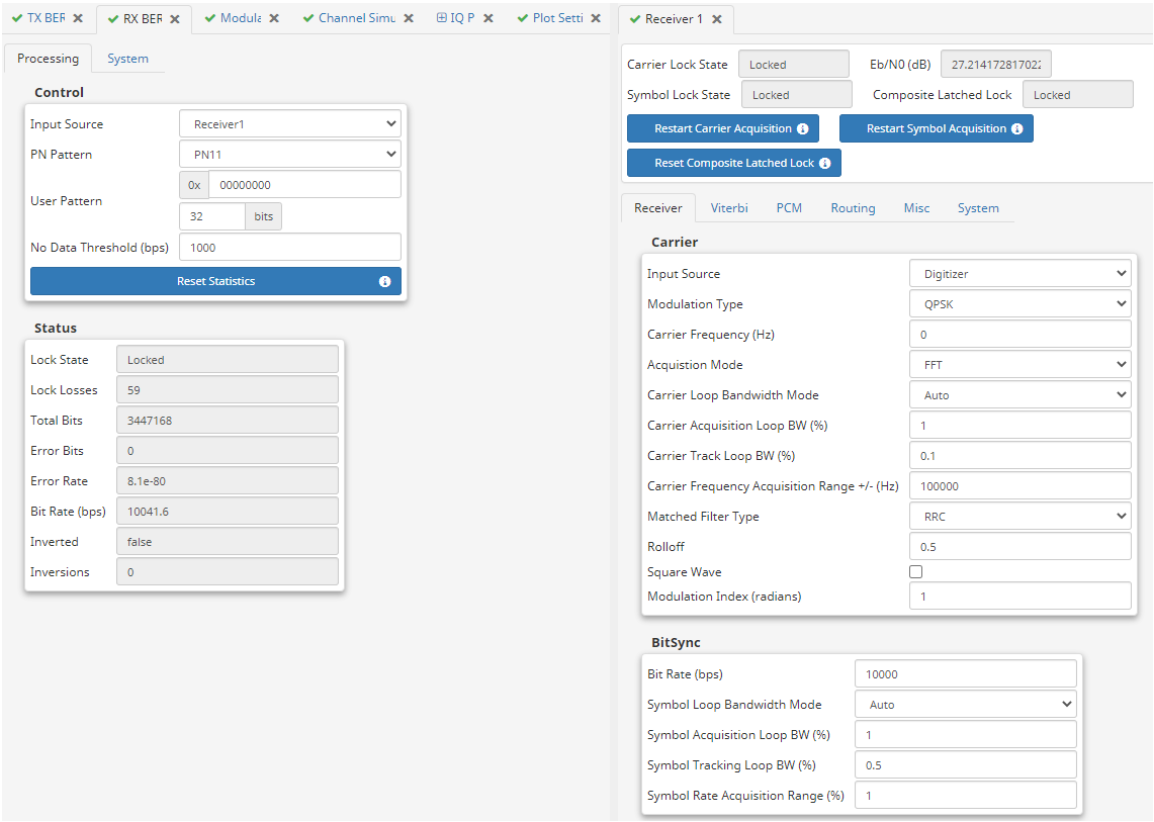

Figure 35. qRadio GUI screenshot with Receiver and RX BERT modules open. Source: qRadio GUI.

In the qRadio GUI, a left-hand side navigation pane enables the selection of different module types to control and set SDR parameters. For instance, opening the "Receiver" module allows the user to select input source and modulation type, as well as view receiver E_b/N_0 and signal lock states. A real-time IQ plot, pictured in Figure 37, may be accessed through clicking the "IQ Plot" module. The various qRadio software module types are listed and described in Figure 36. These modules characterize the processing attributes of uplink and downlink signals, corresponding to the flow of data through respective SpectralNet "RF IN" and "RF OUT" ports of the digitizer.

Module Type	**Instance(s)**	**Purpose**
Digitizer	digitizer	Provides control and status of data interface with digitizer
CMD Input	cmdInput1,cmdInput2	Sends command frames from the network to the modulator
Command Sender	commandSender	Sends command frames from the network to the modulator
Command Acknowledgment	commandAcknowlegment	Supports the command acknowledgment protocol
TX BERT	txBert1,txBert2	Generates a PN pattern at the specified bit rate
Reed Solomon Encoder	reedSolomonEncoder1	Performs block FEC encoding of an input data stream
Modulator	modulator	Generates modulated signal from an information bit stream
PM/FM Modulator	pmFmModulator	Generates a composite output signal by combining subcarrier waveforms
Doppler Compensator	dopplerCompensator	Adjusts the carrier frequency of a signal based upon an input data file
Channel Simulator	channelSimulator	Provides fixed noise capability for link testing
PM Receiver	pmReceiver	Demodulates PM signal waveforms
Receiver	receiver1,receiver2,cadetReceiver	Demodulates a signal into an information bit stream
Frame Sync	frameSync1,frameSync2	Finds frames in a raw bit stream
Reed Solomon Decoder	reedSolomonDecoder1,reedSolomonDecoder2	Performs Reed Solomon decoding and CCSDS derandomization
HDLC Decoder	hdlcDecoder1,hdlcDecoder2	Decodes incoming telemetry using the HDLC Protocol
Network Output	tlmOutput1, tlmOutput2	Provides control and status of an output socket
RX BERT	rxBert1,rxBert2	Detects and locks to PN pattern. Once locked, tracks the number of bit errors in a data stream.
Application Health	applicationHealth	Provides application health status
File Recorder	fileRecorder	Records DSP data to a file
Sample File Player	sampleFilePlayer	Plays back sample data from a file
Time Reference	timeReference	Provides control and status of time reference

Figure 36. qRadio module types. Source: [38].

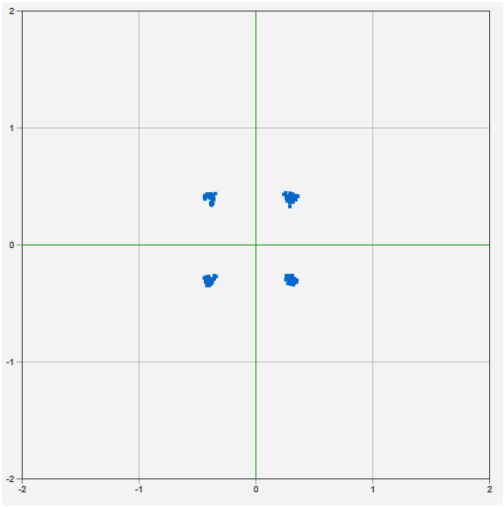

Figure 37. qRadio IQ plot (QPSK demodulation). Source: qRadio GUI.

Comparatively, this thesis research experienced an overall greater ease-of-use with the Kratos system interfaces than the satTRAC interface. The associated documentation and user guides were also clearer and more descriptive for the Kratos SDR. Breaking user access into two GUIs to separately operate Kratos components had its benefits, but AMERGINT's single GUI, with system status portrayed in flow-diagram style, was helpful in quickly accessing and diagnosing errors. For a more detailed comparison of the two receiver GUI experiences, as well as research and testing on specific system performance, refer to preceding thesis work in [2].

THIS PAGE INTENTIONALLY LEFT BLANK

III. X-BAND PAYLOAD

A. DRIVING REQUIREMENTS

The anticipation of increased data requirements for future CubeSats drives MC3 research in the development of higher bandwidth, greater capacity, X-band communication capabilities. As part of the Mola CubeSat mission, the SSAG endeavors to demonstrate cost-effective X-band SDR technology for small satellites. The objective of [1] was to design, build and test a low-cost X-band SDR using COTS components and readily available software (i.e., GNU Radio or MATLAB Simulink), eventually space-qualifying this payload for the Mola spacecraft and integrating it with a CubeSat bus. The Astro Digital Corvus-6 bus was selected, offering a 3U space for payload integration, leaving approximately 0.5U of space and 1 kg of mass for the radio assembly mechanical enclosure [1]. Driving requirements for radio payload development included: S-band uplink, X-band downlink, compatibility with MC3 ground station receivers, frequency shift keying modulation, optimal data rates of 5 to 10 Mbps, FEC coding, and BERs of 10E-5 or less. COTS components were successfully implemented where applicable in SDR design, in order to produce "nominal processing power and RF capability for CubeSat SDR applications, while reducing cost and shortening the development life cycle" [1]. Mola payload interface requirements are outlined in Figure 38.

Payload	Data	Max Power	Max Operating Time @ Peak Power	Approximate Dimensions	Configuration Requirements	Antenna Dimensions
Korimako	RS-232, 115.2 kbps (RS-422 for back door for payload testing, not a required bus interface)	15V, 1.5 A	13 minutes	95.9 x 90.2 x 84.7 mm	1 S-band, 1 X-band patch antennas (nadir facing)	S-band: 100.5 x 82.6 x 20.0 mm X-band: 36.0 x 36.0 x 4.7mm
Terahertz Imaging Camera (TIC)	UART	5V, 1.5A	1 minute	~1.5U	2 x 57 mm diameter cutouts, 24 deg FOV	N/A
X-Band SDR	Ethernet	8V, 4A	10 minutes	~1U	1 X-band patch antenna (nadir facing)	X-band: 36 x 36 mm
Retroreflector	RS-232	5V	TBD	80.0 x 80.0 x 125 mm	Mounted on outside (nadir facing)	N/A

- **Pointing requirements:** <0.1 deg
- **Data flow:** all payloads use bus as bent-pipe to ground station; TT&C link is for both data and commands
- **TT&C Link:** Compatible with MC3 ground network (universal S-band up/down)
- **Thermal requirements:** -40 to 80 °C

Figure 38. Mola payload interface requirement as of preliminary design review (PDR). Source: [4].

The X-band SDR payload, interfacing with the Corvus-6 bus via ethernet, will provide the downlink of TIC data to MC3 network receivers. Projected data flow between Mola payloads is depicted in the block diagram of Figure 39. To support data requirements of the TIC, a data rate of 1 Mbps or greater with QPSK modulation was selected in [1] as an initial threshold objective for thesis work. During functional testing of the assembled X-band SDR payload, a data rate of 2 Mbps was achieved [1]. The causes of data rate limitation to 2 Mbps were identified as: the use of a host PC for SDR operation as opposed to a real-time OS, coding processes ran on the SDR as opposed to the system on a chip (SoC), and the use of a slower USB cable for receipt by the SDR receiver unit chosen for end-to-end testing purposes (ZedBoard/ADFMComms-3 EBZ SDR). With the X-band payload adjustments made by SSAG's Small Satellite Laboratory staff, and integration of MC3 SDR receivers for end-to-end testing, this thesis work saw higher data rates on par with research objectives.

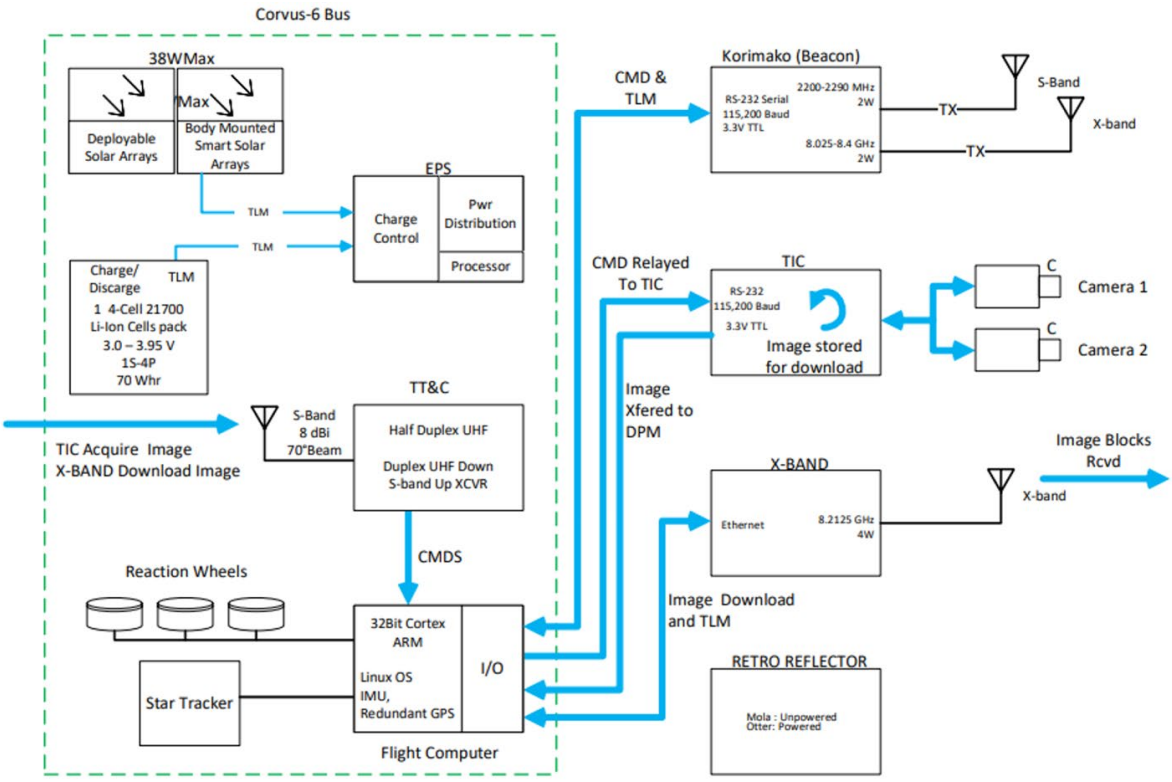

Figure 39. Mola payload data flow. Source: [4].

B. HARDWARE AND SOFTWARE

In development of Mola's X-band SDR payload, the fusion of readily available software, a system on a module (SoM), and drop-in RF parts enabled reduced cost and a more favorable form factor for CubeSat SWaP requirements [1]. The design consists of 4 main hardware components, each made up of various sub-components: the SoM, custom carrier board, convert board, and mechanical enclosure. These hardware components and their features are summarized in the following list [1], with visual depictions in subsequent figures:

- **SoM.** Analog Devices ADRV9361-Z7035 SoM as the SDR platform, with mass 0.0555 kg. Integrates Z-7035 variant of the Zynq-7000 SoC, with processing speeds up to 1 GHz. Incorporates AD9361 RF transceiver (70 MHz to 6 GHz tuning range; 200 kHz to 56 MHz bandwidth).

- **Carrier Board.** Custom-made by the SSAG, referencing the ADRV1CRR-BOB breakout carrier board for design and removing unneeded peripheral components. Approximate mass of 0.047 kg.
- **Convert Board.** Designed using X-MW online tools, utilizing components such as a XM-A9W8-0404D amplifier, and various other XM drop-in parts for RF mixing, filtering, oscillation and voltage regulation. See Appendix A for full breakdown of convert board components.
- **Mechanical Enclosure.** Built by the SSAG to incorporate the SoM, custom carrier board, and convert board while interfacing with the Astro Digital Corvus-6 bus. Measures 9.39 cm x 11.46 cm x 5.63 cm.

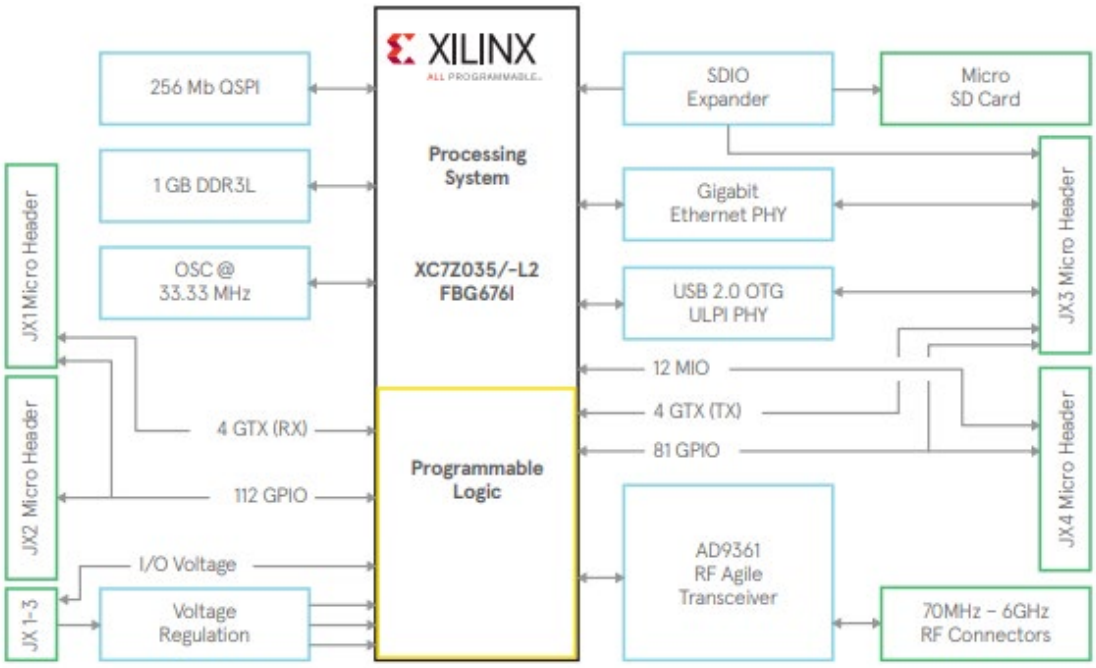

Figure 40. SoM block diagram. Source: [40].

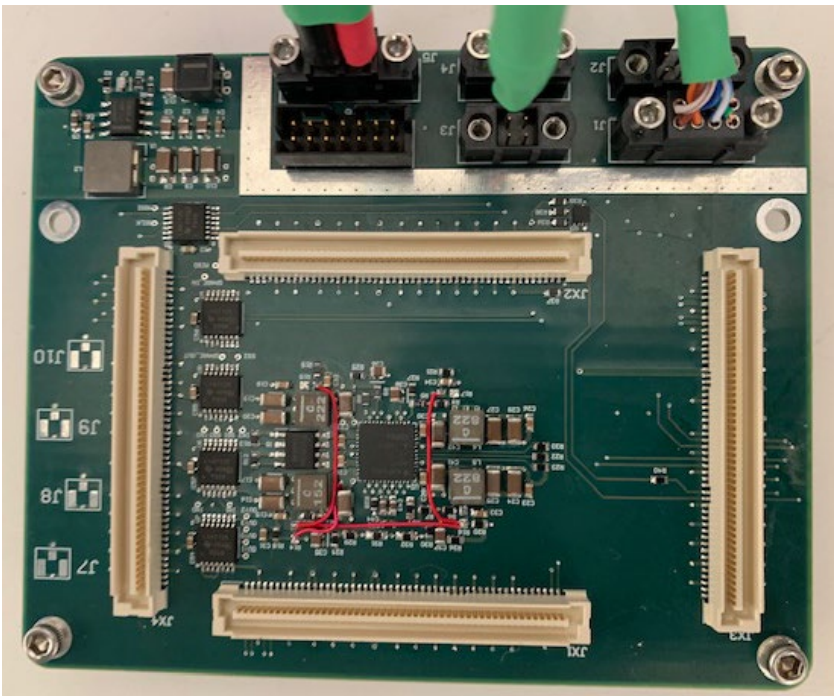

Figure 41. Custom carrier board prototype. Source: [1].

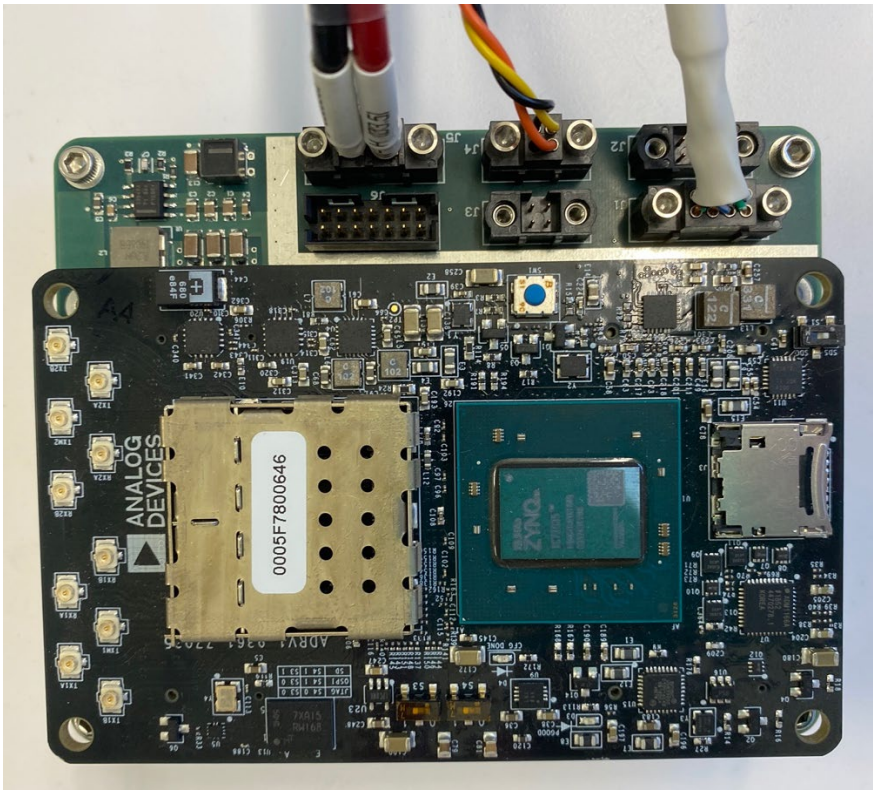

Figure 42. SoM mounted on carrier board.

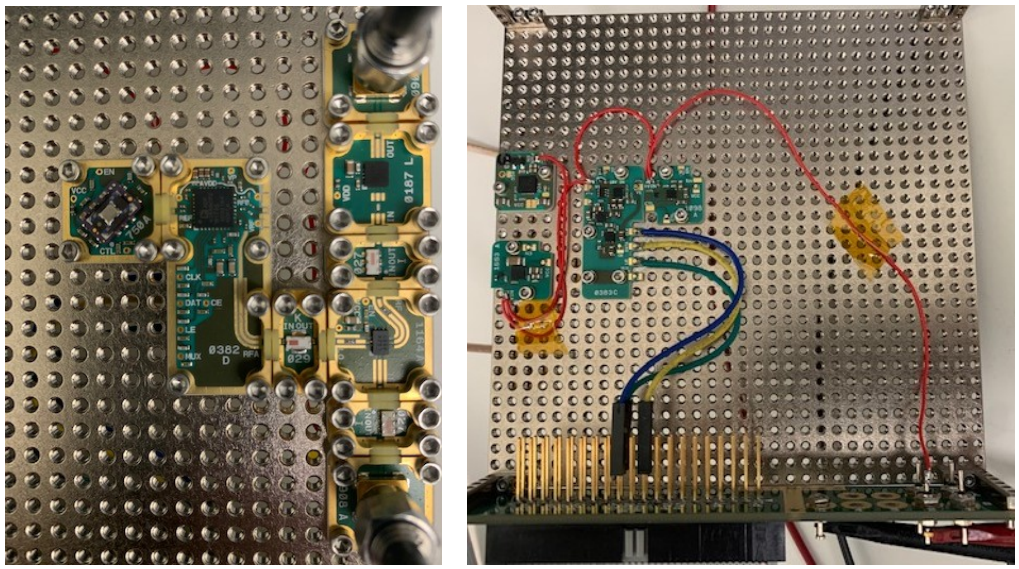

Figure 43. X-MW convert board design, top (left) and bottom (right). Source: [1].

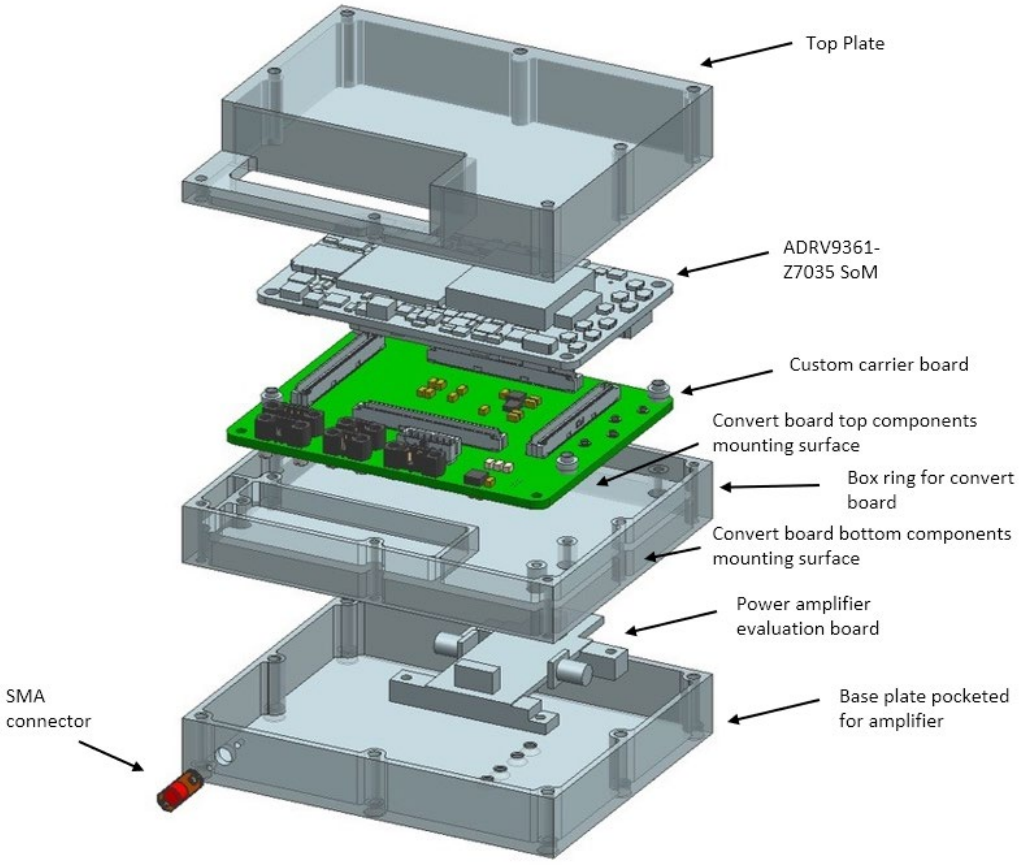

Figure 44. Radio assembly mechanical enclosure. Source: [4].

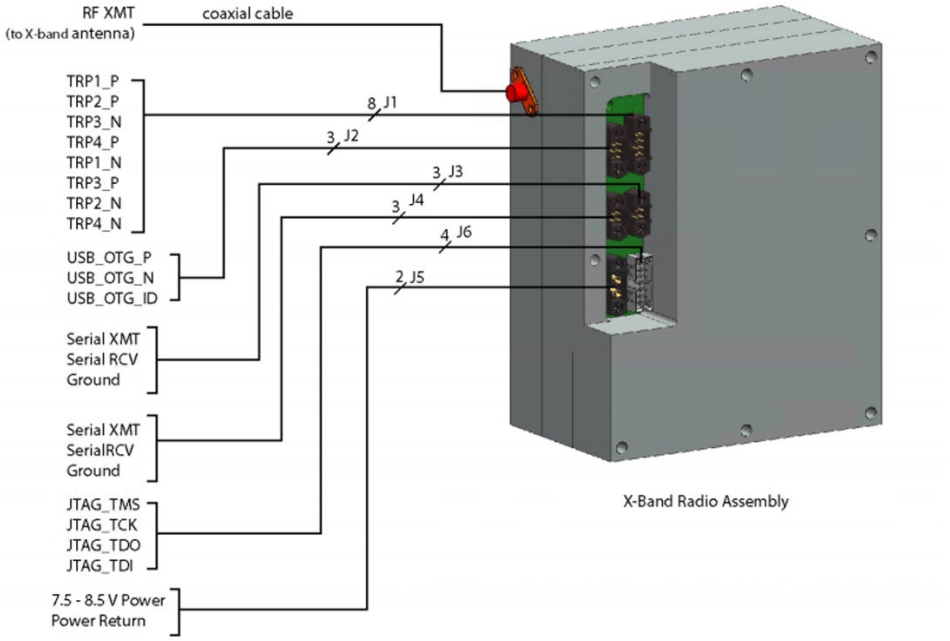

Figure 45. Radio assembly interfaces. Source: [4].

MathWorks MATLAB is the readily available software selected to program and run the X-band SDR payload. Open-source GNU radio was considered as well, but this software requires thorough familiarity with Python, C++ and Linux programming [1]. MATLAB provides user-friendly toolboxes, informative documentation, and practical Simulink models that can be directly executed on the SoC. A QPSK modulation Simulink model was implemented as the payload's baseline program, with appropriate coding adjustments made in MATLAB as needed. MathWorks Simulink's QPSK transmit model, found in the Communications Toolbox Support Package for Xilinx Zynq-Based Radio version 19.2.2, repeatedly sends a QPSK-modulated "Hello World" message on a predetermined center frequency [41]. This module, displayed in Figure 46, activates the Analog Devices AD9361 SDR hardware for bit generation, baseband modulation, pulse shaping, up-sampling and signal transmission [1]. Parameters may be altered via the MATLAB QPSK transmitter initial parameters script provided in Appendix D (zynqRadioQPSKTxAD9361AD9364SL_init.m).

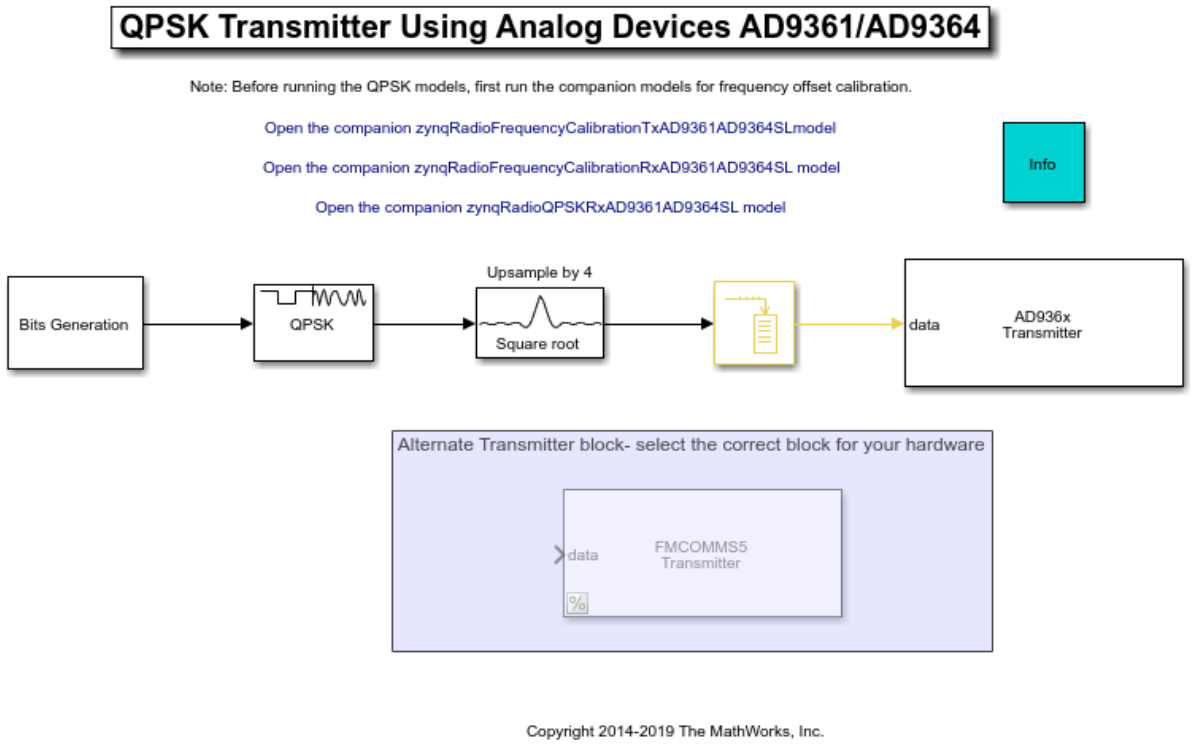

Figure 46. Simulink QPSK transmitter model. Source: [41].

SSAG's Small Satellite Laboratory worked to tweak the coding utilized in [1] to generate a standard PN11 sequence, for compatibility testing with the AMERGINT satTRAC and Kratos quantumRadio receivers designated for Mola's ground segment. In preliminary tests by Small Satellite Laboratory staff, the X-band SDR payload yielded 5 Mbps with 2.6 MHz of occupied bandwidth, and a 2048-bit frame from the PN generator. The RF chip on the X-band SDR ran a 4.096 M-sampled baseband rate. Figure 47 shows the Simulink model, created by lab staff and implemented in subsequent testing with MC3 ground station receivers.

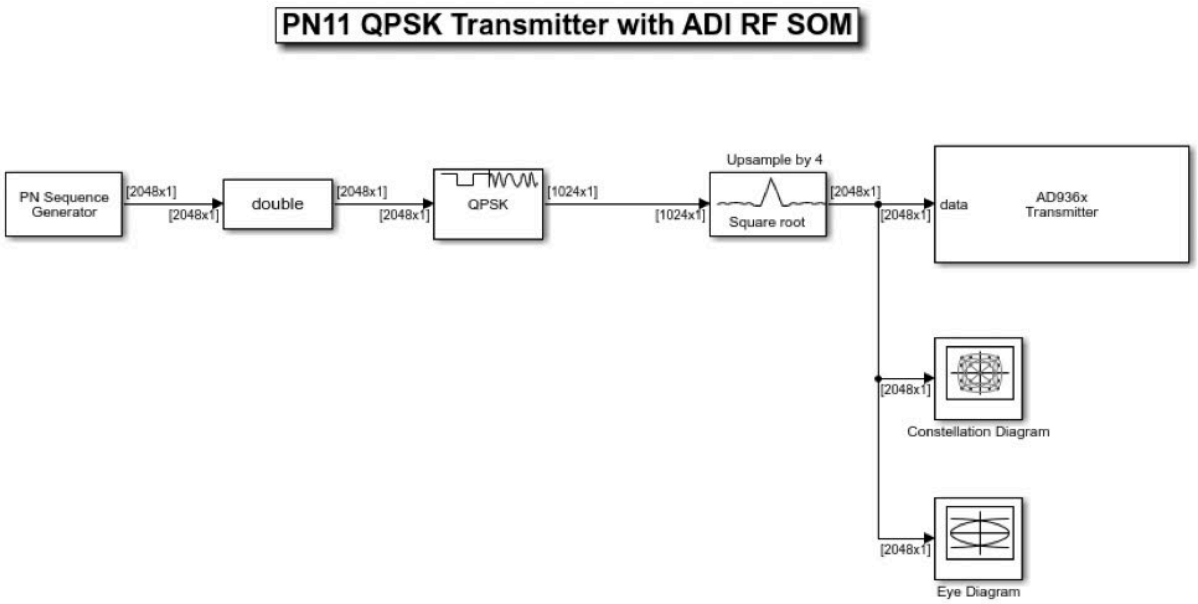

Figure 47. Initial PN11 Simulink model for X-band SDR payload.

C. LINK BUDGET

For this research, link budget calculations were mainly derived from preceding thesis work [1] that built the X-band SDR payload. In [1], link analysis was performed using two cases: a suitable sun-synchronous, LEO with altitude 500 km and elevation 10°, as well as a "worst case" scenario. For the purposes of this thesis work, calculations were updated to reflect the desired parameters included in the X-band SDR research objectives (i.e., a BER of less than 10E-5; data rate of 5 to 10 Mbps). The same SSAG excel spreadsheets from [1] were used for link calculations, provided in Appendix B.

The link budget analysis for the likely Mola orbit scenario is shown in Tables 3 and 4, for data rates of 5 Mbps and 10 Mbps, respectively. In both cases, the positive link margin indicates a closed link with a signal that is successfully detected by the receiver. The link budget analysis for the worst-case scenario presented in [1] is shown in Tables 5 and 6 for 5 Mbps and 10 Mbps data rates. Analysis reveals a successful link in the case of 5 Mbps, but a negative link margin for 10 Mbps.

Table 3. Link budget analysis suitable case (5 Mbps).

Parameter	**Magnitude**	**Units**
Frequency	8.2125	GHz
Elevation angle	10	degrees
Altitude	500	km
Data rate	5	Mbps
Tx losses	-1	dB
Rx losses	-1	dB
Implementation loss	-1.5	dB
Transmit power: 4W	6.021	dBW
Tx antenna gain	4	dB
EIRP	9.021	dBW
Free space loss	-175.32	dB
Antenna G/T	23.40	dB/K
BER	1.5e-5	
Achieved E_b/N_0	16.22	dB
Required E_b/N_0	9.65	dB
Link Margin	**6.57**	**dB**

Table 4. Link budget analysis suitable case (10 Mbps).

Parameter	**Magnitude**	**Units**
Frequency	8.2125	GHz
Elevation angle	10	degrees
Altitude	500	km
Data rate	10	Mbps
Tx losses	-1	dB
Rx losses	-1	dB
Implementation loss	-1.5	dB
Transmit power: 4W	6.021	dBW
Tx antenna gain	4	dB
EIRP	9.021	dBW
Free space loss	-175.32	dB
Antenna G/T	23.40	dB/K
BER	1.5e-5	
Achieved E_b/N_0	13.21	dB
Required E_b/N_0	9.65	dB
Link Margin	**3.56**	**dB**

Table 5. Link budget analysis worst case (5 Mbps).

Parameter	**Magnitude**	**Units**
Frequency	8.2125	GHz
Elevation angle	10	degrees
Altitude	1200	km
Data rate	5	Mbps
Tx losses	-1	dB
Rx losses	-1	dB
Implementation loss	-1.5	dB
Transmit power: 4W	6.021	dBW
Tx antenna gain	4	dB
EIRP	9.021	dBW
Free space loss	-180.65	dB
Antenna G/T	23.40	dB/K
BER	1.5e-5	
Achieved E_b/N_0	10.88	dB
Required E_b/N_0	9.65	dB
Link Margin	**1.23**	**dB**

Table 6. Link budget analysis worst case (10 Mbps).

Parameter	**Magnitude**	**Units**
Frequency	8.2125	GHz
Elevation angle	10	degrees
Altitude	1200	km
Data rate	10	Mbps
Tx losses	-1	dB
Rx losses	-1	dB
Implementation loss	-1.5	dB
Transmit power: 4W	6.021	dBW
Tx antenna gain	4	dB
EIRP	9.021	dBW
Free space loss	-180.652	dB
Antenna G/T	23.40	dB/K
BER	1.5e-5	
Achieved E_b/N_0	7.87	dB
Required E_b/N_0	9.65	dB
Link Margin	**-1.78**	**dB**

This link budget analysis did not include the forward error correction (FEC) coding research objective in calculations, but FEC results in an improved link margin by adding coding gain, and would serve only to improve system performance/signal receipt. In the event attitude control is degraded, which can happen during satellite operations, pointing errors can turn a suitable case into an unsuitable one (also not accounted for in analysis). Link budget calculations helped shape compatibility testing between spacecraft SDR and ground station SDR, for this analysis provides a parameters framework to ensure successful links are achieved between payload and receiver once Mola is launched into orbit.

IV. TESTING

A. PN SEQUENCE GENERATOR

Mola's X-band SDR will provide the downlink of telemetry and TIC payload data to MC3 RGTs. To simulate data transmission, testing leveraged pseudo-random noise (PN) sequence generators to output pseudo-random, binary bit streams. Randomization of the bit stream is important to the receiver synchronization process, removing "long streams of like bits" that can negatively impact decoding [18]. PN sequences carry the statistical characteristics of sampled white noise, but are periodic and "deterministic" in the sense that bit outputs are based on defined initial conditions [17]. Thus, standard PN sequences, such as the PN11 sequence selected for the purposes of this thesis work, are known and interpretable by both radios in a communications link. Simulink's Communications Toolbox includes a PN Sequence Generator block that functions as a linear-feedback shift register (LFSR) to produce sequences [42]. Figure 48 shows the user-defined block parameters, including the initial-condition generator polynomial and initial states binary vector, as well as sample time and samples per frame.

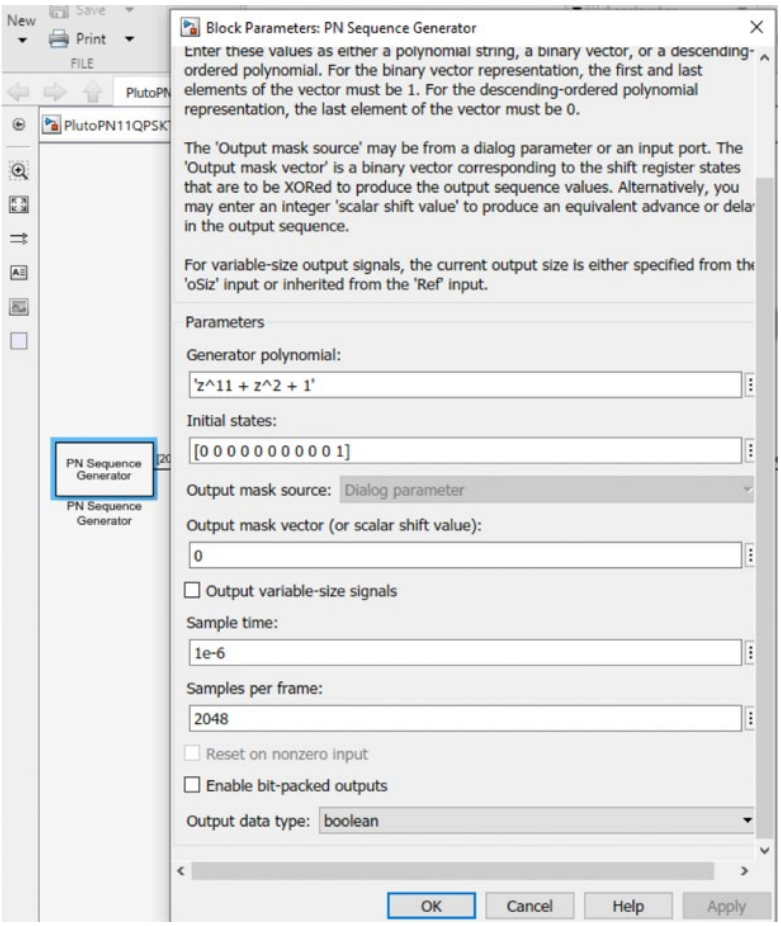

Figure 48. Simulink PN sequence generator block parameters (PN11).

B. PRELIMINARY TESTING OF GROUND STATION RECEIVERS

In order to begin compatibility testing between Mola's X-band SDR payload and MC3 ground station receivers, first it was necessary to study the receivers and become thoroughly acquainted with their operation. Loopback tests, with both the AMERGINT and Kratos radio systems, guided the initial familiarization process. QPSK modulation/demodulation was implemented in the loopback tests, anticipating the desired QPSK signal processing from payload to receiver. Next, test signals were generated between the two ground station SDRs. Establishing a baseline knowledge of satTRAC and qRadio's innerworkings, and how data is demodulated and decoded by each system, allowed testing to transfer to the X-band payload.

1. Familiarization and Loopback Tests

Setting up loopback tests is a straightforward process, useful for system familiarization and troubleshooting, with well-documented instruction in the receivers' respective user guides [26] and [38]. Note that for all preliminary testing and for all bench testing performed during this thesis research, coaxial cable acted as the communications channel for RF signal transmission.

The following figures portray screenshots of the AMERGINT satTRAC GUI during loopback test of a QPSK-modulated, 2 Mbps PN11 data transmission at 2.2 GHz. Conveniently, a loopback system configuration had already been established and saved through the research efforts of [2]. First, the Modem Overview and associated status/controls settings for the softFEP application components are shown, followed by spectrum analyzer and IQ plot screenshots. Then, data analysis for Rx BERT and packet statistics are captured in Figure 53.

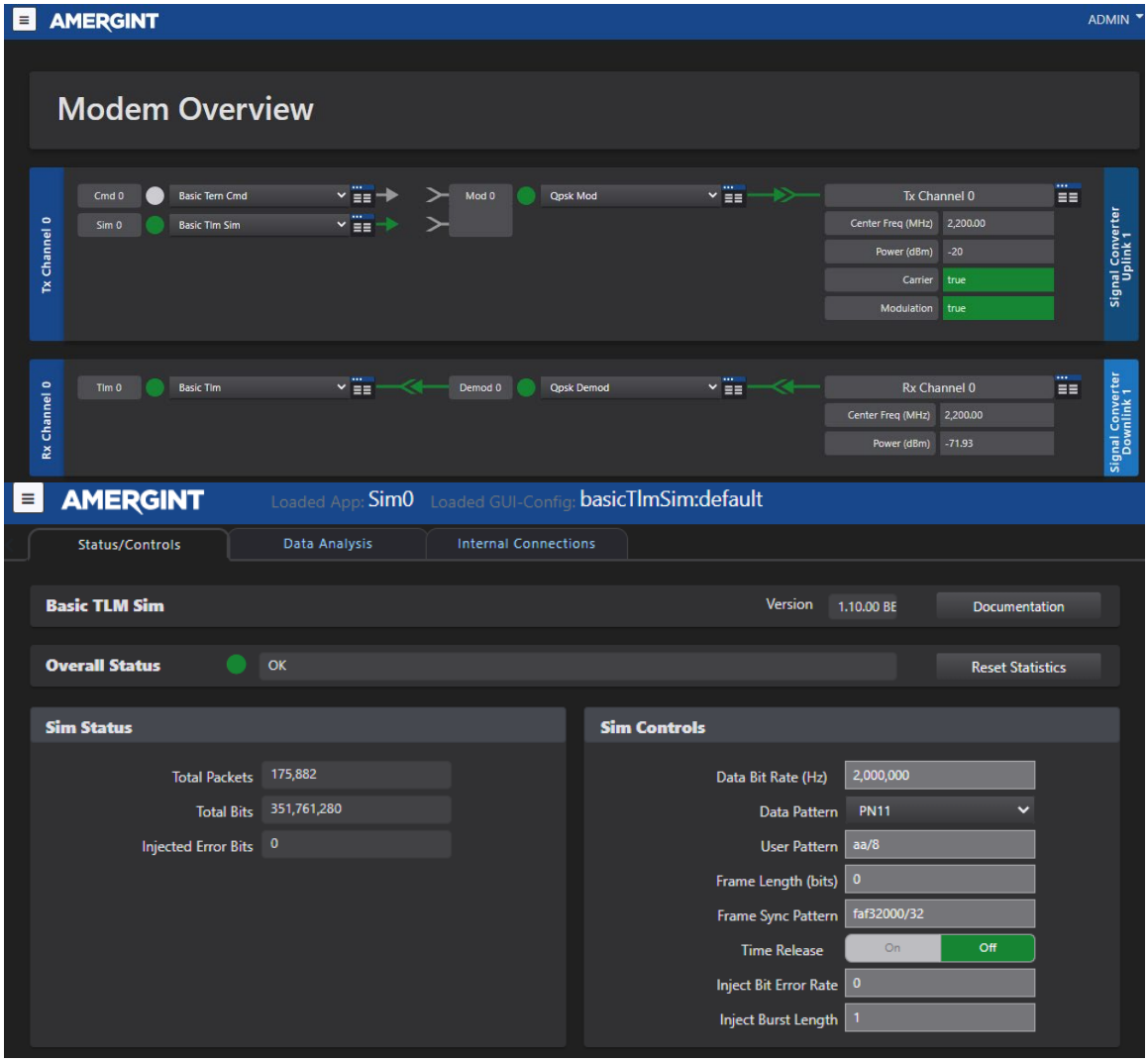

Figure 49. Modem Overview and Sim0 control settings, QPSK loopback test.

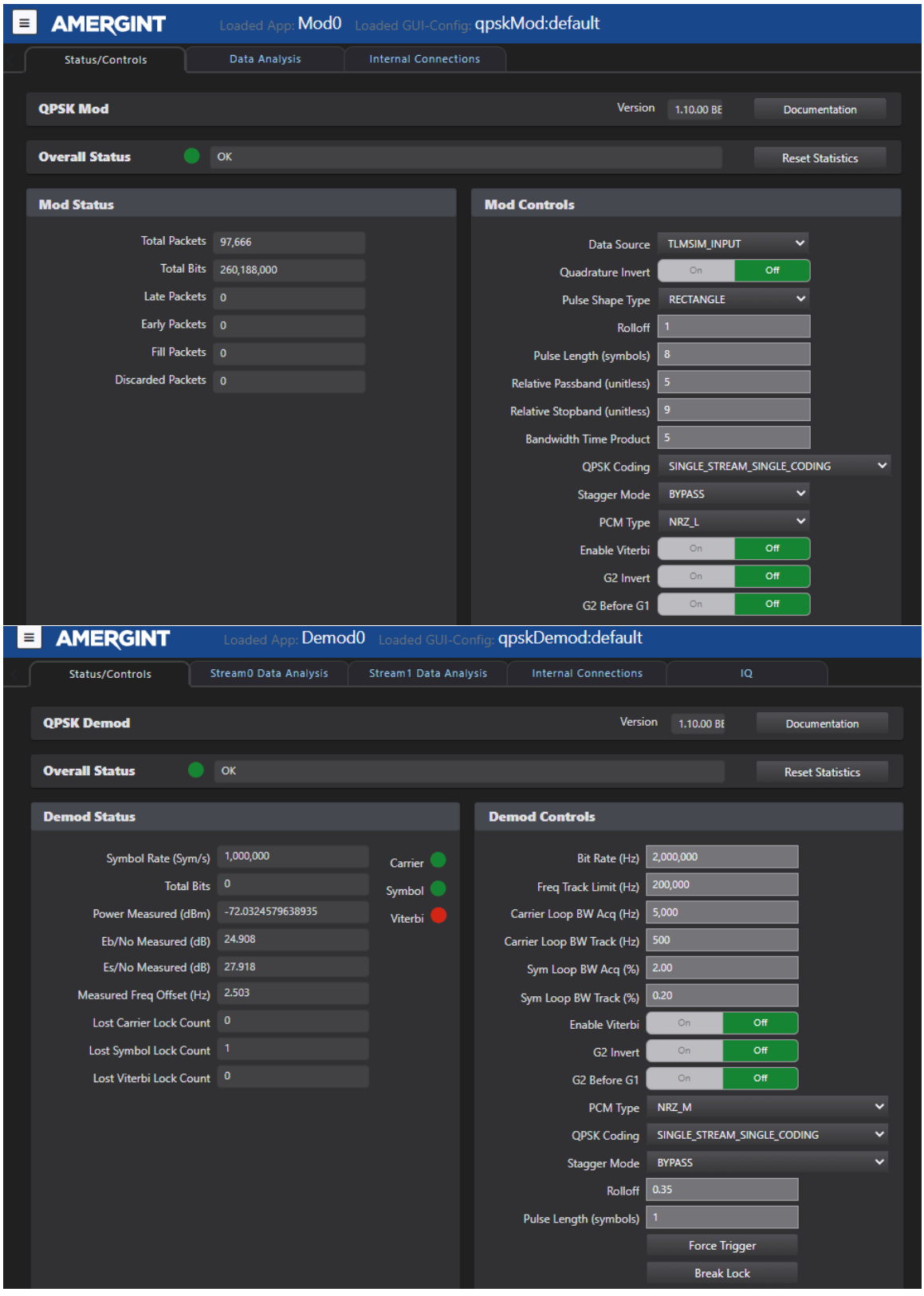

Figure 50. Mod0 and Demod0 control settings, QPSK loopback test.

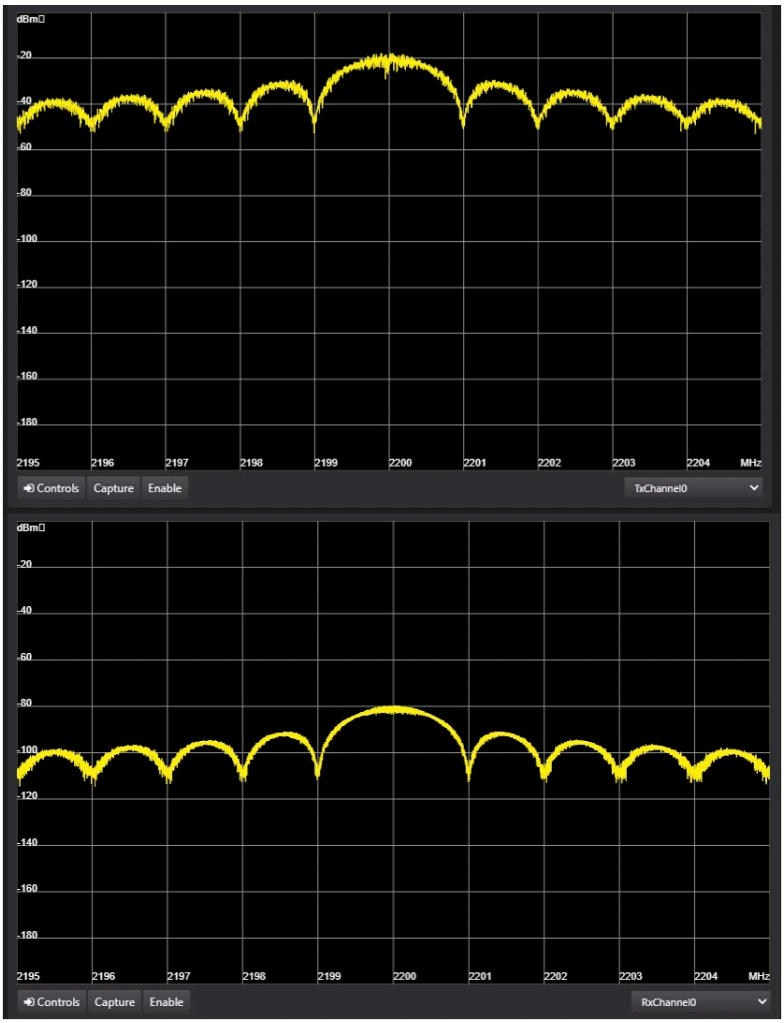

Figure 51. Spectrum analyzer, 2.2 GHz transmit (top) and receive (bottom).

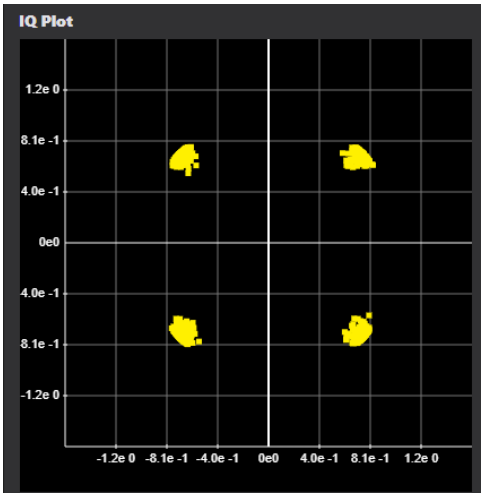

Figure 52. Demodulation, satTRAC QPSK loopback test.

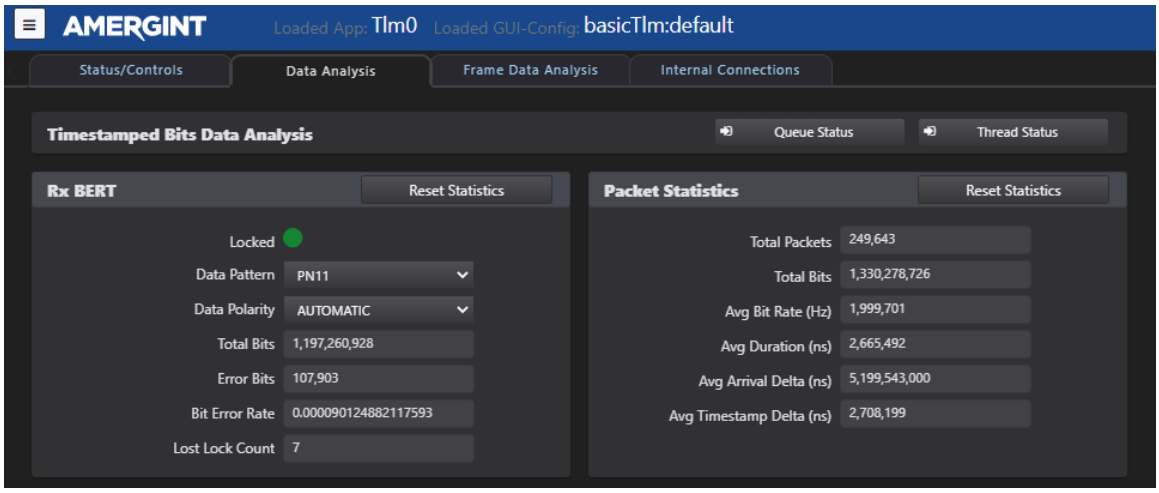

Figure 53. Rx BERT and packet statistics, QPSK loopback test.

As with the satTRAC loopback tests, the Kratos loopback was able to utilize pre-configured settings established by [2] for the SpectralNet and qRadio interfaces (i.e., “Loopback_BERT” system configuration; title included to assist future Small Satellite Laboratory applications). Note that RF IN operates at a -2 MHz center frequency offset from RF OUT, a characteristic inherent to SpectralNet parameters that remained true for the entirety of testing efforts. The Kratos SDR loopback tested a QPSK-modulated, 10 Kbps PN11 data transmission at 1.5 GHz. Screenshots are provided for reference in the figures below.

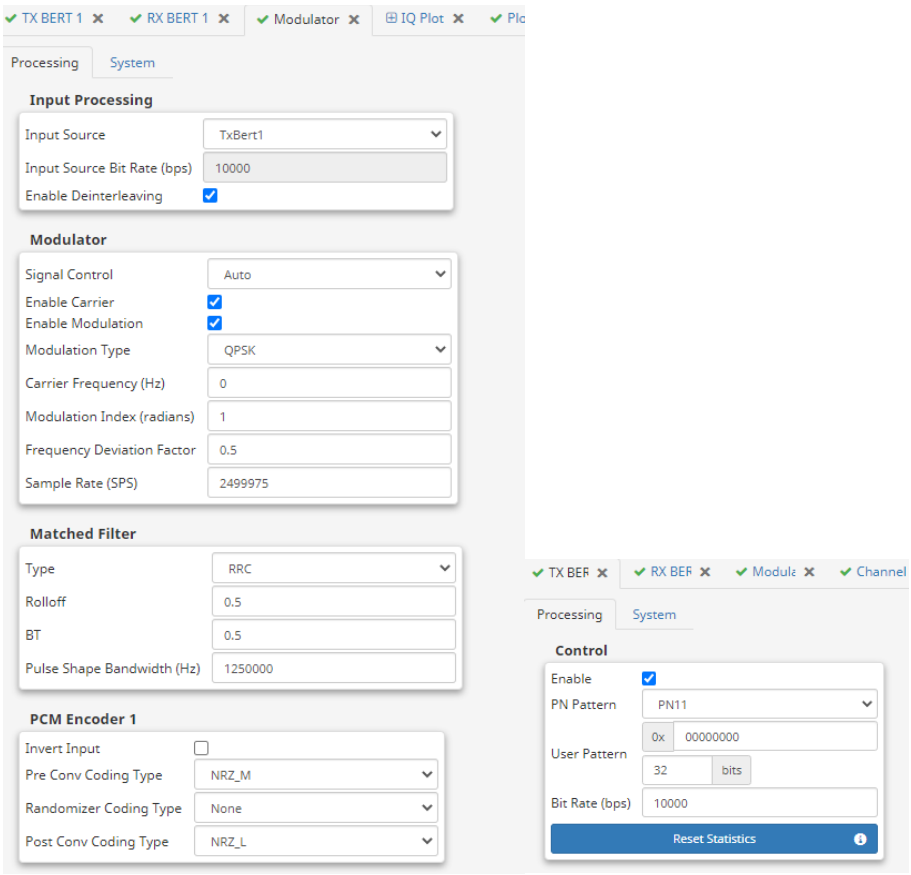

Figure 54. Modulator and TX BERT settings, QPSK loopback test.

Figure 55. SpectralNet RF input GUI, QPSK loopback test.

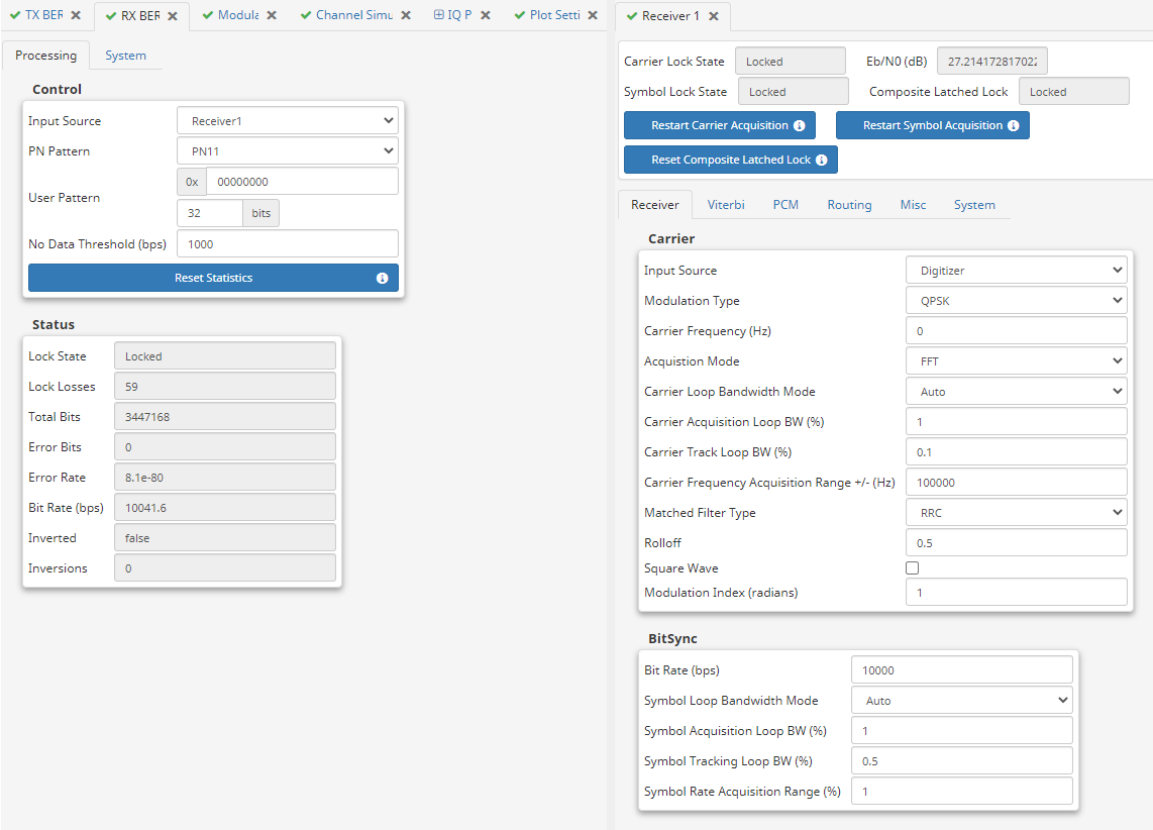

Figure 56. RX BERT and receiver settings, QPSK loopback test.

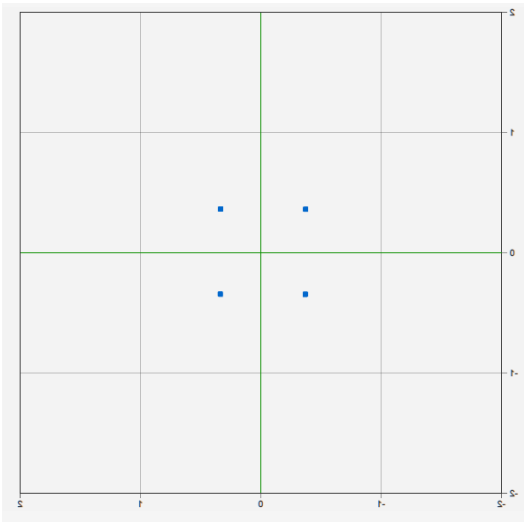

Figure 57. Demodulation, Kratos QPSK loopback test.

2. Kratos to AMERGINT Tests

The Kratos SDR was utilized as the test signal generator for experimentation with the AMERGINT satTRAC system, constituting the first demonstration of satTRAC receiving from another radio since its acquisition by the SSAG. Signal power and carrier frequency was established via the SpectralNet GUI, and waveform parameters selected in the qRadio GUI. Testing began with a standard, unencoded 1 Mbps QPSK PN11 signal, and upon successful receipt by the satTRAC SDR, evolved to 5 Mbps data rates. This test set-up provided a platform upon which to begin QPSK PN11 testing with the payload SDR hardware. The equipment set-up is depicted in Figure 58, showing the Kratos SpectralNet digitizer "RF OUT 1" port wired via coaxial cable to the AMERGINT SDR's Downlink 1 "S-Band In" port (the satTRAC loopback cable connection is also visible as connecting the Uplink "Test Loop Out" port to the Downlink 1 "Test Loop In 1" port).

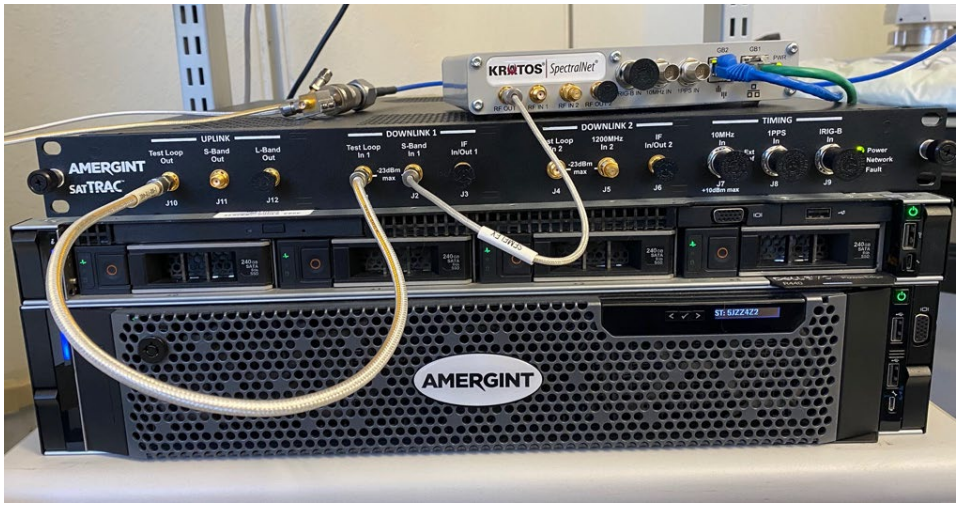

Figure 58. Kratos and AMERGINT test set-up.

The figures that follow capture testing parameters and results of the 5 Mbps QPSK PN11 transmission from Kratos SDR to AMERGINT SDR at 2.25 GHz. The transmit segment graphics are shown first, followed by the satTRAC GUI status displays as data was successfully demodulated and decoded. A BER of 0 was observed as millions of bits were effectively received by the AMERGINT satTRAC system (see Figure 62). Observed

BERs of 0 are plausible with the testing procedures described herein, due to the use of coaxial cable transmission channels and test set-ups devoid of peripheral RF equipment. With minimal noise contribution by the communications link equipment, few opportunities for noise introduction, and no added attenuators/noise introduced to the testing system, a clean signal is expected.

Figure 59. SpectralNet RF output GUI.

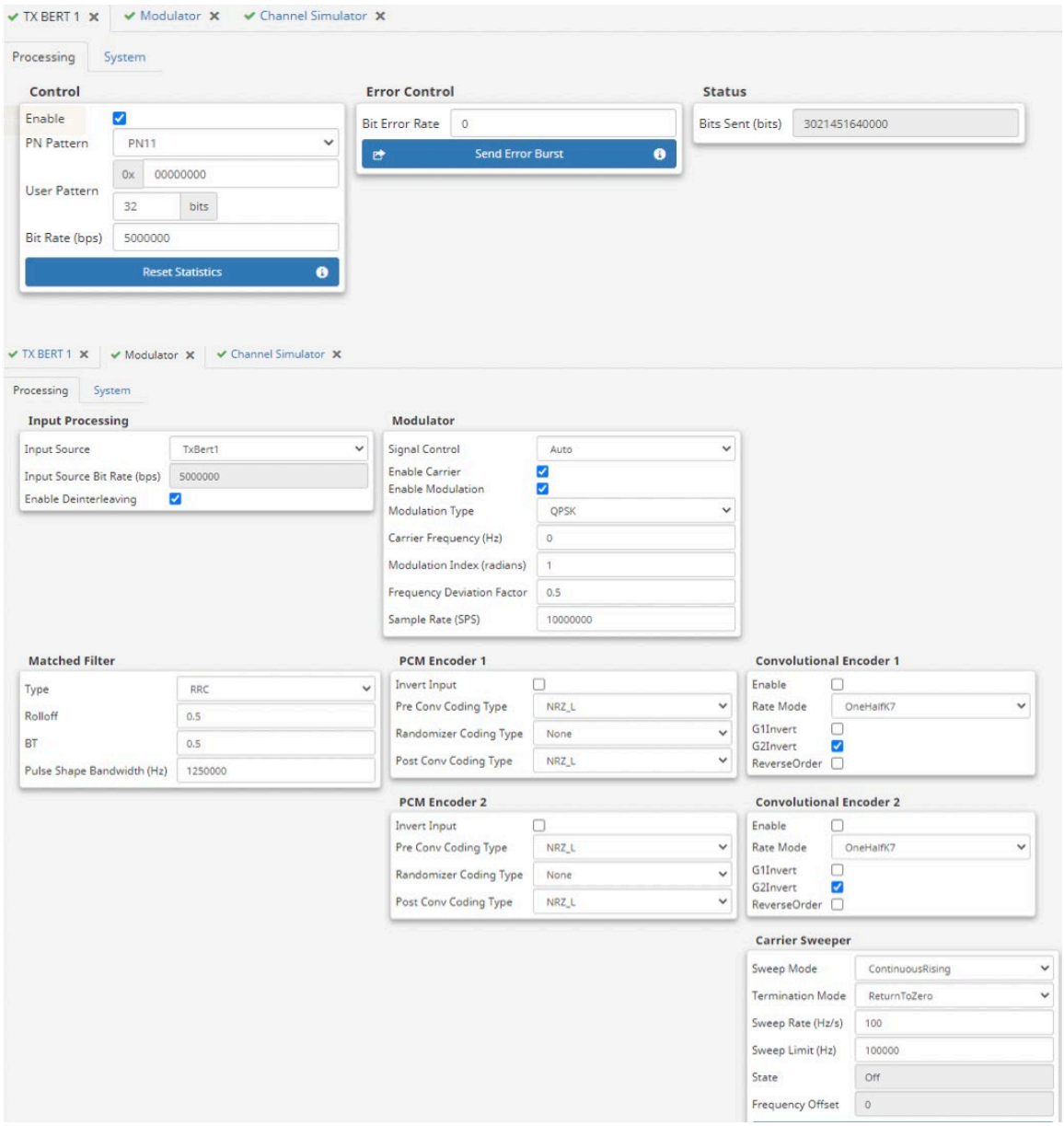

Figure 60. Kratos qRadio GUI.

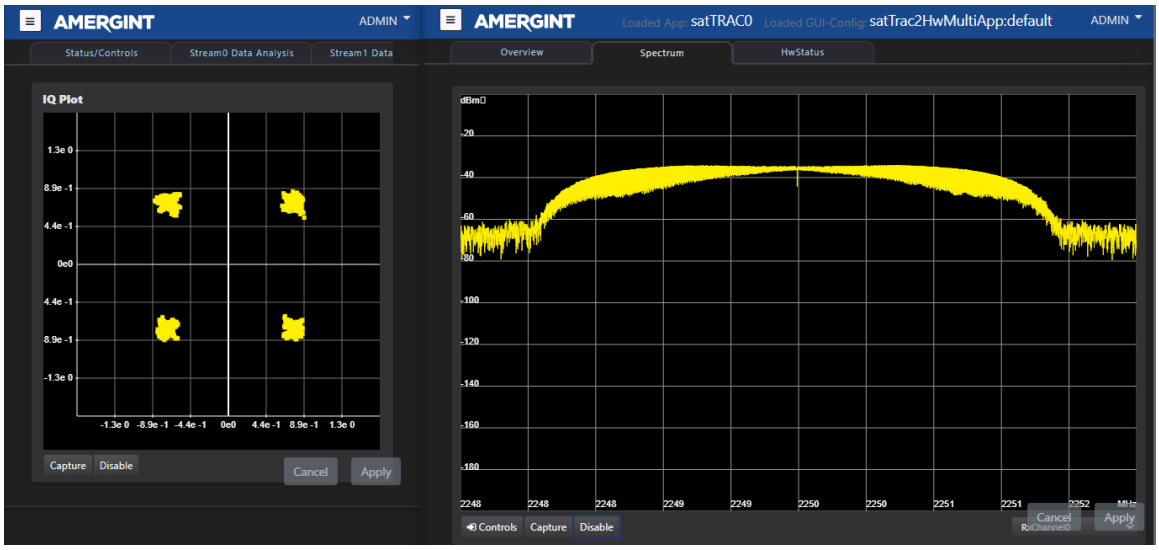

Figure 61. AMERGINT IQ plot and spectrum analyzer.

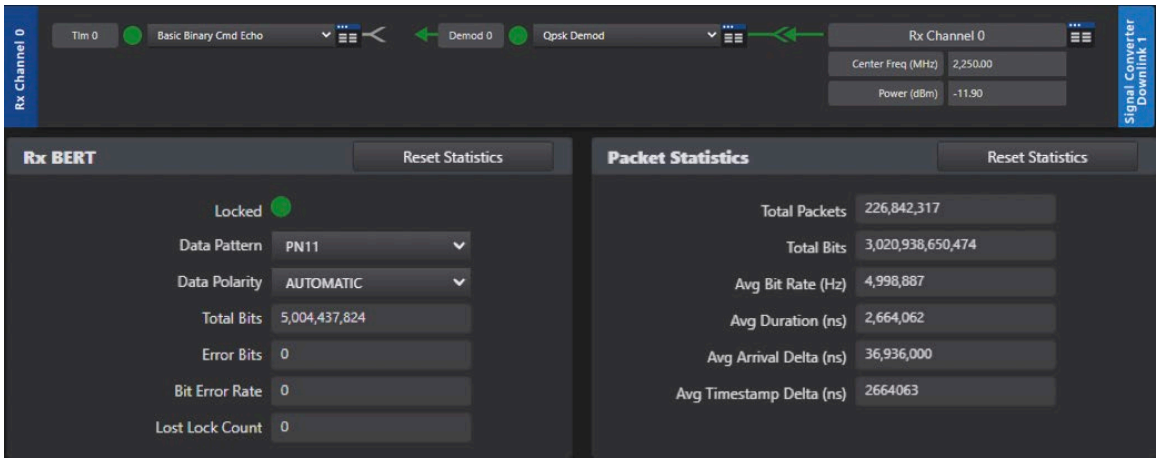

Figure 62. AMERGINT modem overview and data analysis.

C. INTEROPERABILITY TESTING

Serving as a bridge between preliminary receiver testing and later compatibility testing with the X-band SDR payload, tests were executed to verify the previously-discussed PN11 Simulink model developed by Small Satellite Laboratory staff (see Figure 41). Before attempting to run the Simulink model on the higher-complexity, custom-configured hardware of the SDR payload, testing utilized the Analog Devices (AD) ADALM-PLUTO SDR to assess the model's functionality/feasibility of receipt by MC3

ground station receivers. The ADALM-PLUTO SDR Active Learning Module is a user-friendly, commercially-available SDR hardware set that is widely used in academic settings. The Small Satellite Laboratory at NPS frequently uses ADALM-PLUTO SDRs to support various projects and SSAG course offerings. Tests with the ADALM-PLUTO SDR verified a functional Simulink model with PN11 data transmissions effectively demodulated/decoded by both the Kratos SDR and satTRAC SDR. However, once testing transitioned to the flight-like payload hardware (SoM and carrier board), issues were encountered that led to development of a hybrid Simulink model. This new Simulink model combined components of the payload development model provided by the lab staff and the QPSK modulation module that was employed in [1] (see Figure 40). The QPSK modulation module was built-in to Simulink's Communications Toolbox Support Package for Xilinx Zynq-Based Radio. The refined PN11 QPSK transmitter with AD SoM hardware Simulink model yielded successful results that satisfied thesis objectives.

This section covers the testing and interoperability results for both the ADALM-PLUTO SDR platform and the flight-like AD ADRV9361-Z7035 SoM chip set. Several screenshots are provided throughout in order to document the settings/parameters that enabled successful testing outcomes, and allow readers to visualize their implementation within Simulink and within the receiver system GUIs.

1. ADALM-PLUTO SDR

The ADALM-PLUTO SDR is advertised as a "self-contained RF lab in your hand" [43]. This SDR platform, based on an AD9363 and capable of full duplex operation at 325 to 3800 MHz, contains one receive and one transmit channel. ADALM-PLUTO utilizes a USB 2.0 Powered Interface with Micro-USB 2.0 Connector [44] to interface with the host PC, which does not uphold as fast of data rates as ethernet connectors, but was nevertheless useful for initial compatibility testing efforts. Readily-available software packages such as MathWorks MATLAB and Simulink offer a GUI that empowers students to "learn faster, work smarter, and explore more" in regard to SDR technology [43]. Figure 63 provides the ADALM-PLUTO SDR block diagram. Additional specifications/information about the

ADALM-PLUTO SDR Active Learning Module may be found in manufacturer-provided documentation [43] and [44].

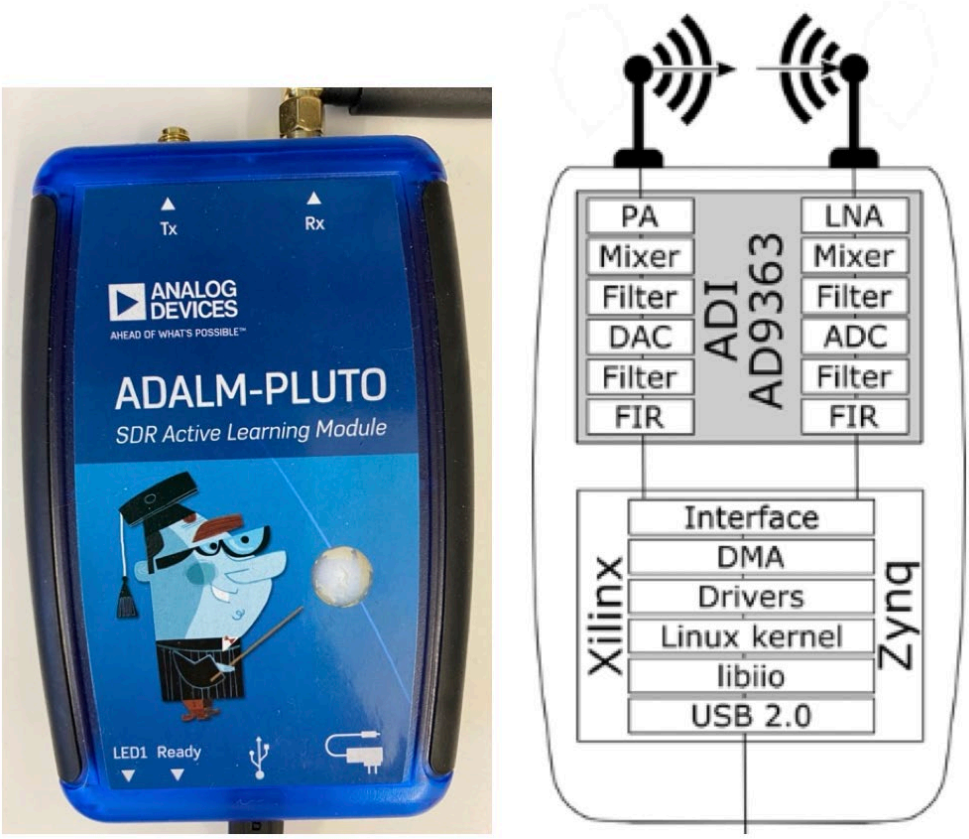

Figure 63. ADALM-PLUTO SDR with block diagram. Source: [44].

In order to test out the lab staff's payload development Simulink model on the ADALM-PLUTO SDR, an ADALM-PLUTO Transmitter block replaced the AD936x Transmitter block, as seen in Figure 64. This block may be accessed via the downloaded Simulink add-on, Communications Toolbox Support Package for ADALM-PLUTO. Figure 65 contains the parameter inputs used for the PN Sequence Generator block and newly added ADALM-PLUTO Transmitter block to generate the PN11 data sequence at 100 Kbps, with QPSK modulation, that yielded the best results with the Kratos and AMERGINT receivers.

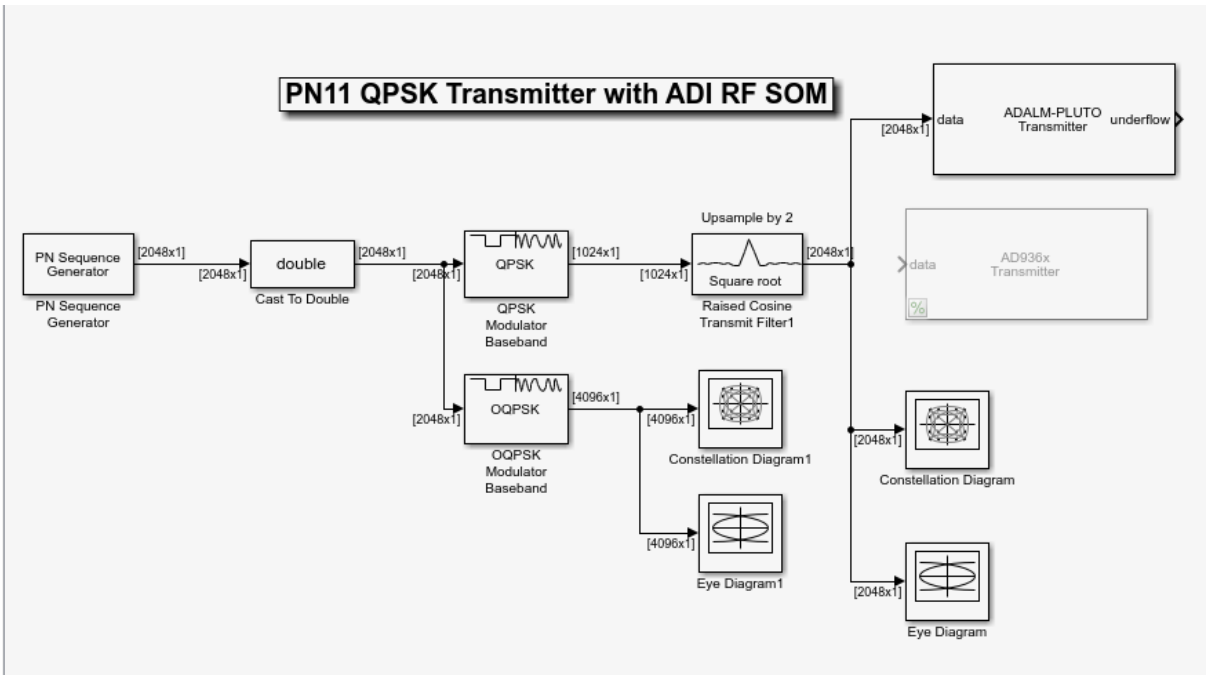

Figure 64. Simulink model for ADALM-PLUTO testing.

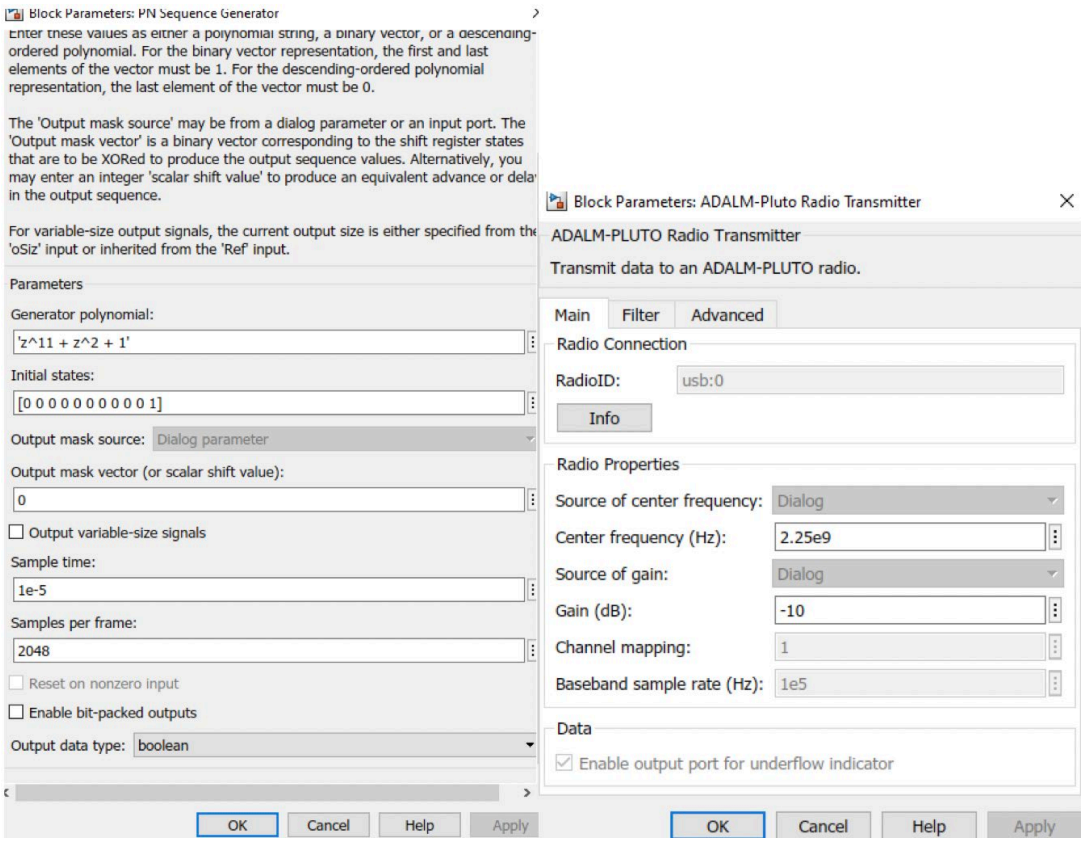

Figure 65. Block parameter inputs, ADALM-PLUTO tests.

Testing resulted in successful signal receipt, demodulation and decoding by both MC3 radio receiver systems, indicating a functioning Simulink model with viability for the interoperability endeavors of this research. The results of AMERGINT satTRAC's receipt of a QPSK-modulated, 100 Kbps PN11 data transmission at 2.25 GHz are depicted in the figures below. The satTRAC receiver maintained carrier and symbol lock over the course of several hours, with BER values of 0 and IQ plot with tidy quadrature points (displayed in Figure 67).

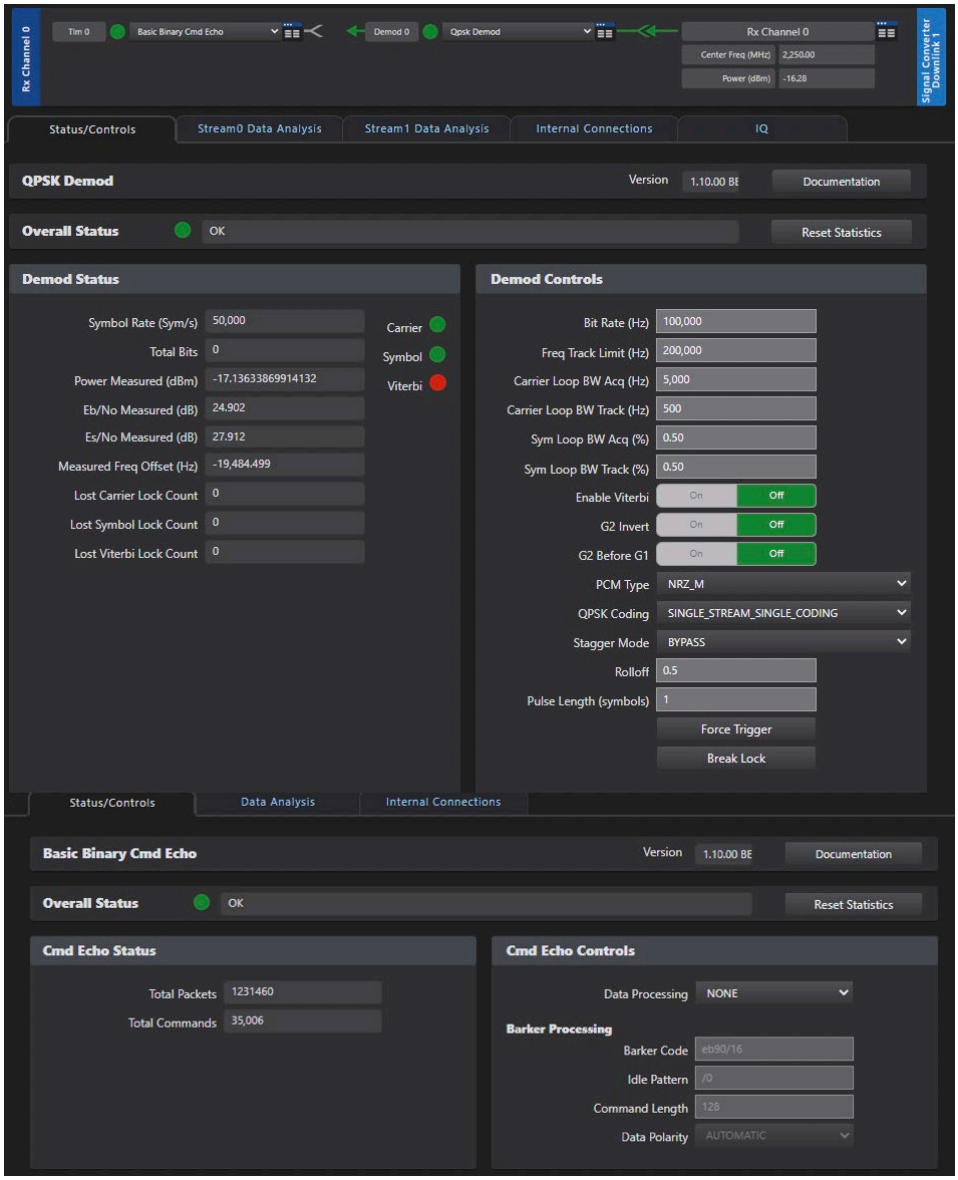

Figure 66. AMERGINT GUI settings, ADALM-PLUTO test.

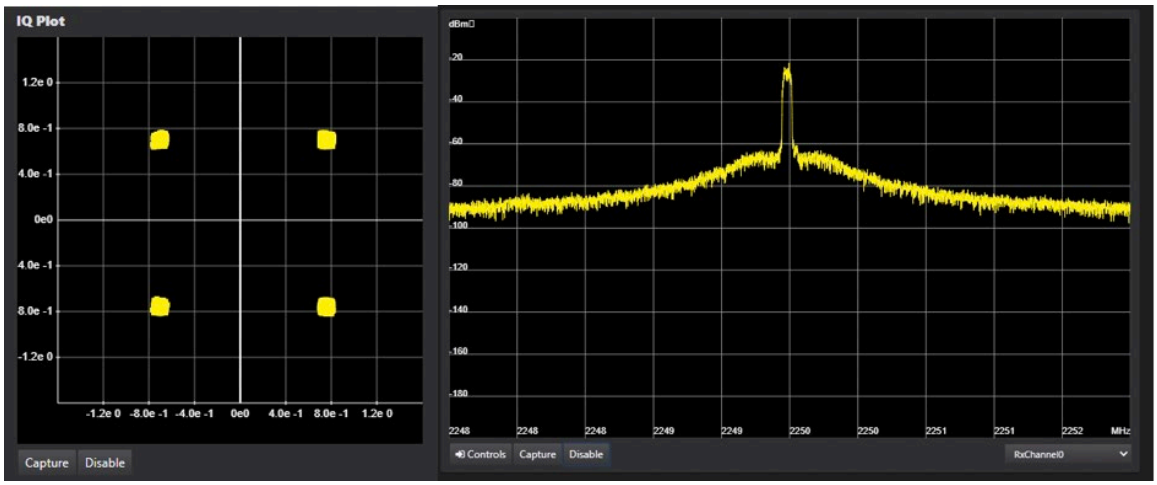

Figure 67. Signal receipt from ADALM-PLUTO SDR.

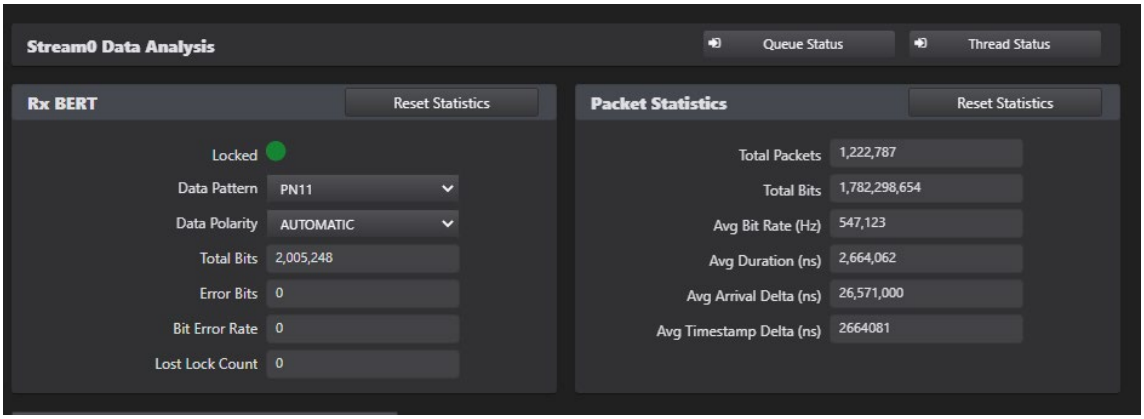

Figure 68. Rx BERT and packet statistics, ADALM-PLUTO test.

2. SoM on Carrier Board Hardware

Once a viable Simulink model was identified, tested and verified via the easy-to-use ADALM-PLUTO SDR platform, testing methods transitioned to flight-like hardware. This hardware consisted of the same AD ADRV9361-Z7035 SoM and carrier board prototype as developed for Mola's X-band SDR payload in [1]. Not only does demonstration of successful data transmission from the payload-like hardware to ground station receivers satisfy objectives of this thesis work, but it also allowed for more flight-like data rates through a 1 GB ethernet connection (as opposed to ADALM-PLUTO's USB). The carrier board employed in testing is larger than the custom-made payload carrier

board (which was engineered to meet payload form factor constraints) but contains exactly the same technology. The SDR hardware of both the test and flight units are shown in Figure 69 for side-by-side comparison.

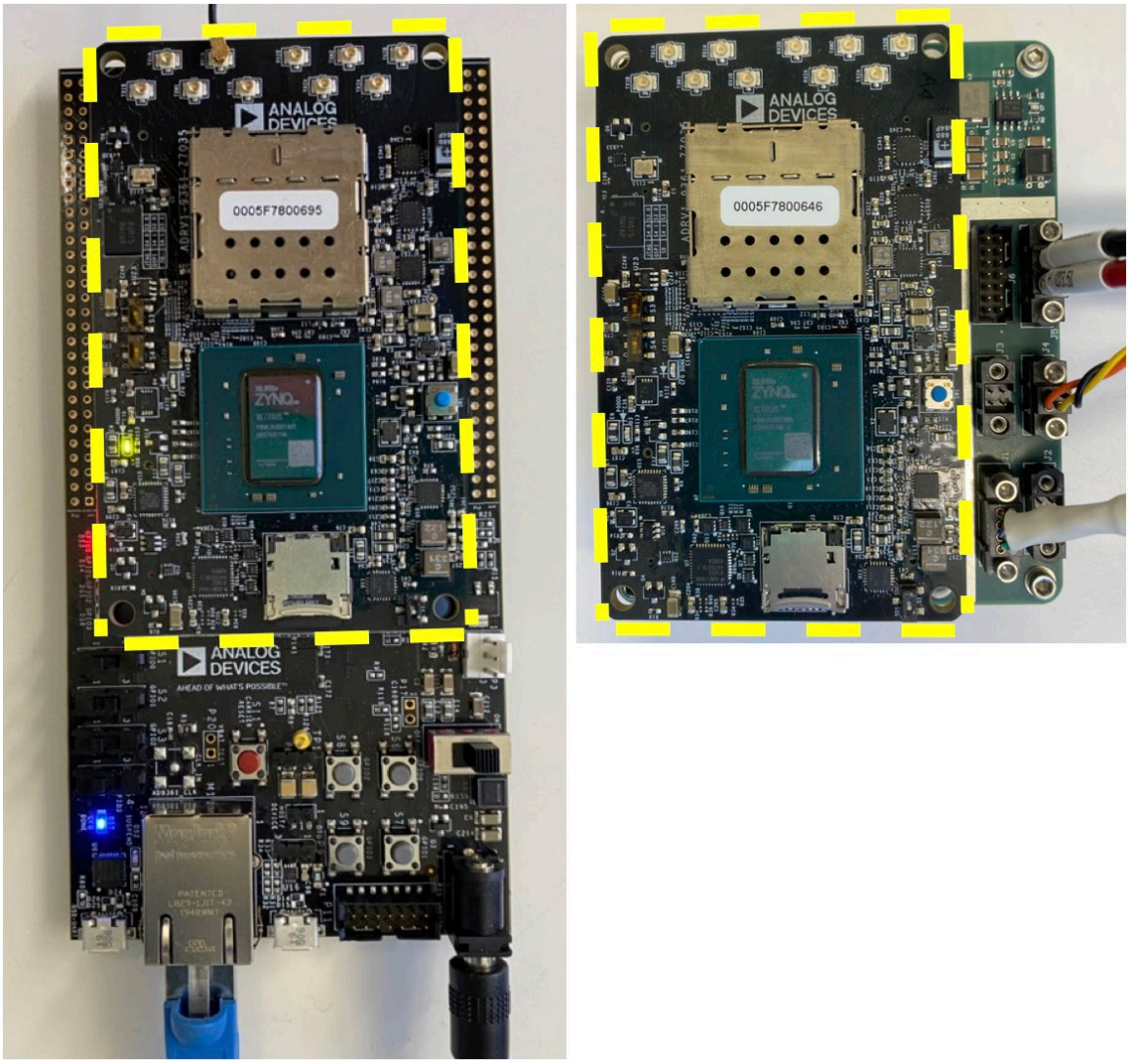

Figure 69. AD ADRV9361-Z7035 SoM (yellow) on carrier board: testing hardware (left), payload hardware (right).

Immediate tests with the PN11 QPSK Simulink model (AD936x Transmitter block) running on the SoM/carrier board hardware proved unsuccessful. Both the Kratos and AMERGINT receivers were unable to maintain symbol lock, nor decode incoming data.

Various parameters and configurations were attempted, including a less intricate BPSK modulation, but neither receiver was able to effectively demodulate/decode the PN11 data transmissions. This led to further research on Simulink models and MATLAB, which resulted in construction of a new model that combined components from the payload development model and the QPSK transmitter model used in [1]. Figure 70 shows the final Simulink model.

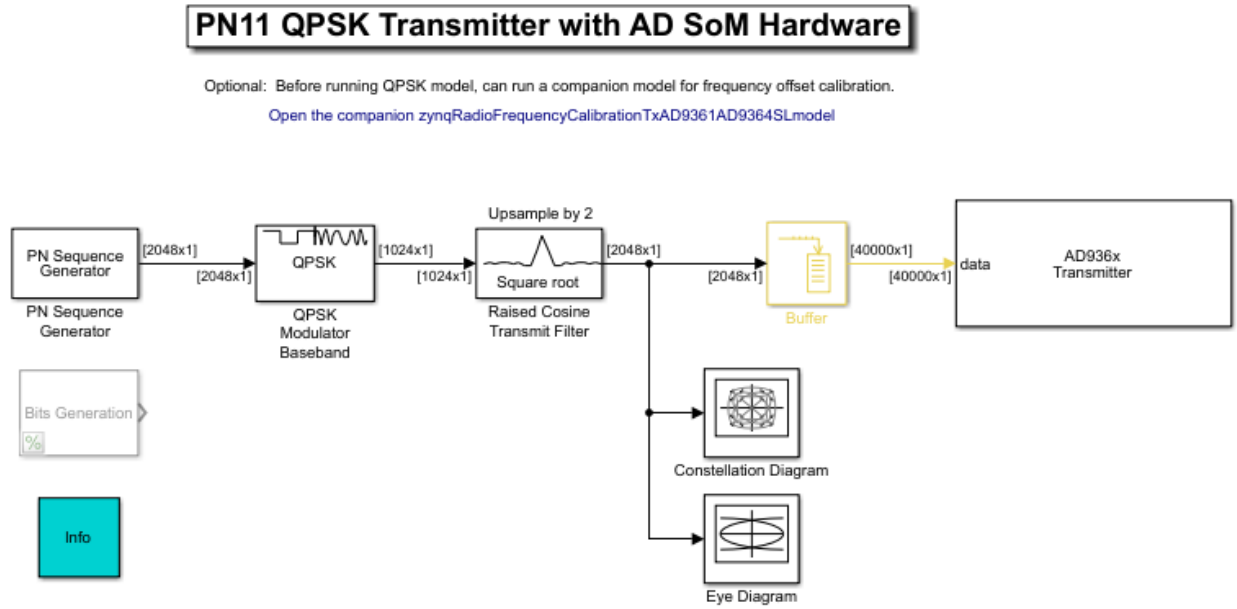

Figure 70. PN11 QPSK transmitter with AD SoM hardware Simulink model.

The most notable change to the model layout is the addition of a Buffer block (highlighted in yellow in Figure 70). According to MathWorks documentation, the Buffer block performs frame-based processing, redistributing input data to produce an output with different frame size [45]. The final PN11 QPSK Simulink model buffers the data stream to a larger frame size, which outputs a slower frame rate. This concept is illustrated in Figure 71. Prior thesis research [3] deduced that frame-based processing is advantageous for interfacing with real-time hardware because it "permits a reduction in the static computational overhead for the acquisition and propagation of samples to/from Simulink." The final Simulink model retained the settings of the Buffer block from [1], depicted in

Figure 72. An output buffer size of 40,000 per channel was the parameter established in [1], and the only buffer size applied in this thesis research. It is suggested that future work delves further into the relationships between buffer size and other model parameters (i.e., sample rate, over-air data rate, frame size). Additional background on the applications of Buffer blocks may be found in [45] as well as preceding thesis research [3].

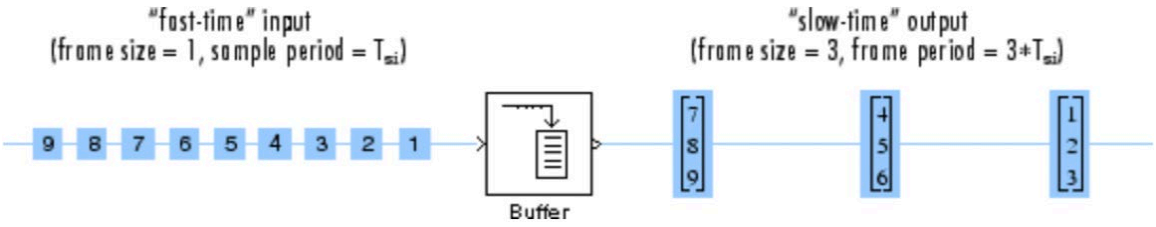

Figure 71. Buffering to larger frame size.

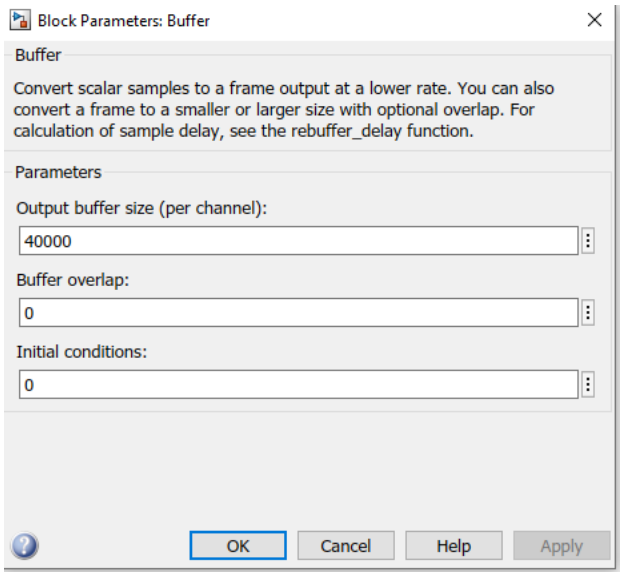

Figure 72. Block Parameters: Buffer.

An additional breakthrough, that led to a successful interoperability testing outcome, was made by employing specific values for the RFFE sample rate (Baseband sample rate parameter of the AD936x Transmitter block). The Simulink model of [1] utilized a sample rate value of 520,841 (Hz). So, to execute tests that would achieve higher

data rates while maintaining resemblance to the parameter structure of [1], testing relied on multiples of 520,841for baseband sample rate (i.e., 1,041,682 and 2,604,205).

Final interoperability tests resulted in the effective receipt/decoding of PN11 data at up to 1.042 Mbps by the AMERGINT satTRAC system, and up to 2.604 Mbps by the Kratos qRadio SDR. The flight-like SDR SoM and carrier board enacted the hybrid Simulink model to transmit a QPSK-modulated, 2.604 Mbps PN11 data transmission at 2.4 GHz center frequency, with successful demodulation and decoding by the Kratos receiver. BERs of 0 were observed throughout the duration of testing. Figure 73 through Figure 77 captures these results. First, the block parameters implemented within the final Simulink model are shown, followed by SpectralNet and qRadio GUI screenshots that show the signal spectra, demodulation, and data decoding by the Kratos system.

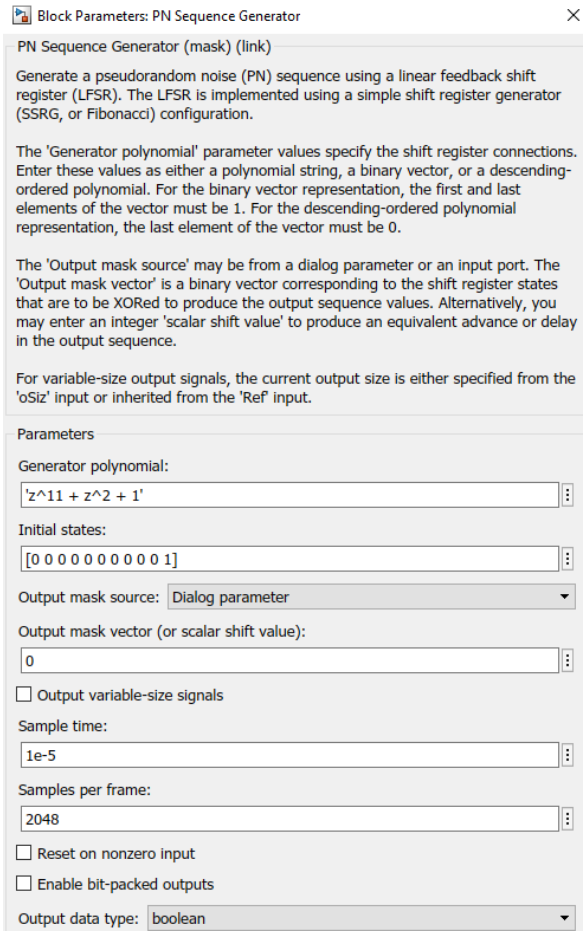

Figure 73. PN sequence generator block, interoperability test.

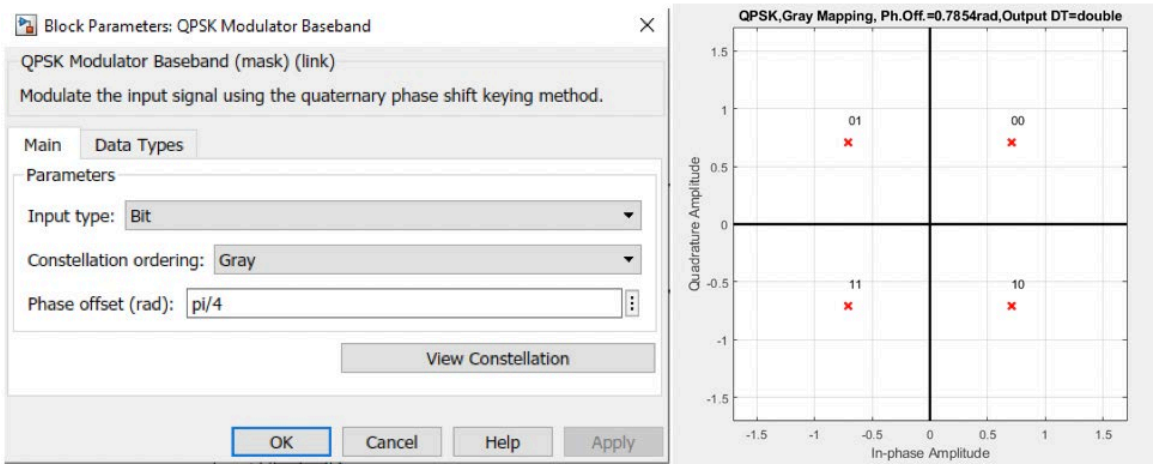

Figure 74. QPSK Modulator settings.

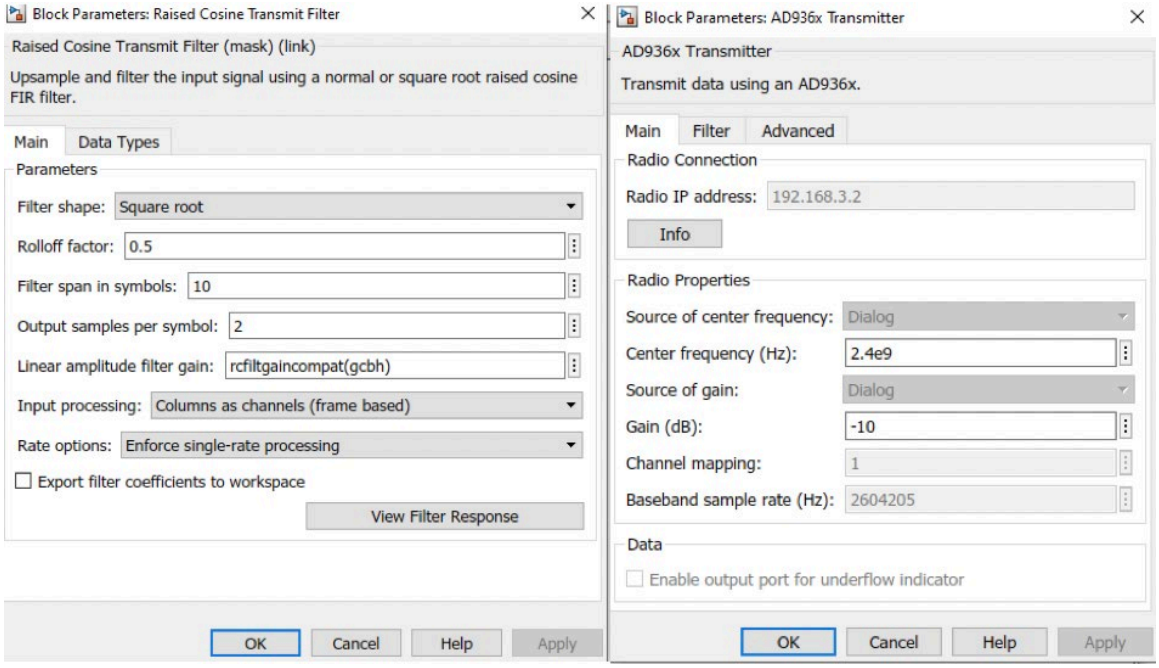

Figure 75. Filter block and AD936x Transmitter settings, interoperability test (Kratos).

Figure 76. SpectralNet GUI, interoperability test.

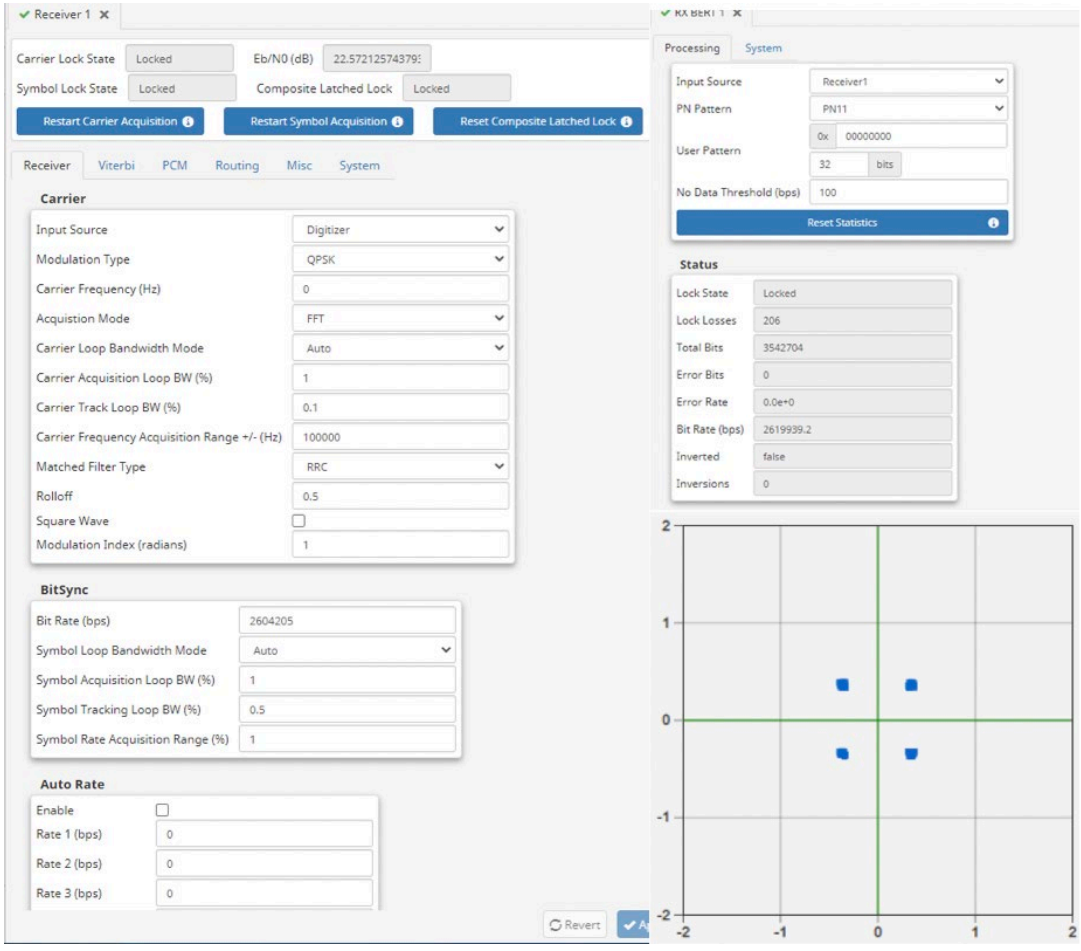

Figure 77. qRadio GUI, interoperability test.

The flight-like SDR SoM and carrier board enacted the hybrid Simulink model to transmit a QPSK-modulated, 1.402 Mbps PN11 data transmission at 2.25 GHz center frequency, with successful demodulation and decoding by the AMERGINT satTRAC receiver. When higher data rates were attempted, the IQ plot showed demodulation occurring, but BERs revealed that data was not being decoded (BER values showing as 1 or approximately 1; a red lock status indicator in the Rx BERT GUI). Efforts to mediate this issue were unsuccessful, but 1.402 Mbps data rates indicate the X-band SDR payload and the AMERGINT satTRAC receiver are interoperable. The results of the 1.402 Mbps test are captured in the figures below. The spectrum analyzer in Figure 80 shows increased energy to either side of the main signal peak, indicative of a filtering issue. Future work could include filter investigation to make the satTRAC radio a more efficient user of the spectrum.

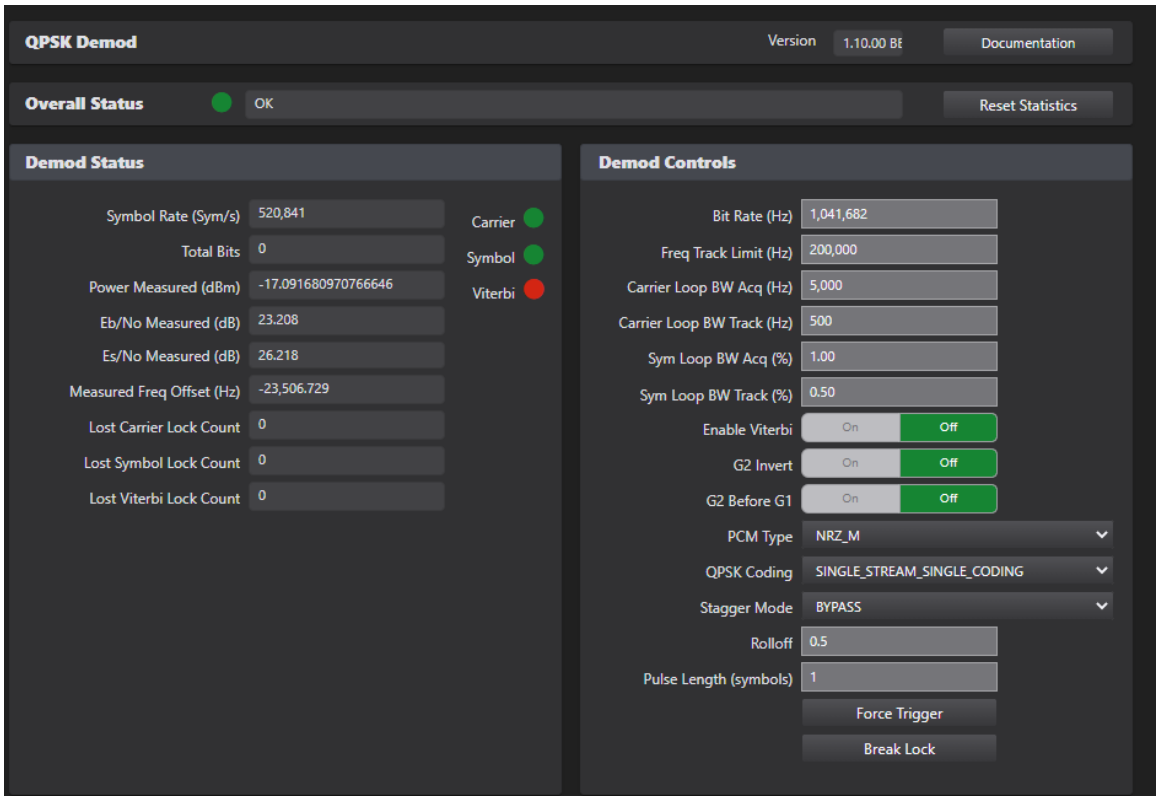

Figure 78. QPSK Demod window, interoperability test.

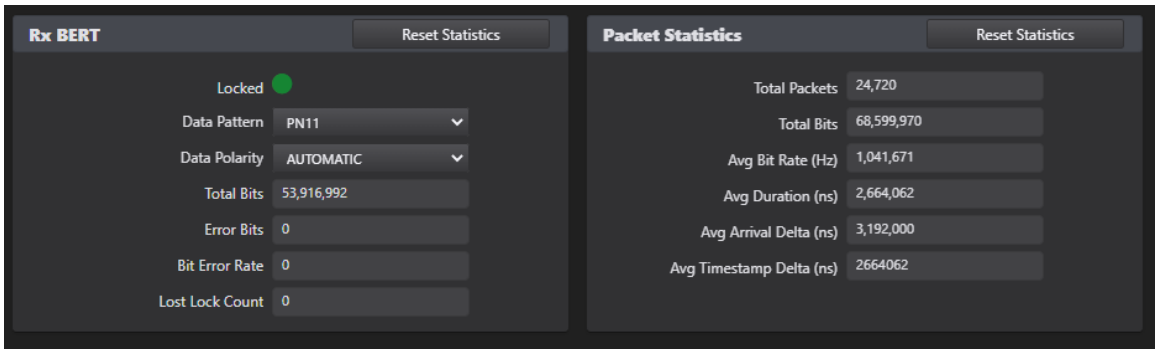

Figure 79. Rx BERT and packet statistics, interoperability test.

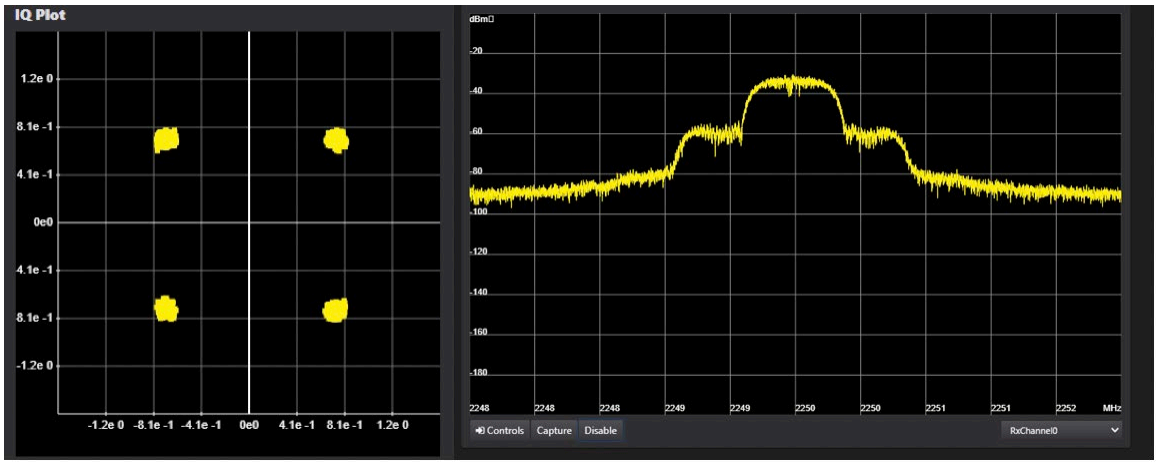

Figure 80. Signal receipt from flight-like hardware.

The block diagrams provided in Figure 81 and Figure 82 portray the final testing configurations, for both the Kratos and AMERGINT satTRAC receiver systems, that effectively satisfied thesis research objectives.

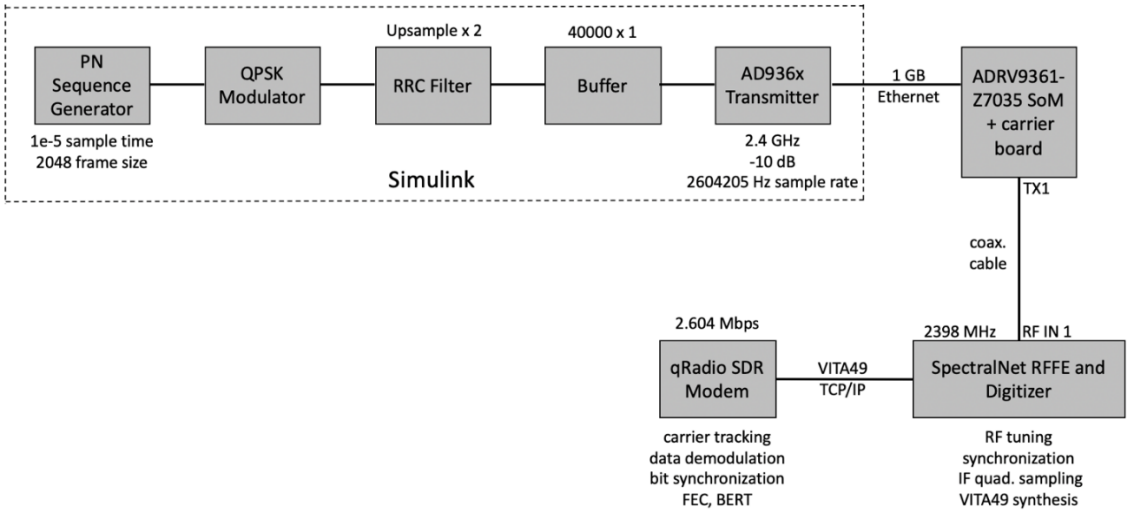

Figure 81. Interoperability testing block diagram (Kratos).

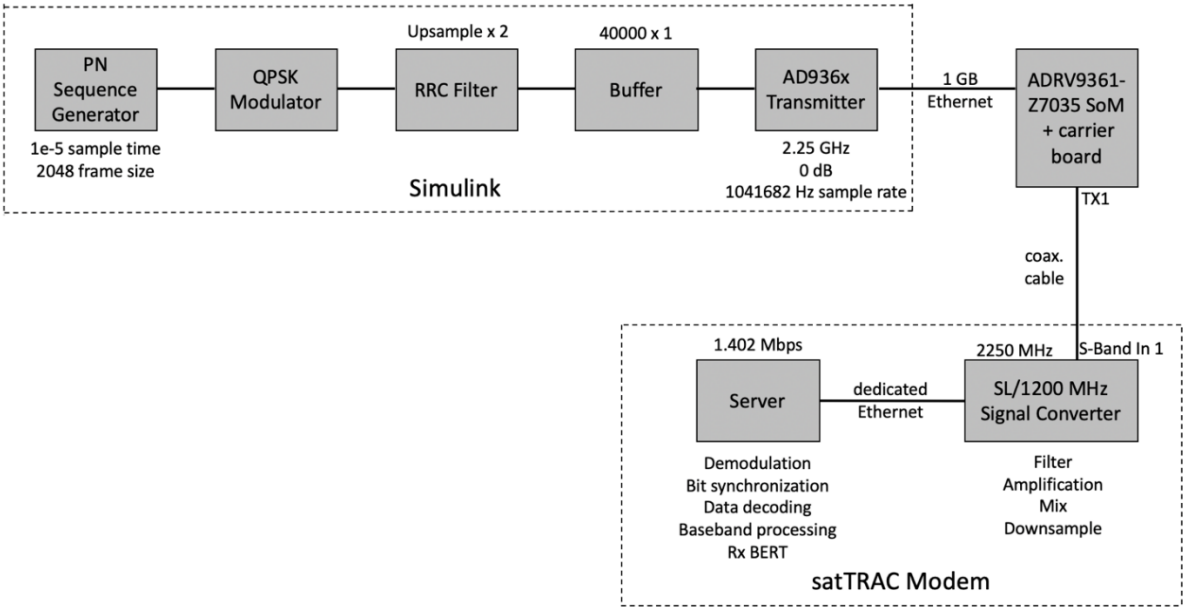

Figure 82. Interoperability testing block diagram (AMERGINT).

THIS PAGE INTENTIONALLY LEFT BLANK

V. CONCLUSIONS

A. SUMMARY

The SSAG at NPS is tackling the goal of demonstrating low-cost X-band SDR technology for small satellites, while seeking to add an X-band communications capability to the MC3 ground station network. This thesis research continued previous work [1], [2], [3] on the X-band SDR payload of the Mola CubeSat and the MC3 X-band initiative. Thesis objectives sought to test and verify a viable, functional communications downlink between the SDR payload and MC3 ground station receivers. The two SDR receiver test-subjects of this thesis effort were the newly-acquired AMERGINT satTRAC system, and the existing Kratos SpectralNet Lite Digitizer/quantumRadio SDR. Mission requirements of Mola's X-band SDR include frequency shift keying modulation, nominal data rates of 5 to 10 Mbps, and BERs less that 10E-5.

Loopback tests and equipment familiarization initiated testing efforts, followed by test signals generated between the two ground station receivers. Establishing a baseline knowledge of satTRAC and qRadio's innerworkings, and how data is demodulated and decoded by each system, allowed testing to transfer to payload-like hardware. But first, before attempting to run the Simulink model (developed for Mola by Small Satellite Lab staff) on the higher-complexity, custom-configured hardware of the SDR payload, the ADALM-PLUTO SDR was employed for model verification. When testing transitioned to the flight-like payload hardware (SoM and carrier board), issues were encountered that led to creation of a hybrid Simulink model. The new Simulink model combined components from the lab staff model design with the built-in Simulink QPSK modulation module utilized in [1]. Final interoperability tests resulted in the effective receipt/decoding of QPSK-modulated, PN11 data transmissions at up to 1.042 Mbps by the AMERGINT satTRAC system, and up to 2.604 Mbps by the Kratos qRadio SDR. Observed BERs remained well within mission requirements, as expected with the baseband testing methods used.

This thesis work culminated in successful demonstration of a baseband link from payload SDR hardware to both the Kratos and AMERGINT receivers. Further functional testing, RF-component integration, and environmental testing will ensure that Mola's X-band SDR payload can effectively communicate on-orbit with the MC3 network, and propel the MC3 X-band initiative towards full fruition.

B. FUTURE WORK

The following focus areas are recommended for future research and thesis work to continue integration of Mola's X-band SDR with the MC3 ground station network, carry the NPS 6U CubeSat project forward, and advance MC3's X-band initiative.

1. Data Rate Limitations

Final test results yielded successful receipt/decoding of PN11 data at up to 2.604 Mbps by the Kratos SDR, and 1.042 Mbps by the AMERGINT satTRAC system. However, research objectives of the X-band SDR include nominal data rates of 5 to 10 Mbps. The Analog Devices ADRV9361-Z7035 SoM and SDR receivers are advertised as able to support data rates in the desired range. It will be necessary to flush out the causes of data rate limitations in the current hardware/software configuration, and make refinements as necessary. Future work should also include progression to more advanced modulation such as offset quadrature phase shift keying (OQPSK), a prominent modulation scheme used in satellite communications.

2. Forward Error Correction (FEC)

Thus far in the Mola X-band SDR project, testing and Simulink model development have not incorporated FEC. Future software iterations should add FEC, which will allow for improved-upon BERs and better link margin. In accordance with communications standards for spaceflight by the Consultative Committee for Space Data Systems (CCSDS), Reed Solomon channel coding is recommended for FEC [1].

3. Flight-Unit Testing

At the conclusion of this research, the flight-unit X-band SDR payload was unavailable for testing due to delays in hardware development. Now that functional bench tests have confirmed a viable software model and successful data transmission from the flight-like SoM/carrier board hardware to MC3 ground station receivers, testing will need to be repeated with the payload itself. Future work should conduct subsequent testing with the fully-constructed radio assembly, seated in its mechanical enclosure (see Figure 44 for depiction of radio assembly mechanical enclosure).

4. Integration of Band Conversion Components

The testing performed during the course of this thesis work verified transmitter-to-receiver functionality at the baseband level. Elements of the final flight communications link (i.e., X-band up-conversion and down-conversion) were not included in testing, but initial demonstration of a working, flight-like hardware set is an important and necessary precursor to final testing efforts. The logical next step for follow-on testing is incorporation of the RF components that will enable real-time CubeSat operations. The RF components designated for MC3's mission with Mola were verified separately by students of the NPS payload design course.

5. Environmental Testing

As with any satellite design/deployment, it is imperative that environmental testing takes place before components are deemed mission-ready. Once the aforementioned functional testing of the X-band SDR payload is complete, the integrated radio assembly must undergo environmental testing. Tests conducted in a thermal vacuum chamber (TVAC), for example, will provide crucial metrics to assess suitability of the flight unit for the LEO space environment, and vibration testing will assess survivability during the CubeSat launch process.

THIS PAGE INTENTIONALLY LEFT BLANK

APPENDIX A. HARDWARE SPECIFICATIONS

A. AMERGINT SATTRAC SYSTEM

satTRAC Modem specifications, as provided by the manufacturer in [26].

RF Output	Specification
Number of Output Channels	1
Frequency Ranges:	
SGLS Up	1750 to 1850 MHz
USB Up	2025 to 2120 MHz
1200 MHz	1150 to 1250 MHz
Test (unfiltered)[1]	1690 to 2400 MHz or 950 to 1450 MHz
Output Power Range	-30 to +10 dBm
P1dB	+26 dBm (S/L) +16 dBm (1200 MHz)
Output Power Accuracy	+/-0.5 dB
Instantaneous Dynamic Range	80 dB
Noise Power Density	-135 dBm/Hz max (S/L) -123 dBm/Hz max (1200 MHz)
Output VSWR	1.3: 1
Output Impedance (nominal)	50 Ohms
Gain Adjustment	60 dB in 0.1 dB Steps
Instantaneous Bandwidth	> 40 MHz (at S/L) > 100 MHz (at 1200 MHz)
Tuning Step Size	< 1 μHz
Output Spurious	< -65 dBc with output power -15 to +10 dBm
Output Spurious with Analog Video I/O Enabled	< -55 dBc with output power -15 to +10 dBm
Frequency Stability and Aging (using internal reference)	+/- 5 ppb over operating temp range, < +/- 100 ppb/yr
Amplitude Response (Flatness)	+/- 0.2dB over 4 MHz
Phase Noise	
10 Hz	-60 dBc/Hz
100 Hz	-80 dBc/Hz
1 kHz	-90 dBc/Hz
10 kHz	-95 dBc/Hz
100 kHz	-97 dBc/Hz
1 MHz	-115 dBc/Hz
10 MHz	-124 dBc/Hz
100 MHz	-136 dBc/Hz

[1] Unfiltered outputs do not meet the output spurious, VSWR and flatness performance specifications.

RF Input	Specification
Number of Input Channels	2
Frequency Ranges:	
SGLS/USB Down	2200 to 2300 MHz
1200 MHz	1150 to 1250 MHz
Test/Echo (unfiltered)[1]	1690 to 2400 MHz or 950 to 1450 MHz
Operational Input Power Range	-100 to -23 dBm
Maximum Input Signal (damage)	+18 dBm
Instantaneous Dynamic Range	> 74 dB
Noise Figure (at max gain)	< 4 dB typical, 8 dB max
Input VSWR	1.3: 1
Input Impedance (nominal)	50 Ohms
AGC (50 dB range) Time Constant	0.001 to 1 seconds
Instantaneous Bandwidth	> 40 MHz (at S/L) > 100 MHz (at 1200 MHz)
Tuning Step Size	< 1 μHz
In-Band Spurious	< -59 dBc
Amplitude Response (flatness)	+/- 0.2dB over 4MHz

Timing and Reference Signals	Specification
Frequency Reference	10 MHz
Internal Frequency Reference Accuracy	< 0.1 ppm
External Frequency Reference Input	
Level Range	-10 to +10 dBm
Impedance	50 Ohms
Phase-Lock Frequency Range	+/-5 Hz
Spurious	-60 dBc max
Phase Noise at Offset ≥ 10 Hz	-86 dBc/Hz max
Time References Supported	IRIG-B, 1PPS, NTP
Time Reference Voltage Levels (for IRIG and 1PPS)	0.3 to 5 V peak-to-peak
Time Reference Impedance (for IRIG and 1PPS)	10K Ohms

Analog Video I/O	Specification
Video Input & Output Channels	2 In, 2 Out
Video Bandwidth	7.5 MHz
Input/Output Impedance	50 Ohms

B. KRATOS SPECTRALNET LITE DIGITIZER AND QUANTUMRADIO SDR

Kratos system specifications, as provided by the manufacturer in [37] and [38].

4. DOWNLINK (TELEMETRY)

4.1 ANALOG INTERFACES

Description	Specification
RF Frequency Range:	50 MHz to 2500 MHz
RF Tuning Step Size:	0.1 Hz
RF Input Power Levels:	-60 dBm to 0 dBm
RF Connector Type:	SMA
A/D Resolution	Selectable from 4 through 12 bits.
Instantaneous Bandwidth:	125 kHz to 10 MHz[4]
Number of Receive Channels:	1

4.2 RECEIVER SPECIFICATIONS

Description	Specification
Number of Receive Channels:	1
Direct Demodulation Types:	BPSK QPSK DQPSK (Normal / Alternate) OQPSK 8PSK FSK MSK GMSK SOQPSK_TG PCM PM PCM FM
Symbol Rate:	7 sps to 5 Msps[5]
Mod Index (PM):	0.0 to 3.0 Radians
Frequency Deviation (FM):	0 to 4 MHz
Match Filter:	None Raised Cosine Root Raised Cosine
Match Filter Rolloffs:	User Defined from 0% to 100%
Number of Subcarrier Channels:	2
Subcarrier Types:	Sine Square
Subcarrier Minimum IF/RF Freq.:	1 kHz
Subcarrier Maximum IF/RF Freq.:	Limited by bandwidth
PCM Decoding:	NRZ-L,M,S Biϕ-L,M,S D-Biϕ-L,M,S
Dual PCM Decoders:	Supported

[4] The instantaneous bandwidth of the SpectralNet Lite device for *RF transport* is 54 MHz. The quantumRadio supports processing a maximum of 10 MHz of instantaneous bandwidth. When using the SpectralNet Lite as the front end for quantumRadio, the instantaneous bandwidth is limited to quantumRadio's maximum instantaneous bandwidth (10 MHz.).

[5] Max rate assumes a bandwidth of 10MHz > 5 Msps @ 8PSK > 15 Mbps and that they data is unencoded.

quantumRadio's Key Features

Modulation (Transmit)	Demodulation (Receive)	Features
• Number of Channels: 1 - Digital Spectrum up to 20MHz instantaneous bandwidth[2]	• Number of Channels: 1 - Digital Spectrum up to 20MHz instantaneous bandwidth	• Reference Signals - External generated 1PPS - External generated IRIG - Monitoring and Control
• Compatible Hardware Front-ends - SpectralNet Narrowband - SpectralNet Wideband	• Compatible Hardware Front-ends - SpectralNet Narrowband - SpectralNet Wideband	• Ethernet TCP/IP remote M&C interface - Web-based GUI - File record/playback
• BPSK/PM or BPSK/FM - Symbol Rate: 7 sps to 5 Msps[2] - Modulation Index (PM): 0.0 to 3.0 Radians - Frequency Deviation (FM): 0 to 4 MHz • FSK/AM - Symbol Rate: 1, 2, and 10 Ksps	• BPSK/PM or BPSK/FM - Symbol Rate: 7 sps to 10 Msps[2] - Number of Subcarriers (Per Channel): 1 - Subcarrier frequency: 1 kHz to 4 MHz - Modulation Index (PM): 0.0 to 3.0 Radians - Frequency Deviation (FM): 0 to 4 MHz	• Ranging - Tone Ranging - ESA, ESA-Like - SGLS PRN[1] - Up to 5 MHz of bandwidth
• Direct PSK (BPSK/QPSK/OQPSK/UAQPSK) - Symbol Rate: Up to 10 Msps[2]	• Direct PSK (BPSK/QPSK/OQPSK/UAQPSK) - Symbol Rate: Up to 10 Msps[2]	• Command Echo[3] - Single Channel - Symbol Rate: Up to 5 Msps
• PCM Coding: NRZ-L,M,S, and BIØ-L,M,S	• PCM Coding: NRZ-L,M,S, and BIØ-L,M,S	CPU instruction set architecture: x86_64; AVX512[4]
• Convolutional Encoding: Rate ½, k=7	• Viterbi Decoding: Rate ½, k=7	
• Reed-Solomon Decoding: (223, 255), (239, 255) - Interleave: 0 to 8	• Reed-Solomon Decoding: (223, 255), (239, 255) - Interleave: 0 to 8	
• HDLC Encoder - Bitwise		

[1] SGLS functionality is not part of standard quantumRadio baseline; a separate license is required. SGLS requires a separate export license as it is EAR controlled.
[2] Standard license supports 10 MHz of instantaneous bandwidth and 5 Msps; a separate license is required to achieve rates of 20 MHz of instantaneous bandwidth and 10 Msps.
[3] Command echo requires either two SpectralNet Narrowband units or a single SpectralNet Wideband unit with dual RF cards to support.
[4] Higher bandwidths and symbol rates require an AVX512 instruction set.

C. X-BAND SDR PAYLOAD CONVERT BOARD

Convert board bill of materials and design diagrams (top and bottom), as provided by thesis work in [1].

ID	Part Number	Feature	QTY	Each	Total
1	XM-PB4-SMA	SMA connector	2	$59.95	$119.90
2	XM-ANCHOR2	Anchor	15	$9.95	$149.25
3	XM-GSGJ	gsgJumper	8	$4.00	$32.00
4	XM-A2R9-0404D	Voltage regulator	1	$65.00	$65.00
5	XM-A9W8-0404D	Amplifier	1	$110.00	$110.00
6	XM-A7J3-0404D	Oscillator	1	$110.00	$110.00
7	XM-A7T8-0404D	Bias controller	1	$150.00	$150.00
8	XM-A3R9-0409D	Bias controller	1	$180.00	$180.00
9	XM-A5Y8-0409D	PLL VCO	1	$204.00	$204.00
10	XM-A1F4-0204D	High pass filter	1	$44.00	$44.00
11	XM-A718-0204D	Band pass filter	1	$44.00	$44.00
12	XM-A9V7-0404D	Mixer	1	$199.00	$199.00
13	XM-C6A1-0404D	Bias controller	1	$65.00	$65.00
14	XM-A166-0204D	Band pass filter	1	$44.00	$44.00
	TOTAL (USD)				**$1516.15**

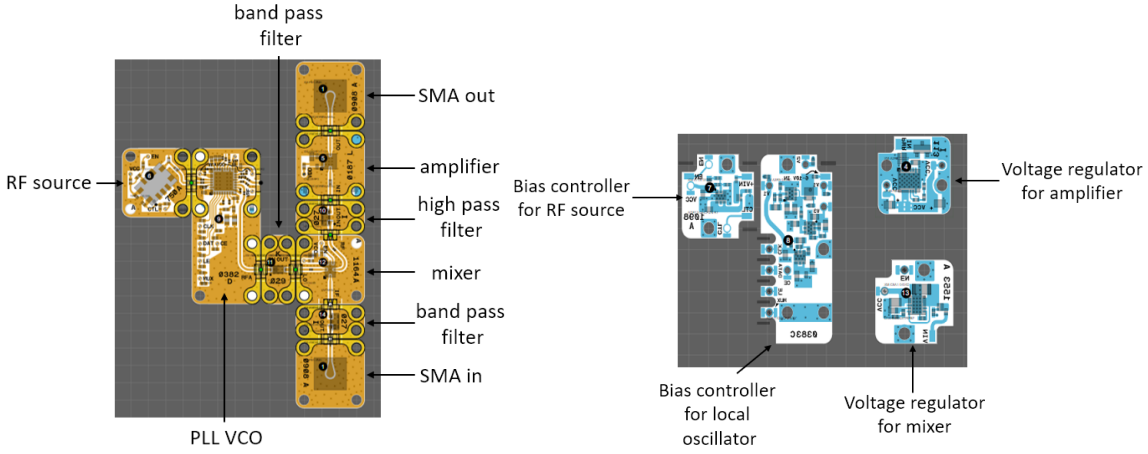

APPENDIX B. LINK BUDGET SPREADSHEETS

Parameter	Symbol	Value	Units	Alt units				Mission Geometry					
Speed of light	c	300000000	m/s					R_earth	6378	km			
Frequency	f	8.21	Ghz					elevation angle	10	deg	0.174533	rad	
Tx power	P	4.00	W	6.021	dBW	36.021	dBm	altitude	500	km			
Tx line loss	L_i	-1.00	dB					slant range (D)	1695.081	km			
Effective Tx antenna Gain	G_t	4.00	dB					Subtended angle	2.722	rad			
Equivalent Isotropically Radiated Power	EIRP	9.021	dBW					Earth Central angle	0.245	rad			
Slant range	d	1695.08	km										
Free space path loss	FSPL	-175.32	dB										
Propogation and polarization losses	L_a	-1.00	dB										
Theoretical System G/T	G/T	23.40	dB/K										
Data Rate	R	5000000	bps	66.99	dB-bps								
Implimentation loss	L_i	-1.50	dB						1 Mbps	->	1200 km		
Bit error rate	BER	0.00001	<N/A>						2.5 Mbps	->	1200 km		
Carrier power to noise power per unit bw	C/N0	83.21	dB-Hz						5 Mbps	->	725 km		
Achieved Eb/N0	Eb/N0	**16.22**	dB						10 Mbps	->	450 km		
Required Eb/N0	Req Eb/N0	9.65	dB										
Margin	LKM	**6.57**	dB										

Parameter	Symbol	Value	Units	Alt units				Mission Geometry					
Speed of light	c	300000000	m/s					R_earth	6378	km			
Frequency	f	8.21	Ghz					elevation angle	10	deg	0.174533	rad	
Tx power	P	4.00	W	6.021	dBW	36.021	dBm	altitude	500	km			
Tx line loss	L_i	-1.00	dB					slant range (D)	1695.081	km			
Effective Tx antenna Gain	G_t	4.00	dB					Subtended angle	2.722	rad			
Equivalent Isotropically Radiated Power	EIRP	9.021	dBW					Earth Central angle	0.245	rad			
Slant range	d	1695.08	km										
Free space path loss	FSPL	-175.32	dB										
Propogation and polarization losses	L_a	-1.00	dB										
Theoretical System G/T	G/T	23.40	dB/K										
Data Rate	R	10000000	bps	70.00	dB-bps								
Implimentation loss	L_i	-1.50	dB						1 Mbps	->	1200 km		
Bit error rate	BER	0.00001	<N/A>						2.5 Mbps	->	1200 km		
Carrier power to noise power per unit bw	C/N0	83.21	dB-Hz						5 Mbps	->	725 km		
Achieved Eb/N0	Eb/N0	**13.21**	dB						10 Mbps	->	450 km		
Required Eb/N0	Req Eb/N0	9.65	dB										
Margin	LKM	**3.56**	dB										

Parameter	Symbol	Value	Units	Alt units				Mission Geometry					
Speed of light	c	300000000	m/s					R_earth	6378	km			
Frequency	f	8.21	Ghz					elevation angle	10	deg	0.174533	rad	
Tx power	P	4.00	W	6.021	dBW	36.021	dBm	altitude	1200	km			
Tx line loss	L_i	-1.00	dB					slant range (D)	3132.026	km			
Effective Tx antenna Gain	G_t	4.00	dB					Subtended angle	2.548	rad			
Equivalent Isotropically Radiated Power	EIRP	9.021	dBW					Earth Central angle	0.419	rad			
Slant range	d	3132.03	km										
Free space path loss	FSPL	-180.65	dB										
Propogation and polarization losses	L_a	-1.00	dB										
Theoretical System G/T	G/T	23.40	dB/K										
Data Rate	R	5000000	bps	66.99	dB-bps								
Implimentation loss	L_i	-1.50	dB						1 Mbps	->	1200 km		
Bit error rate	BER	0.00001	<N/A>						2.5 Mbps	->	1200 km		
Carrier power to noise power per unit bw	C/N0	77.87	dB-Hz						5 Mbps	->	725 km		
Achieved Eb/N0	Eb/N0	**10.88**	dB						10 Mbps	->	450 km		
Required Eb/N0	Req Eb/N0	9.65	dB										
Margin	LKM	**1.23**	dB										

Parameter	Symbol	Value	Units	Alt units				Mission Geometry				
Speed of light	c	300000000	m/s					R_earth	6378	km		
Frequency	f	8.21	Ghz					elevation angle	10	deg	0.174533	rad
Tx power	P	4.00	W	6.021	dBW	36.021	dBm	altitude	1200	km		
Tx line loss	L_i	-1.00	dB					slant range (D)	3132.026	km		
Effective Tx antenna Gain	G_t	4.00	dB					Subtended angle	2.548	rad		
Equivalent Isotropically Radiated Power	EIRP	9.021	dBW					Earth Central angle	0.419	rad		
Slant range	d	3132.03	km									
Free space path loss	FSPL	-180.65	dB									
Propogation and polarization losses	L_a	-1.00	dB									
Theoretical System G/T	G/T	23.40	dB/K									
Data Rate	R	10000000	bps	70.00	dB-bps							
Implimentation loss	L_i	-1.50	dB						1 Mbps	->	1200 km	
Bit error rate	BER	0.00001	<N/A>						2.5 Mbps	->	1200 km	
Carrier power to noise power per unit bw	C/N0	77.87	dB-Hz						5 Mbps	->	725 km	
Achieved Eb/N0	Eb/N0	**7.87**	dB						10 Mbps	->	450 km	
Required Eb/N0	Req Eb/N0	9.65	dB									
Margin	LKM	**-1.78**	dB									

APPENDIX C. MATLAB QPSK TRANSMITTER CODE

zynqRadioQPSKTxAD9361AD9364SL_init.m (MATLAB QPSK transmitter initial parameters script).

```
function SimParams = zynqRadioQPSKTxAD9361AD9364SL_init
% Set simulation parameters



%SDR receiver parameters
SimParams.RadioFrontEndSampleRate = 520.841e3;
SimParams.RadioFrontEndSamplePeriod = 1 / SimParams.RadioFrontEndSampleRate;
SimParams.RadioChannelMapping = 1;

% General simulation parameters
SimParams.Upsampling = 4; % Upsampling factor
SimParams.Fs = SimParams.RadioFrontEndSampleRate; % Sample rate
SimParams.Ts = SimParams.RadioFrontEndSamplePeriod; % Sample time
SimParams.FrameSize = 100; % Number of modulated symbols per frame
SimParams.FrameTime = SimParams.Ts * SimParams.FrameSize * SimParams.Upsampling;
% Tx parameters
SimParams.BarkerLength = 13; % Number of Barker code symbols
SimParams.DataLength = (SimParams.FrameSize - SimParams.BarkerLength)*2; % Number of data
payload bits per frame
SimParams.MsgLength = 105; % Number of message bits per frame, 7 ASCII characters

SimParams.RxBufferedFrames = 10; % Received buffer length (in frames)
SimParams.RCFiltSpan = 10; % Group delay of Raised Cosine Tx Rx filters (in symbols)
```

THIS PAGE INTENTIONALLY LEFT BLANK

LIST OF REFERENCES

[1] L. West, "Design, build and test of a low-cost, high-bandwidth X-Band software-defined radio for CubeSats," M.S. thesis, Space Systems Academic Group, NPS, Monterey, CA, USA, 2020. [Online]. Available: https://calhoun.nps.edu/handle/10945/66741.

[2] S. H. Wood, "Trade study of commercial software-defined radio technologies for small satellite ground station network command and control applications," M.S. thesis, Space Systems Academic Group, NPS, Monterey, CA, USA, 2020. [Online]. Available: https://calhoun.nps.edu/handle/10945/65475.

[3] E. Bower, "Software defined radio implementation using MathWorks Simulink and MATLAB with commercially available hardware," M.S. thesis, Space Systems Academic Group, NPS, Monterey, CA, USA, 2020.

[4] "Mola PDR." Space Systems Academic Group, NPS, December 2020.

[5] National Aeronautics and Space Administration, "CubeSat 101: Basic concepts and processes for first-time CubeSat developers," October 2017. [Online]. Available: https://www.nasa.gov/sites/default/files/atoms/files/nasa_csli_cubesat_101_508.pdf.

[6] E. Mabrouk, "What are SmallSats and CubeSats?," NASA, 2017. Accessed December 14, 2020. [Online]. Available: https://www.nasa.gov/content/what-are-smallsats-and-cubesats.

[7] A. Johnstone, "CubeSat design specification (1U-12U) rev 14 CP-CDS-R14." The CubeSat Program, Cal Poly SLO, July 2020.

[8] National Aeronautics and Space Administration, "PropCube 3," April 2021. [Online]. Available: https://nssdc.gsfc.nasa.gov/nmc/spacecraft/display.action?id=2015-058K.

[9] D. Hill, "The CubeSat Launch Initiative Celebrates its 100th CubeSat Mission Deployment," NASA, 2020. Accessed December 14, 2020. [Online]. Available: https://www.nasa.gov/feature/the-cubesat-launch-initiative-celebrates-its-100th-cubesat-mission-deployment.

[10] Mobile CubeSat Command & Communications (MC3) *User's Guide*. 07 Jan 2019.

[11] "X-Band SDR Meeting Notes 20200731." Space Systems Academic Group, NPS, July 2020.

[12] G. Minelli, L. Magallanes, N. Weitz, D. Rigmaiden, J. Horning and J. Newman, "The mobile CubeSat command and control (MC3) ground station network: An overview and look ahead," presented at the 33rd Annual AIAA/USU Conference on Small Satellites, Logan, UT, USA, 7 Aug 2019.

[13] J. Walker, *Fundamentals of Physics*, 10th ed. Hoboken, NJ, USA: John Wiley & Sons, Inc.

[14] J. G. Proakis, *Digital Communications*, 4th ed., Boston, MA, USA: McGraw-Hill, 2001.

[15] AMERGINT Technologies, *A Really Simple Introduction to Satellite Links*, 2019. [Online]. Available: https://www.amergint.com/wp-content/uploads/AMERGINT-tutorial-Really-Simple-Introduction-to-Satellite-Links.pdf.

[16] Federal Communications Commission, "Radio spectrum allocation," March 02, 2011. [Online]. Available: https://www.fcc.gov/engineering-technology/policy-and-rules-division/general/radio-spectrum-allocation.

[17] B. Sklar, *Digital Communications: Fundamentals and Applications*, 2nd ed. Upper Saddle River, NJ, USA: Prentice Hall, 2001.

[18] A. B. Carlson, *Communication Systems: An Introduction to Signals and Noise in Electrical Communication*. 2nd ed. New York, NY, USA: McGraw-Hill, 1975.

[19] J. Wertz, D. Everett, and J. Puschell, *Space Mission Engineering: The New SMAD*, Hawthorne, CA, USA: Microcosm Press, 2011.

[20] E. Grayver, *Implementing Software Defined Radio*, 2013th ed., New York, NY, USA: Springer, 2013.

[21] R. Keim, A. White, O. Hoilett, and Texas Instruments, "Active components in RF circuits," All About Circuits, 2017. Accessed October 3, 2019. [Online]. Available: https://www.allaboutcircuits.com/textbook/radio-frequency-analysis-design/rf-principles-components/active-components-in-rf-circuits/.

[22] W. Tuttlebee, *Software Defined Radio: Enabling Technologies*, 2nd ed. New York, NY, USA: J. Wiley & Sons, 2002.

[23] M. Kolawole, *Satellite Communication Engineering*, 2nd ed. Boca Raton, FL, USA: CRC Press, Taylor & Francis Group, LLC, 2013.

[24] AMERGINT Technologies, *SatTRAC Modem Training,* Delivered media, Document Number: AT-19-1593, October 2019.

[25] T. Kuphaldt, *Understanding I/Q Signals and Quadrature Modulation Radio Frequency Demodulation Electronics Textbook*, 2000. [Online]. https://www.allaboutcircuits.com/textbook/radio-frequency-analysis-design/radio-frequency-demodulation/understanding-i-q-signals-and-quadrature-modulation/.

[26] AMERGINT Technologies, *Modem/Baseband Unit User Guide*, Delivered media, Document Number: AT-satTRAC-F0507-USR-AT-19-AT-1586, Version: 1.0, October 2019.

[27] T. F. Collins, R. Getz, D. Pu, and A. M. Wyglinski, *Software-defined radio for engineers*. Norwood, MA, USA: Artech House, 2018.

[28] Wireless Innovation, "What is Software Defined Radio?" Accessed August 21, 2020. [Online]. Available: https://www.wirelessinnovation.org/assets/documents/SoftwareDefinedRadio.pdf.

[29] A. M. Wyglinski and D. Pu, *Digital Communication Systems Engineering with Software-Defined Radio*. Boston: Artech House, 2013.

[30] D. Oikonomou, P. Nomikos, G. Limnaios, and K. Zikidis, "Passive radars and their use in the modern battlefield," Journal of Computations & Modeling, vol. 9, no.2, pp. 37–61, 2019.

[31] L. Wilson, *SDR Receiver System's Tests & Performance Evaluation Techniques - Working Report*, December 2020.

[32] C. Racoosin, "SS3610-EO3510 Exam #3 Graphs & Equations_Mar 2020," Space Systems Academic Group, Naval Postgraduate School, Monterey, CA, USA, 2020.

[33] AMERGINT Technologies, *AMERGINT satTRAC Brochure*, 2019. [Online]. Available: https://www.amergint.com/wp-content/uploads/AMERGINT-satTRAC-brochure-2019-07-23-m.pdf.

[34] AMERGINT Technologies, *Signal, Network, and Data Processing*, 2019. [Online]. Available: https://www.amergint.com/products/.

[35] AMERGINT Technologies, *AMERGINT WANFEC Ground Technology and Info to Meet Laser Communications Requirements*, 2017 [Online]. Available: https://www.nasa.gov/sites/default/files/atoms/files/06_amergint_ground_technology_for_laser_comm_requirements.pdf.

[36] Kratos, *About Kratos Defense & Security Solutions*. [Online]. Available: https://www.kratosdefense.com/about/about-kratos.

[37] Kratos, *Software Modem quantumRadio*, DS-274. [Online]. Available: https://www.kratosdefense.com/-/media/datasheets/rtl-dst_qradio.pdf.

[38] Kratos Defense and Security Solutions, *quantum quickStart Guide*, Version 2.0, Real Time Logic Corporation, June 2018.

[39] M. B. Matthews, "Laboratory 12 – radio study," Space Systems Academic Group, Naval Postgraduate School, Monterey, CA, USA, 2020.

[40] AVNET, *PicoZed SDR 2x2 Product Brief*, 2019. [Online]. Available: http://zedboard.org/sites/default/files/product_briefs/PB-AES-Z7PZ-SDR2-PicoZed-SDR-SOM-V1.pdf.

[41] MATLAB, "QPSK transmitter using Analog Devices AD9361/AD9364 - MATLAB & Simulink example." Accessed. March 4, 2021. [Online]. Available: https://www.mathworks.com/help/supportpkg/xilinxzynqbasedradio/ug/qpsk-transmitter-using-analog-devices-ad9361-ad9364.html.

[42] The MathWorks, Inc., "PN sequence generator." Accessed March 4, 2021. [Online]. Available: https://www.mathworks.com/help/comm/ref/pnsequencegenerator.html.

[43] Analog Devices, Inc., "ADALM-PLUTO overview," March 10, 2021. [Online]. Available: https://wiki.analog.com/university/tools/pluto.

[44] Analog Devices, Inc., "ADALM-PLUTO evaluation board." Accessed March 10, 2021. [Online]. Available: https://www.analog.com/en/design-center/evaluation-hardware-and-software/evaluation-boards-kits/ADALM-PLUTO.html.

[45] The MathWorks, Inc., "Buffer." Accessed May 14, 2021. [Online]. Available: https://www.mathworks.com/help/dsp/ref/buffer.html?searchHighlight=buffer%20block&s_tid=srchtitle.

INITIAL DISTRIBUTION LIST

1. Defense Technical Information Center
   Ft. Belvoir, Virginia

2. Dudley Knox Library
   Naval Postgraduate School
   Monterey, California